Application of Forward Osmosis for the reduction of pre-treatment sludge volume in desalination: Modelling and Experiments

A thesis submitted in fulfilment of the requirements for the degree of Doctor of Philosophy

Susanthi Liyanaarachchi

Bsc Engineering (hons.) (University of Peradeniya)

School of Engineering

College of Science, Engineering and Health

RMIT University

June 2017

Declaration

I certify that except where due acknowledgement has been made, the work is that of the author alone; the work has not been submitted previously, in whole or in part, to qualify for any other academic award; the content of the thesis is the result of work which has been carried out since the official commencement date of the approved research program; any editorial work, paid or unpaid, carried out by a third party is acknowledged; and, ethics procedures and guidelines have been followed.

……

Susanthi Liyanaarachchi

Dedication

This thesis is dedicated to Dr. Dimuth Navarathna, Victoria University.

Your encouragements throughout this study are highly acknowledged.

Acknowledgements

First and foremost, I would like to express my sincere gratitude to my principal supervisor Prof. Jega V Jegatheesan for his excellent guidance, technical expertise and continuous support throughout this research. Thanks for being my principal supervisor, mentor and friend throughout this study. I also thank my co-supervisor Prof. Felicity Roddick for her guidance and valuable inputs to this work. Dr. Shobha Muthukumaran, Victoria University, is also highly acknowledged for her guidance and continuous support throughout my candidature. Prof. Bas Baskaran, Deakin University and Dr. Shu Li, RMIT University are also thanked for their support. I am grateful to these supervisors for the education, direction, encouragement and examples they have provided.

The financial support I received from Deakin University and then from RMIT University is gratefully acknowledged. I acknowledge the support I have received for my research through the provision of an Australian Government Research Training Program Scholarship.

I also would like to thank the friendly technical staff of civil engineering laboratory, Deakin University, namely Mr. Steve Bagshaw, Mrs. Leanne Farrago and Mr. Lube, for their immense support, assistance and technical advice. Their support for setting up and assisting with laboratory experiments are highly acknowledged.

I thank the RMIT environmental engineering laboratory technicians, Mrs.Peggy Chang, Mr.Cameron Crombie and Dr. Sandro Logano. Dr. Babu Iyer is gratefully acknowledged for assisting with seawater sampling which wasn't practically easy.

I would like to thank my research colleagues, Harish Ravishankar, Shamima Moazzem and Shruthi Sakarkar. It was pleasure to work with you all conducting laboratory experiments, learning and sharing knowledge.

Finally, I would like to thank my family for their steady support. Thanks my mother for your enormous support and guidance since my childhood and being my role model. I'm also grateful to my husband, Chana, for your encouragement and patience during past few years!

Contribution to the knowledge

Published peer reviewed journal papers

1. **S. Liyanaarachchi**, V. Jegatheesan,S. Muthukumaran, Stephen Gray, L. Shu, Mass balance for a novel RO/FO hybrid system in seawater desalination. Journal of Membrane Science, 501 (2016) 199–208.

2. **S. Liyanaarachchi**, V. Jegatheesan, I. Obagbemi, S. Muthukumaran, L. Shu, Effect of feed temperature and membrane orientation on pre-treatment sludge volume reduction through forward osmosis. Desalination and Water Treatment 54 (2014) 1-7.

3. **S. Liyanaarachchi**, L. Shu, S. Muthukumaran, V. Jegatheesan, K. Baskaran, Problems in seawater industrial desalination processes and potential sustainable solutions: a review, Reviews in Environmental Science and Bio/Technology, 13 (2014) 203-214.

4. **S. Liyanaarachchi**, V. Jegatheesan, L. Shu, S. Muthukumaran, K. Baskaran, A preliminary study on the volume reduction of pre-treatment sludge in seawater desalination by forward osmosis, Desalination and Water Treatment 52 (2013) 556–563.

5. Shu, L., Obagbemi, I. J., **Liyanaarachchi, S**., Navaratna, D., Parthasarathy, R., Aim, R. B. and Jegatheesan, V. (2016). "Why does pH increase with $CaCl_2$ as draw solution during forward osmosis filtration." Process Safety and Environmental Protection 104, Part B, 465-471.

6. L. Shu, I. Obagbemi, V. Jegatheesan, **S. Liyanaarachchi** and K. Baskaran, Effect of multiple cations in the feed solution on the performance of forward osmosis, Desalination and Water Treatment 54, (2015), 845-852.

Peer reviewed conference papers

1. **Susanthi Liyanaarachchi**, Felicity Roddick, Shobha Muthukumaran, Jega V. Jegatheesan, Li Shu, A novel approach for waste management in desalination, Ozwater'16: Water: For Liveable Communities and Sustainable Industries. Held on May 12 -14 2016, Melbourne, pp 1-7, paper number 129 (Oral presentation) (available online at https://awa.sharefile.com/share?#/view/s84a7abf484848c1b).

Journal papers in preparation

1. **S. Liyanaarachchi**, S. Muthukumaran, V. Jegatheesan, L. Shu, Modelling the Performance of a Forward Osmosis Membrane using a range of Salt Mixtures, Desalination.

2. **S. Liyanaarachchi**, V. Jegatheesan, L. Shu, F. Roddick, S. Muthukumaran, Optimising the water flux through hollow fibre FO membrane during sludge dewatering and comparison with flat sheet FO membranes, desalination.

3. **S. Liyanaarachchi**, V. Jegatheesan, L. Shu, F. Roddick, Fouling behaviour of the flat sheet FO membrane during sludge dewatering, Journal of Membrane Science.

Table of Contents

List of Figures

List of Tables

List of Abbreviations

A	Area of FO membrane (m^2)
A	Water permeability coefficient
B	Salt permeation coefficient
C_p	Salt concentration of diluted brine (mg/L)
C_0	Salt concentration of intake seawater (mg/L)
C_R	Salt concentration of RO 1st pass inlet (mg/L)
C_{PR}	Salt concentration of permeate of 1st pass RO unit (mg/L)
C_{0ut}	Salt concentration of treated water (mg/L)
C_f	Salt concentration of backwash sludge (mg/L)
C_c	Salt concentration of concentrated sludge (mg/L)
C_d	Salt concentration of draw solution/ brine from 1st pass RO unit (mg/L)
C_{PR2}	Salt concentration of permeate from 2nd pass RO unit (mg/L)
C_w	Salt concentration of blended RO concentrate- reject (mg/L)
$C_{D,b}$	Salt concentration of the bulk draw solution
$C_{F,b}$	Salt concentration of the bulk feed solution
$C_{D,m}$	Salt concentration near the membrane surface of draw side
$C_{F,m}$	Salt concentration near the membrane surface of feed side
$C_{D,i}$	Salt concentrations of draw solution at the porous and dense layers' interface
$C_{F,i}$	Salt concentrations of feed solution at the porous and dense layers' interface
d	Channel equivalent diameter
D/D_s	Diffusion coefficient (m^2/s) of a single solute
D_{eff}	Effective diffusion coefficient (cm^2/s) of multiple solutes
d_h	Hydraulic diameter
FO	Forward Osmosis
J_w	Water flux through FO unit(LMH)
K	Solute resistivity (s/m)
k	Mass transfer coefficient (m/s)
KD_{eff}	Structural constant (m)
PRO	Pressure retarded osmosis
Q_B	Backwash sludge flow rate (m^3/day)
Q_{in}	Intake flow rate (m^3/day)
Q_R	Inlet flow rate to 1st pass RO unit (m^3/day)
Q_{PR}	Permeate flow rate of 1st pass RO unit (m^3/day)
Q_f	Feed flow rate to the FO unit (m^3/day)
Q_P	Diluted brine flow rate (m^3/day)
Q_r	Recycle flow rate of concentrated sludge (m^3/day)
Q_c	Concentrated sludge flow rate (m^3/day)

Q_d	Draw flow rate to the FO unit (m^3/day)
Q_{RR}	Brine flow rate of 1st pass RO unit (m^3/day)
Q_{RR2}	Reject flow rate of 2nd pass RO unit (m^3/day)
Q_w	Concentrated brine- waste flow rate (m^3/day)
R	Overall recovery of the proposed system (%)
$R1$	Recovery of the 1st pass RO (%)
$R2$	Recovery of the 2nd pass RO (%)
RO	Reverse Osmosis
ROC	Reverse Osmosis Concentrate
Re	Reynolds number
Sc	Schmidt number
Sh	Sherwood number
ρ	Density (kg/m^3)
v	Velocity of a fluid (m/s^1)
μ	Viscosity (Pa·s)
$\pi_{D,b}$	Bulk osmotic pressure of draw solution (bar)
$\pi_{F,b}$	Bulk osmotic pressure of feed solution (bar)
ΔΠ	Osmotic pressure difference (bar)

Abstract

Forward osmosis (FO) is a novel water treatment process that potentially can be used as an alternative technology for both sludge and brine treatment due to its low energy requirement. In the FO process, a solution of high salt concentration (known as draw solution) is utilized to generate an osmotic pressure gradient across a semipermeable membrane to extract freshwater from a solution with lower salt concentration (known as feed solution). The FO process requires low energy to operate as it capitalizes on the phenomenon of natural osmosis. FO has been given significant attention over the past few years due its superior characteristics. However, this technology is still in the developmental stages. A few studies have been carried out using FO for the treatment of industrial wastewater, landfill leachate and food industry effluents. However, to date, there has been no research on sludge treatment and brine management using the FO process, other than this research, which could be another promising application of FO.

Therefore, in this study FO was proposed as an additional process to the seawater reverse osmosis (RO) process to dilute the brine before it is discharged back to the ocean and to reduce the volume of pre-treatment sludge before mechanical dewatering. Diluting of brine have number of advantages depending on the industrial requirements such as (1) it can increase the brine diffusion rate as the concentration is low (2) it can keep the same diffusion rate however adverse effect to flora and fauna near the diffusers are low as the salt concentration is low (3) it can be sent back to the RO desalting process to increase the overall water recovery as the diluted brine is already pre-treated.

Most of the current seawater desalination plants have two-stage reverse osmosis (RO) processes. Therefore, the proposed FO systems utilize 1st stage RO concentrate (brine) as the draw solution (since osmotic pressure of brine is higher due to higher salinity) and pre-treatment sludge as feed solution (lower salt concentration). After passing through the FO system, as a consequence of water permeation from feed to draw solution, the pre-treatment sludge volume becomes lower and the brine gets diluted. Diluted brine can either be sent back to the 1st pass RO process to increase the overall water recovery or blended with the 2nd pass RO brine before being discharged to the ocean. By doing the latter, the diffusion rate of the brine within the water body can be increased.

In this study, laboratory experiments to assess the viability of applying the FO process for an RO desalination system at different sludge conditions (pH, temperature) were conducted. Further, biofilm growth on the membrane surface up to 8 weeks of continuous filtration was

analysed. In addition, mass balance calculations were used to predict the reduced sludge volume and power requirement arising from large scale (340 ML/day intake) and small scale (15 ML/day intake) hybrid FO/RO desalination plants.

The electrical conductivity (EC) of the brine and seawater EC were 73.0 mS/cm and 44.5 mS/cm, respectively. As EC is directly proportional to osmotic pressure, there was a sufficient osmotic pressure difference between the draw and feed solutions to have adequate water flux through the FO system. However, the total organic carbon (TOC) of the brine and sludge were 3.10 mg/L and 8.92 mg/L, respectively. Therefore, there is a potential for biofilm growth on the membrane surface. When the pH of feed solution was increased from 6 to 8, there was a marginal change in water flux. Therefore, the as is pH (normally pH 8) of feed solution is recommended for the hybrid system. When the temperature increased from 20 to 40 ^{o}C, the average water flux slightly increased (5.6 to 6.0 LMH). However, considering the economic benefits, it is recommended to operate at room temperature.

The water flux of continuous filtration experiments declined with time due to fouling as well as dilution of the draw solution. However, flux increased when the draw and feed solutions were replaced with the fresh solutions. This increased flux was lower than the initial flux of the previous batch and was due to fouling on the membrane. After one week of filtration, the flux declined further due to the thickened fouling layer deposited on the membrane. The layer may have contained microorganisms in addition to salt deposits as both draw and feed solutions contained salt ions. However, scanning electron microscopy (SEM) spectrum showed salt deposits on the membrane surface after 5 week of continuous filtration without cleaning in between. This fouling can easily be overcome by providing regular flushes at high cross flow velocities as deposited layers are thin and loose and therefore readily removed. After 8 weeks of continuous filtration large salt deposits were observed. Further, after 8 weeks there was no water permeation through membrane. After analysing SEM EDX images and spectra, weekly membrane cleaning is recommended to avoid biofouling and inorganic fouling.

After analysing water flux values and the fouling behaviour during FO filtration, mathematical modelling was carried out for the proposed RO/FO systems. Since, daily pre-treatment sludge generation varies (both in volume and solids content) with the desalination plant size, calculations were made for two plant sizes: large-scale plants (LSP, 340 ML / day intake) and small-scale plants (SSP, 15 ML / day intake). When the membrane area is 100 m^2 (minimum area considered in this study) it can reduce sludge volume up to 7% in a SSP, however this depends on the water flux through FO. When the membrane area increases, sludge volume reduction increases in both large and small scale plants. The sludge solids content can

be increased from 3 to 10% TS with a small power requirement (17.3 kW h /day). Interestingly, when the membrane area of a LSP is increased to 900 m^2, the sludge volume is reduced by 50%. This yields a sludge stream having a final solids content of 7.6%. Proposed system requires lower OPEX and CAPEX compared to existing system; however, they are marginal.

With all the results obtained through laboratory scale experiments and mathematical modelling, it is evident that the proposed hybrid system is a promising technology to reduce the volume of pre-treatment sludge and increase the overall water recovery of RO process.

Chapter 1: Introduction

1.1 Seawater Desalination Process

Seawater desalination is a good option to answer the fresh water demand faced by most of the arid regions in the world. Among the desalination processes available, seawater reverse osmosis (SWRO) is the well-known and most famous process which produces high quality product water with a lower production cost. Before passing through the RO process, seawater needs to be pre-treated to increase the productivity and life of the RO membrane by removal of foulants. Pre-treatment is done using conventional method (media filtration) or membrane technology (micro-filtration and ultra-filtration) where both methods generate pre-treatment sludge. Generated pre-treatment sludge volume is significant and it needs further volume reduction before sending to a landfill. Current option for sludge dewatering is mechanical treatment (such as centrifuging or belt presses) or evaporation ponds, which needs high operation and maintenance cost.

Following pre-treatment process, seawater is then passed through the reverse osmosis (RO) membrane where RO permeate is sent for post treatment, until it meets drinking water quality. Most of the current single stage RO units have around 50% water recovery. Therefore, a 100 ML / day plant produces only around 50, 000 m^3 of product water /day, where rest of the 50, 000 m^3/day (which is highly saline) needs to be disposed of as a waste stream. This waste water stream is called RO concentrate (ROC) and its salinity is nearly or more than twice the salinity of seawater. Therefore, proper disposing of the ROC, most commonly back into the ocean, is one of the areas needed research and development in the desalination industry. Because improper discharge of ROC back into the ocean is a threat for marine flora and fauna.

1.2 Can Forward Osmosis Give a Solution?

Therefore, this study focused on addressing above mentioned drawbacks namely, sludge volume reduction and ROC management, using the novel emerging Forward Osmosis (FO) membrane technology. FO drives using natural osmosis process. When two solutions which

have two different salinities are passed through a FO membrane, water will permeate from lower saline solution to higher saline solution due to the difference in osmotic pressure. However, due to the difference in salinity gradient some amount of salts will pass from higher to lower saline solution as well which is called reverse salt flux (RSF). RSF is one of the disadvantages in FO applications as it will reduce the quality of the lower salinity solution. FO has been used in lab scale and pilot plant scales for several applications, such as for diluting fertilisers, concentrating sugar solutions, in food processing applications to concentrate tomato, pine apple juices and dairy products and in pharmaceutical industry etc. However, no research has been carried out to reduce pre-treatment sludge volume in desalination using this novel technology.

1.3 Research Aims

Therefore, this study aimed to reduce volume of pre-treatment sludge using the FO technology. Since the FO process needs a higher salinity solution (termed draw solution) to draw water from lower saline solution (termed feed solution) and ROC was selected as the draw solution. Therefore, water will permeate from the feed solution (pre-treatment sludge solution) to ROC thereby reducing the volume of pre-treatment sludge and diluting the ROC stream. Hence, both sludge and ROC are benefited during the FO process. Sludge can undergo further treatment, if needed, before being sent to the landfill. In addition, ROC can either be return to the ocean in a higher diffusing rate as its concentration is much lower, or it can be sent back to the RO desalting process to increase the overall water recovery.

So, in this study a novel FO/RO hybrid process was proposed to reduce volume of pre-treatment sludge and to dilute the ROC. To check the feasibility of this proposed system laboratory experiments and mathematical modelling were carried out. Laboratory experiments were conducted to find the optimum water flux through FO membrane when sludge and ROC are used as feed and draw solutions. This was done by changing the sludge properties (pH, temperature, cross flow velocity, and solids content). Further, as membrane is susceptible to bio-fouling as sludge and ROC pass through the membrane, effect of bio-fouling on the membrane surface during long term filtration was analysed. Once the optimum experimental water flux through membrane was obtained, the value was applied for the mathematical modelling of the proposed system to check the applicability of the hybrid system in terms of

increase in water recovery, sludge volume reduction and brine dilution. In addition, CAPEX and OPEX cost for the proposed systems were calculated and compared with the existing systems.

1.4 Research Questions

1. How can we apply FO technology economically to address the bottlenecks in RO desalination? Can the existing systems be retrofitted with FO?
2. What are optimum process conditions to have a higher water flux through flat sheet FO membrane?
3. How will the FO membrane withstand bio-fouling when sludge and ROC are passed through the membrane?
4. Will hollow fibre membranes perform better than flat sheet membranes in the presence of pre-treatment sludge and ROC?
5. How can we characterise the FO membrane in terms of effective diffusion coefficient to answer the theoretical lag in the literature?

1.5 Summary of the Thesis Structure

This thesis consists of nine chapters (Figure 1) where ninth chapter contains the overall conclusion of this work and recommendations for future work. Chapter 2 explains the literature behind the SWRO and FO. Theory related to FO technology is explained in detail. In Chapter 3 experimental procedure will be explained including the materials and the analytical methods used.

Chapters 4 to 8 contain the results obtained during the laboratory experiments and mathematical modelling as shown in Figure 1. FO membrane was characterised in terms of diffusion and the experimental results and modelling calculations are explained in Chapter 4.

Chapter 5 details the results for the water flux optimisation experiments with comprehensive discussions. This chapter contains the results with flat sheet cellulose tri acetate (CTA) membranes and the impact of pH, cross flow velocity and temperature of the sludge on the water flux.

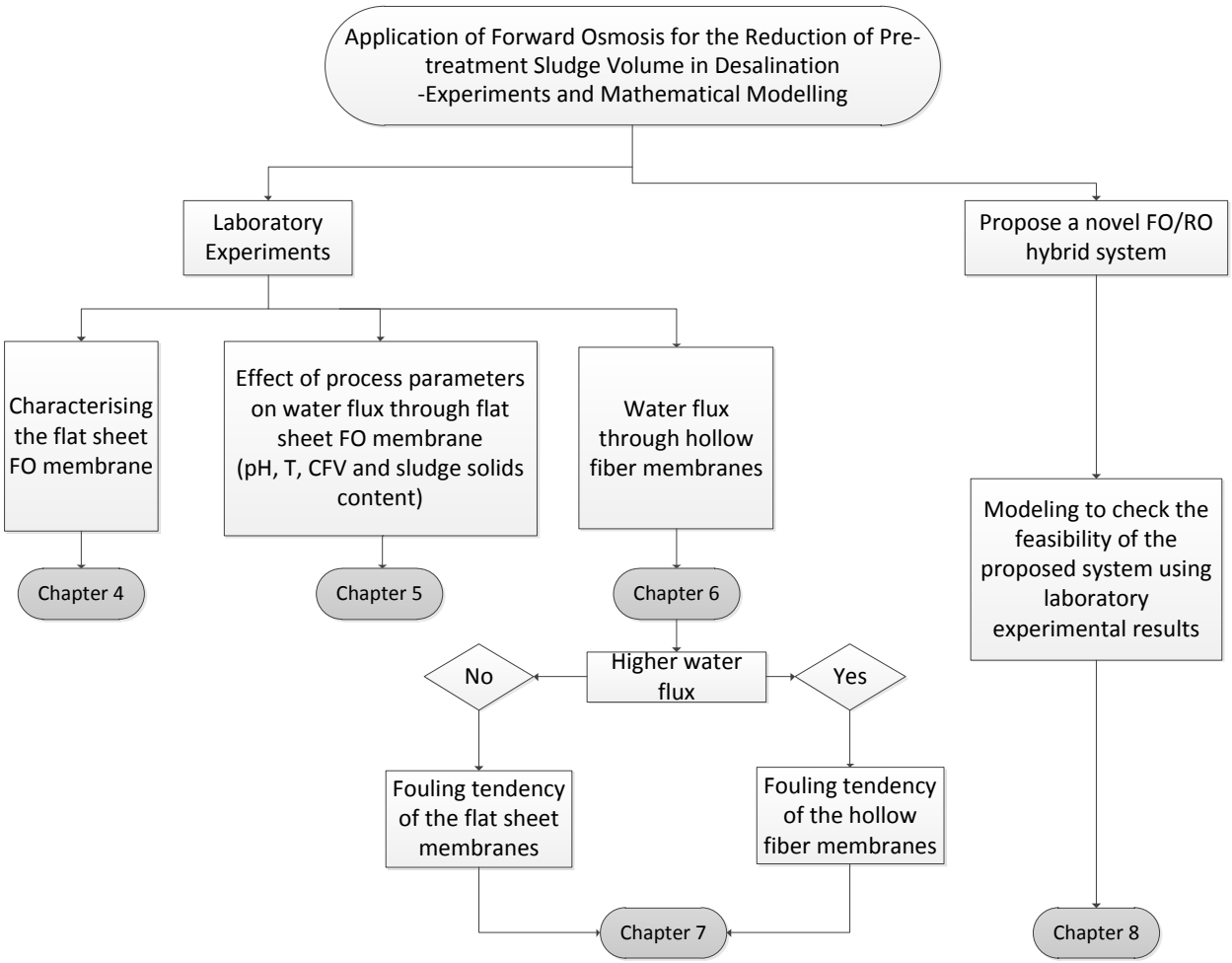

Figure 1: Research plan and thesis outline

Chapter 6 contains the water flux optimisation results with discussion for polyamide hollow fibre membranes. Reynolds number of the feed and draw solutions were varied to optimise the water flux. At the optimum process flow conditions, sludge and brine were run at different sludge solids conditions.

Chapter 7 consists of the results on the fouling behaviour of CTA flat sheet membranes. Continuous filtration experiments were run and the filtered membrane coupons were analysed for any susceptibility to bio fouling.

Finally, mathematical modelling was applied to the proposed FO/RO hybrid system and is given in Chapter 8. This chapter includes the mass and salt balance calculation with cost calculations. Maximum experimental water flux obtained was used for the calculations.

Conclusions from each Chapter (from 4 to 8) and future recommendations are given in Chapter 9.

Chapter 2: Literature Review

2.1 Seawater Desalination

Desalination, removal of salt and minerals from seawater, brackish water and wastewater effluent, is becoming one of the promising solutions for increasing fresh water demand in the world. In 2005, approximately 98% of domestic water supply in UAE was satisfied by desalted water (Mohamed et al., 2005). Hoang et. *al* (2009) predicted that seawater desalination capacity in Australia will increase to over 450 GL/year by 2013 (Hoang et al., 2009). This is 10 times larger compared to the capacity in 2006. There are two types of desalination processes available to date, *viz* phase change process which includes multistage flash (MSF), multiple effect distillation (MED) and vapour compression (VC) and membrane process which includes reverse osmosis (RO) and electro-dialysis reversal (EDR). Table 1 illustrates installed capacity, unit cost, water recovery and energy demand of the available desalination processes.

Table 1: Desalination capacity, unit cost, energy demand and recovery of available large scale desalination processes (Greenlee et al., 2009, Blank et al., 2007a, Karagiannis and Soldatos, 2008, Semiat, 2008, Wittholz et al., 2008).

Desalination process	Worlds' installed desalination capacity[1] (%)	UPC[2] (US$)	Combined energy demand[3] (kW h_e /m^3)
MSF	40	0.62-1.97	10-16
MED	3	0.60-1.17	6-12
VC	5	Only small scale plants are available.	
RO	44	0.45-0.95	3-6
ED	6	Only small scale plants are available.	

[1] as at 2002; 2% use desalination processes other than mentioned.

[2] $UPC = Unit\ Production\ Cost = \frac{\left(Capital\ Cost / Plant\ life\right) + Annual\ Operating\ Cost}{Plant\ Capacity \times Plant\ Availability}$

[3] equivalent energy (for heat and electricity requirements) in terms of electrical energy

From the total installed production capacity, seawater desalination plant capacity is nearly 59%. Current seawater RO (SWRO) plants consume around 3-6 kW h electricity to produce one cubic meter of product water. Phase change processes are more expensive as large amount of energy is required. Energy demand for MSF and MED processes are 10-16 and 6-12 kW h/ m^3, respectively. Water unit production cost (UPC) using MSF and MED processes are 0.6 - 1.97 US$ and 0.60 - 1.17 US$ respectively. Interestingly, UPC for RO is 0.45 - 0.95 US$ with a combined energy demand (demand for both heat (thermal) and electricity (pumping) requirements) of 3 - 6 kW/h. The production costs significantly vary with the plant capacity. Obviously, large scale desalination plant water cost is comparatively smaller. Water recovery from single stage RO process lies from 40-60%.

Out of all the discussed desalination processes, RO has the most potential and robust technology for large scale seawater desalination since it produces well purified water with a lower unit product cost (Nooijen and Wouters, 1992, Ebrahim and Abdel-Jawad, 1994, Abou Rayan and Khaled, 2003, Semiat, 2008, El-Sadek, 2010) as well as is simpler to operate and maintain compared to other desalination processes (Misdan et al., 2012). Coupled with lower unit product cost and lower energy demand, refer Table 1, global SWRO production capacity has increased drastically in few years' time. As per Table 1, desalination production capacity using RO process technology in the world is 44 % , (Greenlee et al., 2009) and it is used by majority of Australian desalination plants (Hoang et al., 2009). A list of large scale SWRO plants available in Australia is given in Table 2.

Table 2: Large scale desalination plants available in Australia (Palmer, 2012)

Location	**Owner**	**Process**	**Capacity (MLD)**	**Status**	**Completion date**
Kwinana, WA	WCWA	MMF/RO	145	Operating	2006
Bunbury, WA	WCWA	UF/RO	150	Operating	2011
Karratha, WA	CITIC Iron	UF/RO	175	Planning	2012
Adelaide, SA	SA Water	UF/RO	300	Operating	2011
Whyalla, SA	BHP Blliton	-	280	Planning	2014
Wonthaggi, VIC	DSE	MMF/RO	450	Operating	2012
Kurnell, NSW	Sydney Water	MMF/RO	250	Operating	2010
Gold coast, QLD	SEQ Water	MMF/RO	125	Operating	2009

All the large scale plants are currently in operation or planning. All these large scale plants use RO technology. Opportunely, large scale RO plants have the highest potential for further improvements compared to other available processes (Blank et al., 2007a).
RO membrane technology employs semi permeable membranes which allow saline water to separate into two streams; (1) Permeate - purified water that passes through the membrane and (2) RO concentrate (ROC) or brine - which contains concentrated salts and other minerals.

However, the source water needs to undergo several treatment processes before and after RO membrane treatment in order to make SWRO process economical and environmentally friendly. Thus, a typical SWRO plant could be divided into five major steps (Figure 2);

1. Intake,
2. Feed water pre-treatment,
3. High pressure pumping,
4. Membrane separation (or desalting process)
    a. Performance of membranes,
    b. Concentrate disposal/resource recovery, and
5. Product Quality

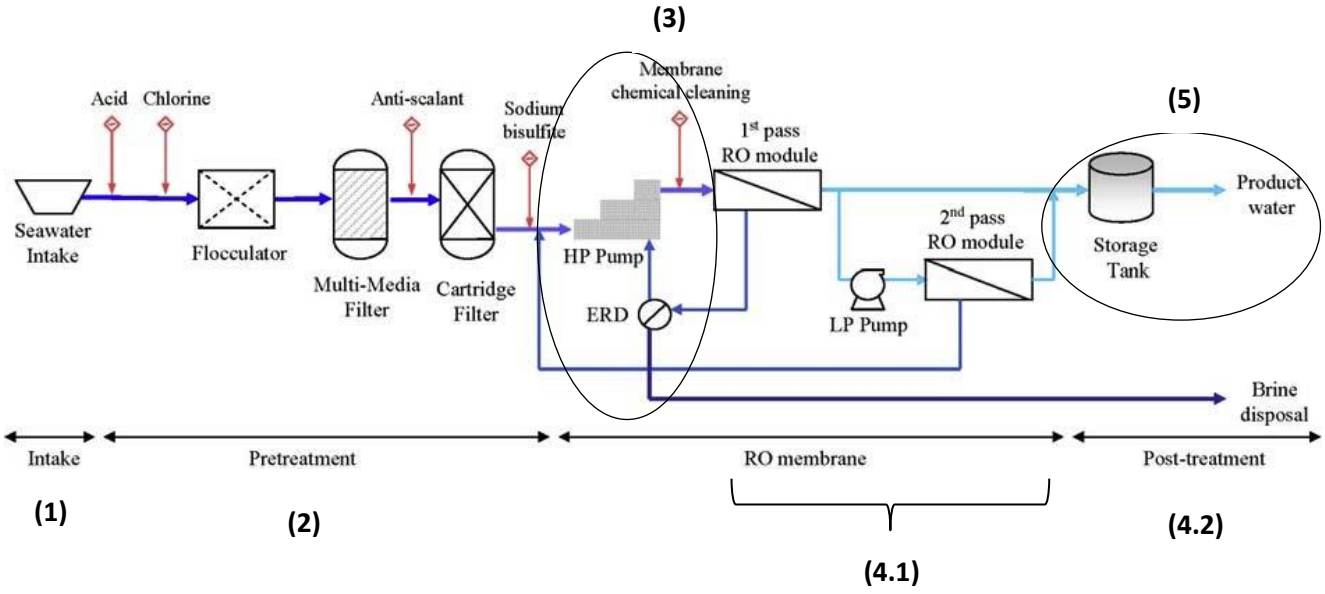

Figure 2: Schematic of a typical SWRO plant (Kim et al., 2009), where ERD, HP and LP denote energy recovery device, high pressure and low pressure, respectively.

During this PhD study, problems encountered in each step were surveyed. Furthermore, existing solutions and drawbacks of them were comprehensively discussed. In addition, solutions for the current drawbacks were suggested and highlighted the mandatory research areas in seawater desalination. These outcomes were published as a review paper entitled ***Problems in seawater industrial desalination processes and potential sustainable solutions: a review*** in the journal of Reviews in environmental engineering and bio/technology (Liyanaarachchi et al., 2013). Table 3 summarises the published/reported issues in each process with existing solutions and suggestions.

Table 3: Key issues in seawater desalination, current solutions and suggestions for drawbacks (Morton et al., 1997, Latorre, 2005, Mohamed et al., 2005, Jacob, 2007, Tularam and Ilahee, 2007, Vedavyasan, 2007, Sarp et al., 2008, Agus et al., 2009, Jeppesen et al., 2009, Martinetti et al., 2009, Ji et al., 2010, NCED, 2010, VOLLPRECHT, 2013, Liyanaarachchi et al., 2013).

SWRO step	Associated problems	Existing Solutions	Essential study areas
Intake	1. Rust and valve problems 2. Entrainment and Impingement of small marine organisms 3. Threat to marine environment as pipe lines acts as artificial reefs 4. Pipe lines disturb the seafloor; surf zone hence changes coastal hydrology.	1. Shock chlorination to remove entrained marine organisms in intake pipes. 2. Use corrosion resistant pumps	1. Development of higher corrosion resistant piping materials/coating materials, valves. 2. Alternative for shock chlorination. 3. Proper intake systems in a way that it minimizes disturbing coastal hydrology.
Pre-treatment (Low Pressure Membrane)	1. MF-UF cleaning (Cost of cleaning exceeds cleaning costs associated with RO membranes) 2. Replacing and transportation cost (increase the cost of water production) 3. MF-UF cartridge discharge.	1. Land disposal.	1. Alternatives for UF/MF (current ISI[1] research) 2. Conventional pre-treatment with novel chemicals 3. Development of longer life cartridge filters (NCED suggestion and Siemens carrying out a research)
Pre-treatment (chemical)	1. Pre-treated sludge disposal. 2. Amount of sludge generated. 3. Higher chemical usage.	1. Landfill disposal.	1. Alternative coagulants for sludge reduction 2. Recycling of ferric sludge 3. Sludge volume reduction (*this study*).

Table 3 (continued): Key issues in seawater desalination, current solutions and suggestions for drawbacks continued *(Morton et al., 1997, Latorre, 2005, Mohamed et al., 2005, Jacob, 2007, Tularam and Ilahee, 2007, Vedavyasan, 2007, Sarp et al., 2008, Agus et al., 2009, Jeppesen et al., 2009, Martinetti et al., 2009, Ji et al., 2010, NCED, 2010, VOLLPRECHT, 2013).*

SWRO step	Associated problems	Existing Solutions	Essential study areas
High pressure pumping	1. Corrosion in pumps. 2. Carbon emission from the desalination plant.	1. Offset with renewable energy. 2. Use corrosion resistant pumps.	1. Use of alternative membranes such as lower hydraulic pressure membranes. 2. Corrosion resistance coating to pumps.
Membrane separation	1. Brine disposal on land has a significant adverse effect on aquifer. 2. Brine discharge to sea cause impacts on marine fauna and flora. 3. Low water recovery (30-50%). 4. RO fouling (Chemical cleaning agents increase the cost of water production). 5. Disposal of used RO.	1. Concentrated brine diffuses to land or sea. 2. Metal recovery before discharging (research stage). 3. High recovery of RO brines using FO and membrane. distillation (research stage) 4. Alternative membranes (e.g. FO still in research stage).	1. Reduce brine volume. 2. Brine management guidelines (current ISI[1] research). 3. Improvements in high recovery. 4. Development of better membranes. 5. Proper pre-treatment methods. 6. Assessment of alternatives to disposal of used RO membranes (current ISI[1] research).
Product quality	1. Higher concentration of Br^- in product water. 2. Treatment of Br^- and I^- (DBFs). 3. Boron removal.	1. Boron removal using ion exchange, multi stage RO, EDR, and electro-coagulation.	1. Proper boron removal method. 2. Proper guidelines for limits.

[1]*ISI -Institute for Sustainability and Innovation, Australia*

As Table 3 explains, pre-treatment sludge and ROC management needs more attention. During this PhD study, application of FO as a solution to sludge and ROC management was studied. Therefore, among five major SWRO processes, pre-treatment process and RO membrane desalting process were selected to explain in detail in this dissertation.

2.1.1 Feed Seawater Pre-treatment

Pre-treatment is the most important part in SWRO as it will lead to the reduction in membrane fouling, higher recovery, longer membrane life and higher quality product water. Intake seawater is pre-treated to filter debris, suspended particles, dissolved organics, and micro-organisms providing significant operational benefits such as lower RO replacement rates and reduced backwash frequencies. Pre-treatment methods may vary depending on the influent water qualities such as suspended solids (SS) concentration and Silt Density Index (SDI), investment cost, and environmental impact assessments. Table 4 shows characteristics of intake seawater at Perth Seawater Desalination Plant (PSDP), Australia (VOLLPRECHT, 2013). Drawing water typically contains 35,000 - 37,000 mg/L salinity and at this particular day it was 36,500 mg/L.

Blank et al (2007) have summarised most areas needing R&D in each large scale desalination process. According to their report, pre-treatment is one of the areas needing the most R&D in large scale RO desalination process (Blank et al., 2007a). Intake seawater is being pre-treated using either (1) chemical treatments (conventional coagulation and filtration) and/or (2) low pressure membrane treatment (Microfiltration / Ultrafiltration). Conventional pre-treatment needs more space and improved sludge management options, but requires lower investment cost and lower energy requirements compared to low pressure membrane treatment (NCED, 2010). A surface seawater SDI of 13-25 was reduced to below 1 through ultrafiltration pre-treatment whereas conventional pre-treatment failed to reduce SDI below 2.5 (Brehant et al., 2002). Even though SDI below 3 is typically acceptable for RO systems, much lower SDI reduces the RO flushing frequency required (Kremen and Tanner, 1998). RO cleaning frequency with conventional pre-treatment (coagulation + 2 stage sand filtration) is 4-12 times per year whereas only 1-2 times per year with UF membrane pre-treatment (Kim et al., 2009).

Table 4: Intake seawater properties as at July 2012 at Perth Seawater Desalination Plant (PSDP) (VOLLPRECHT, 2013)

Parameter	**Concentration (mg/L)**
pH	8.17
Conductivity at 25 ^{o}C	5100 mS/m
Total filtered solids	36500
Suspended solids	30
Total alkalinity	116
Alkalinity as HCO_3	139
Carbonate	<1
Calcium – unfiltered	420
Magnesium—unfiltered	1342
Hardness as $CaCO_3$	6590
Aluminium—unfiltered	<0.16
Manganese– unfiltered	<0.04
Potassium– unfiltered	175
Sodium– unfiltered	11300
strontium– unfiltered	7.5
Boron– unfiltered	4.9
Sulphate– unfiltered	2889
Sulphur– unfiltered	964
Barium– unfiltered	<0.004
Silicon (as SiO_2) by DA	<0.2
Nitrogen-Ammonia	<0.005
Nitrogen -Kjeldahl	<0.02
Nitrogen -NO_2+NO_3	0.010
Nitrogen -NO_2	<0.002
Nitrogen -NO_3	0.010
Total Nitrogen	<0.02
Total Iron	<0.06
Phosphorous- Total	0.016
Chloride	20510
Bromide	72.6
Fluoride	0.70
Total organic carbon (TOC)	0.9

In general, chemical pre-treatment is most often used technique in current operating SWRO plants (Hoang et al., 2009). Large scale SWRO plants (Perth plant in Austarlia and worlds' largest desalination plant, Fujairah, UAE plant which produce 144 ML/day and 170 ML/day, respectively) pre-treat their seawater using chemical treatment methods. Perth plant's process flow diagram is given in Figure 3. Furthermore, among 32 desalination plants surveyed by CSIRO, Australia, approximately half of plants use conventional pre-treatment options (Hoang et al., 2009). $FeCl_3$, $FeSO_4$ and Alum are the commonly used coagulants and additional chemicals as coagulant aids, disinfectors and scaling control agents are used.

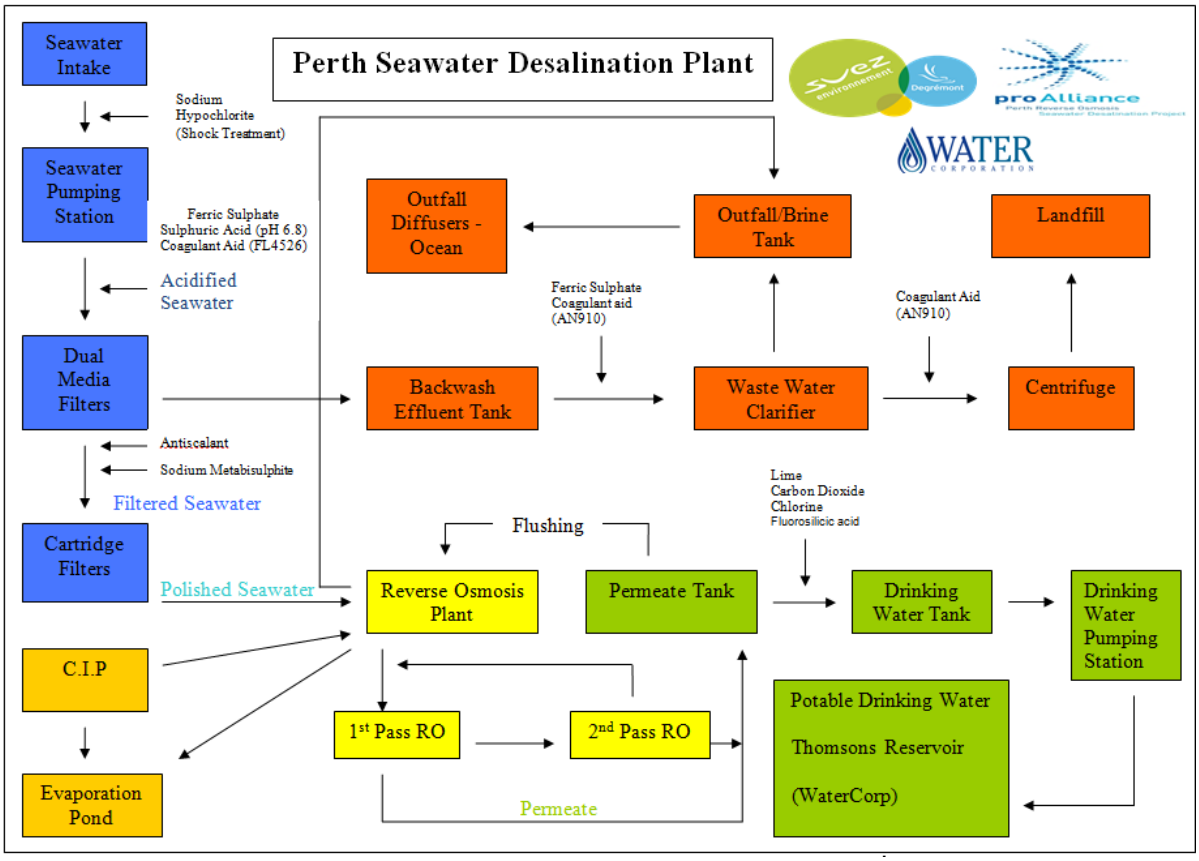

Figure 3: Process flow diagram of Perth Seawater Desalination Plant (PSDP)(VOLLPRECHT, 2013).

Generated sludge needs to be disposed in a way that it minimizes the negative effects to the environment. However, major issue in sludge management is transportation and disposal which takes more than 75% of total sludge treatment O&M cost (VOLLPRECHT, 2013). Figure 4 shows a cost analysis for sludge treatment (these values have calculated considering one specific day at the Perth desalination seawater desalination plant). Chemicals and power take only 1.9% and 1.4% of the total operation and maintenance (O&M) cost, respectively. Transportation and disposal take 18.4% and 78.3%, respectively, which is significantly a higher amount. Therefore, it is evident that reduced sludge volume could significantly reduce transportation and disposal expenses associated with chemical treatment method.

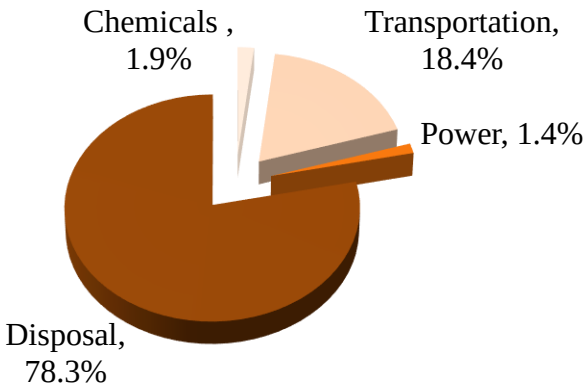

Figure 4: Sludge treatment operating and maintenance cost analysis at PSDP (VOLLPRECHT, 2013).

2.1.2 Desalting Process

RO membrane separates pre-treated seawater into two streams; permeate and RO concentrate (ROC) under a hydraulic pressure higher than the osmotic pressure, and therefore has a higher energy requirement (65-85%) compared to other SWRO steps (Refer Table 5). Permeate requires further treatment before distribution to communities. ROC needs further management options before discharge. Properties of permeate and ROC depend on the performance of membrane unit. Membrane fouling, which leads to poor membrane performance, is the major factor that limits use of RO technology to treat seawater (Luo and Wang, 2001).

At present, ROC is discharge back to the sea (diffuses at a specific rate at which they get blend with seawater), land (ground infiltration, evaporation basin, discharge to beach, Zero Liquid Discharge (ZLD)) and dispose to sewer lines (Morton et al., 1997, Ahmed et al., 2001, Sadhwani et al., 2005). Evaporation ponds and ZLD (brine concentrators) are the most expensive options due to statutory groundwater regulations and energy requirements, respectively (Greenlee et al., 2009). Post treatment of ROC take up a significant percentage of the total cost of desalination. Therefore, recent research has been focused on reducing ROC volume which will reduce the operational and maintenance cost. Brine volume can be reduced by further concentrating it (Martinetti et al., 2009), applying alternative membranes for RO (Elimelech, 2007) and increasing recovery of RO unit. Currently, these options have attracted a lot of research interest and pilot scale plants have been used. ROC disposal on land has a significant adverse effect on aquifer (Mohamed et al., 2005). On the other hand by discharging

back to the sea there can be impacts on marine fauna and flora (Latorre, 2005), and algae formation near the beach (Ahmed et al., 2001). Many of the Disinfection By-products (DBPs) formed during pre-treatment and post treatment (a result from reactions between organic and inorganic matter in water with chemical disinfection agents such as bromide, ozone, Cl_2 etc) will be discharged with the ROC and they could affect marine ecosystems if they are not diluted sufficiently after discharge (Agus et al., 2009). On the contrary, after monitoring four years continuously, Western Australia University's Palmer reports that (Palmer, 2012) there is not any impact on marine fauna and flora. However, there could be an impact on the marine system as Palmer, 2012 reports only from a short period research. Therefore, implementing national/global level guidelines and standards for seawater ROC discharge (either to sea or land) would be a better initiative to control impacts on environment.

Table 5: Percentage cost and specific energy comparison at each SWRO step (Wilf and Klinko, 1998, Dreizin, 2006, Semiat, 2008, Charcosset, 2009, WaterReuseAssociation, 2011)

SWRO step	Cost/ total water price	Specific energy (kW h_e^*/m^3 of product)	Energy / total power requirement (%)
Intake		0.79[1]	
Pre-treatment	4.1% (chemicals)		8-12%
Conventional		0.07[2]	
Membrane		0.10[2]	
High pressure pumping	25.4% (energy)	2.83[3]	65-85%
Desalting process	5.4%		
Post treatment	1.8%		< 2%

**e*-electric , [1] (intake + raw water supply + feed booster), [2] kWh/m^3 of effluent, [3] (pumps + turbine + motors + auxiliary + lighting)

2.1.2.1 Brine management

Brine has high salinity value depending on the recovery rate of the RO unit and is sent for further treatment before being discharged to a land or to a water body. Generally, the TDS of the brine will be double the value of seawater (source) however will depend on the recovery of RO. Concentrated brine has TDS values of more than 65, 200 mg/L. Figure 5 shows the process flow diagrams of two SWRO plants namely, Eni Gela plant and Fujairah plant.

(a)

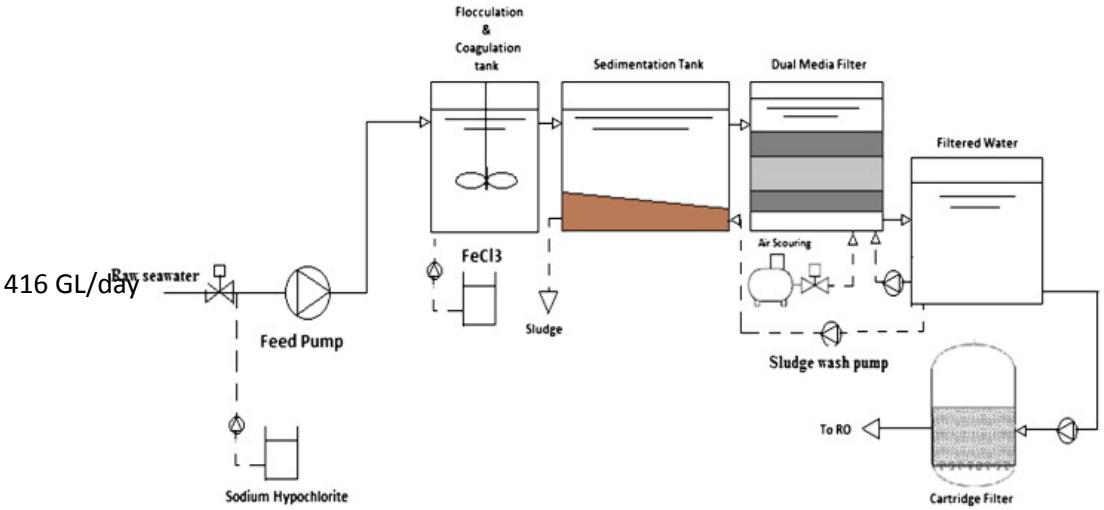

(b) (c)

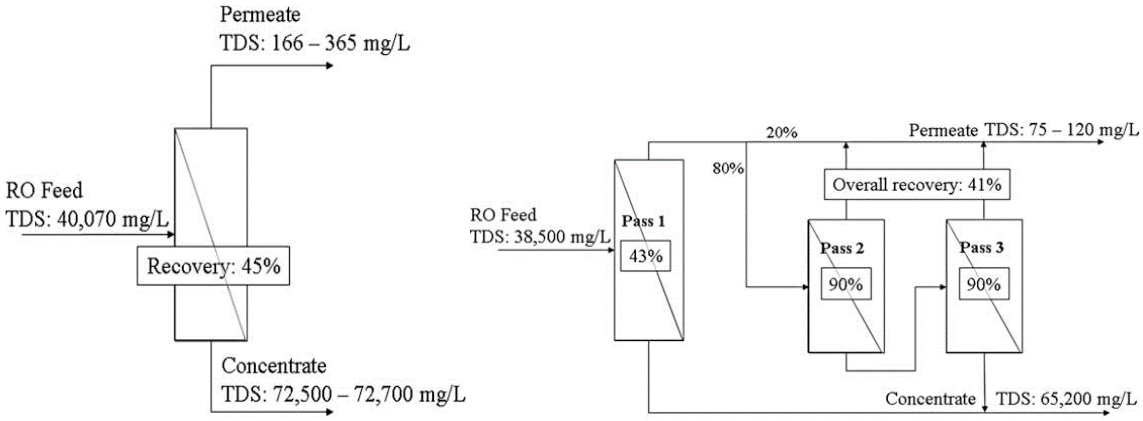

Figure 5: (a) Schematic of current conventional pre-treatment of Fujairah SWRO desalination plant (Al-Sarkal and Arafat, 2013); Process flow diagram of (b) one-stage SWRO plant in Eni Gela, Sicily and (c) two - stage SWRO plant in Fujairah, UAE.

Currently, brine from most SWRO plants is discharged back to the sea (diffused at a specific rate at which they get blended with seawater (Water-Technology.net, 2013, Ahmed et al., 2001)) or to the land (ground infiltration, discharge to beach (Ahmed et al., 2001). Solar evaporation (Greenlee et al., 2009), wind aided intensified evaporation (has been only demonstrated at laboratory scale (Katzir et al., 2010), spray irrigation (Sethi, 2006)) and disposal to sewer lines (Morton et al., 1997, Ahmed et al., 2001, Sadhwani et al., 2005), zero liquid discharge (Greenlee et al., 2009) are other options for brine management. Evaporation

ponds and zero liquid discharge (brine concentrators) are the most expensive options due to statutory groundwater regulations and energy requirements, respectively (Greenlee et al., 2009, Sethi, 2006). From a survey of 137 drinking water plants which are having capacity of greater than 98 m3/day, brine disposal methods have been divided as shown in Figure 6 (Ahmed et al., 2001).

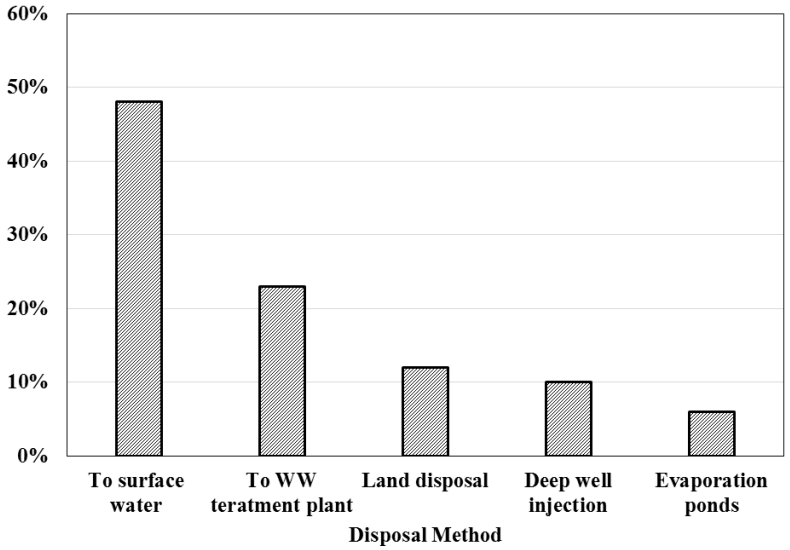

Figure 6: Brine disposal methods from a survey (Ahmed et al., 2001).

Post treatment of brine takes up 5-33% of the total cost of desalination (Ahmed et al., 2001). Therefore, recent research focuses on reducing brine volume which will reduce the O&M cost. Brine volume can be reduced by further concentrating (Martinetti et al., 2009) (using membrane distillation or electro-dialysis, recovering commercial products (Jeppesen et al., 2009)), applying alternative membranes for RO and increasing recovery of RO unit. Water recovery of single stage RO process lies between 40-60%. As Figure 6 depicts the recovery of RO process at single stage Eni Gela plant and two-stage Fujairah plant to be 45% and 41 % respectively. Hence, increase in water recovery would undoubtedly reduce the volume of concentrate. However, when the volume is less, concentration of minerals and chemicals are higher. This can cause more negative issues since many disposal regulations are based on concentrations but not on volume (Ahmed et al., 2001). Further, SWRO plants are based near beaches and major brine disposal method is diffusing it back to the sea. Therefore, if the brine is discharged back to sea, having lower concentrations is an added advantage. Main advantage

would be the rapid rate of diffusion/dispersion. Therefore, this study focuses on brine management while reducing the volume of sludge of the SWRO process.

2.1.3 Future Perspective

Forward Osmosis (FO) is a novel emerging technology which could possibly support and improve the SWRO process by increasing water recovery. FO is being used in desalination industry to concentrate the brine (Martinetti et al., 2009), to replace the second stage of two staged RO system etc. However, this technology is still in laboratory scale and pilot plant scale (McCutcheon and Elimelech, 2006, Elimelech and Phillip, 2011) due to various disadvantages compared to RO such as significantly lower flux, higher reverse salt flux, and complexity of regeneration of draw solution from product water. Therefore, much research is being conducted on application of FO in SWRO and this is a competitive research area to date in the field of desalination.

Next section of this literature review comprehensively explains the theory behind FO technology and its applications and limitations.

2.2 Forward Osmosis (FO) Technology

Osmotically driven membrane process, Forward Osmosis (FO) or Pressure Retarded Osmosis (PRO), is a promising technology which is being used in different pure water separation, diary, food processing and pharmaceutical applications. When a diluted solution and a concentrated solution are separated by a semi-permeable membrane, water permeates through the membrane from diluted solution to the concentrated solution due to the difference in water chemical potential (osmotic pressure). Consequently, diluted solution (known as feed) gets concentrated whereas concentrated solution (known as draw) gets diluted. The driving force for the water permeation is the osmotic pressure difference between the two solutions and this phenomenon is called osmosis. However, due to the concentration gradient between feed and draw solutions, there is an unwanted salt flux from draw to feed solutions, which is known as reverse salt flux (RSF).

2.2.1 Theoretical background of FO

Osmotic pressure (π) is the pressure which, if applied to the more concentrated solution, would prevent transport of water across the membrane (Cath et al., 2006). Figure 7 shows osmotic pressures of few selected salt solutions, obtained using OLI Stream Analyser® software. Osmotic pressure of a solution is a function of its concentration; the higher the concentration the higher the osmotic pressure. At present, $MgCl_2$ has the highest osmotic pressure at a similar concentration compared to other available potential salt solutions.

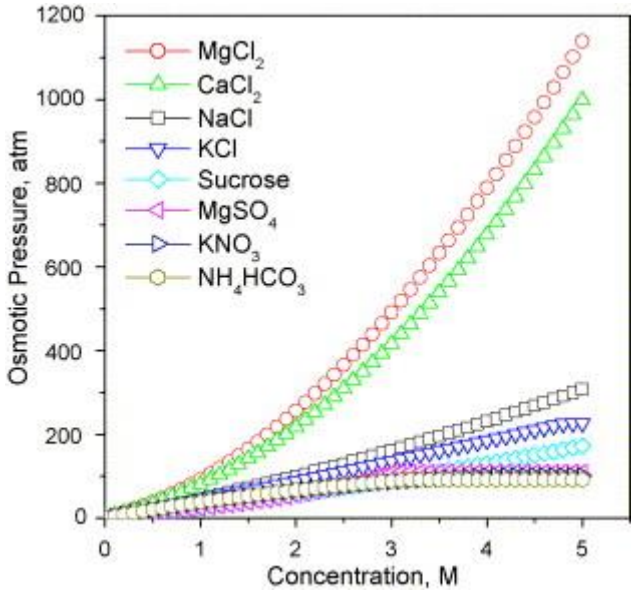

Figure 7: Osmotic pressure as a function of solution concentration at 25°C (Cath et al., 2006).

Figure 8 shows the water permeation through membrane during Forward Osmosis (FO), Pressure enhanced Osmosis (PEO), pressure retarded osmosis (PRO) and RO. Water flux direction is from lower concentration solution to the highly-concentration solution for FO, PRO and PEO. However, in RO water flux is from the highly-concentrated solution due to applied pressure, which is significantly higher than osmotic pressure.

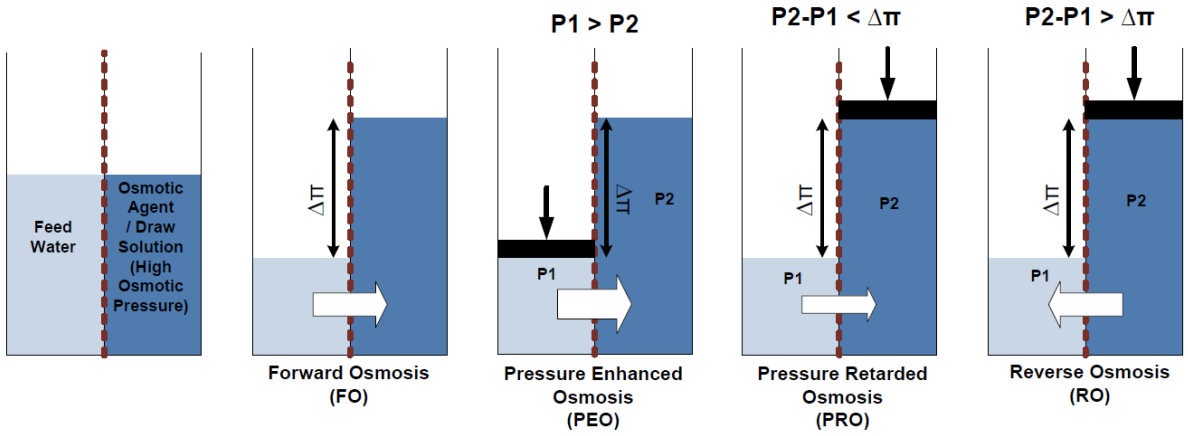

Figure 8: Different osmosis processes (Nicoll).

The general equation describing water transport through FO, RO, PEO or PRO is given by:

$$J_w = A(\sigma\Delta\pi - \Delta P) \qquad (1)$$

Where, J_w is the water flux, A, σ, $\Delta\pi$ and ΔP are water permeability coefficient of the membrane, reflection coefficient, osmotic pressure difference and applied pressure, respectively. For RO, $\Delta\pi < \Delta P$ and for PRO $\Delta\pi > \Delta P$. But for FO operations, ΔP is zero as FO operates with no applied pressure but with natural osmotic pressure difference.

Let's consider FO operation. One would expect to have a water flux through the FO membrane as explained by basic water transport equation (1):

$$J_w = A\sigma\left(\pi_{D,b} - \pi_{F,b}\right) \qquad (2)$$

Where $\pi_{D,b}$ and $\pi_{F,b}$ are bulk osmotic pressure of draw solution and bulk osmotic pressure of feed solution, respectively.

However, in real applications membranes do not perform perfectly. Often, we get lower water flux than theoretical value as effective osmotic pressure difference is lower than expected. This lower than expected osmotic pressure difference is due to salt leakage from highly concentrated solution to lower concentrated solution, simply from draw solution to feed solution (Hancock and Cath, 2009, K.L et al., 1981) as well as due to the concentration polarisation (CP) effect. CP can affect internal to the membrane (ICP), that is in the porous support layer of the membrane or externally (ECP), that is on the surface of the membrane. Figure 9 shows the schematic representation of ECP and ICP effects when membrane filtration happens in active layer - facing draw solution (AL-DS) and active layer - facing feed solution (AL-FS) modes.

$C_{D,b}$ and $C_{F,b}$ are the salt concentration of the bulk feed solution and bulk draw solution and $C_{D,m}$ and $C_{F,m}$ are salt concentration near the membrane surfaces of draw and feed sides. $C_{D,i}$, and $C_{F,i}$ are the salt concentrations of draw and feed solutions respectively at the porous and dense layers' interface.

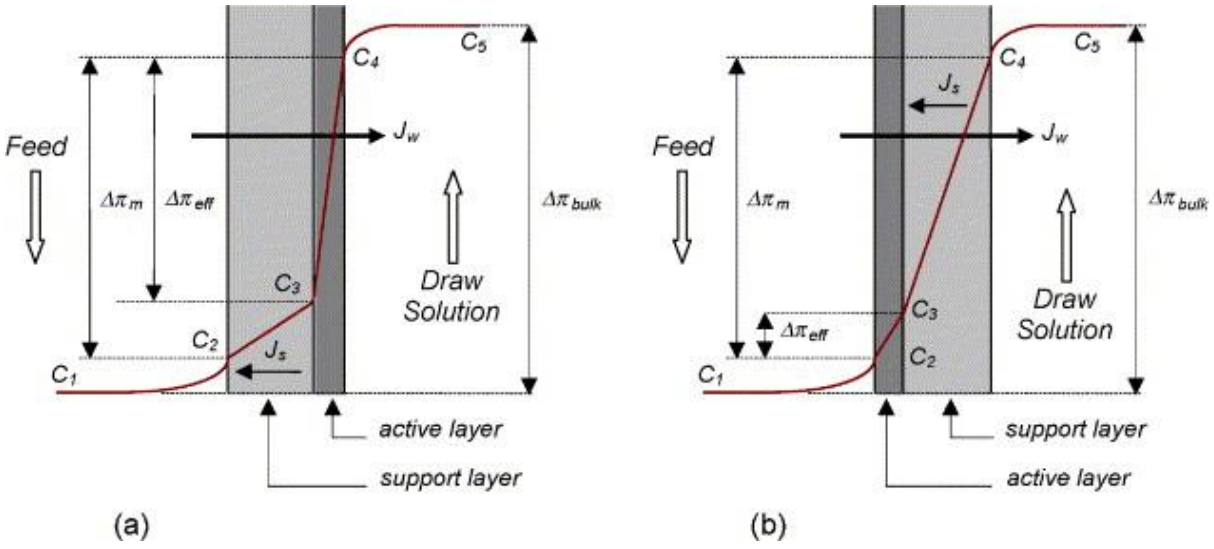

Figure 9: Schematic representation of external and internal concentration polarisation (ECP and ICP) effect across FO membrane during water permeation. Figure adapted from (Cath et al., 2006).

As Figure 9 depicts, due to ICP and ECP effects on the sides of the membrane, effective osmotic pressure (which is directly proportional to the concentration) drives the water flux less than expected. Therefore, corresponding water flux considering this ECP and ICP effects is given by:

$$J_w = A\sigma(\pi_{D,m} - \pi_{F,i}) \qquad (3)$$

Where, $\pi_{F,i}$ is the osmotic pressure at the active dense layer and support porous layer interface. However, $\pi_{F,i}$ and $\pi_{D,m}$ cannot be measured or predicted.

From theory, $\pi_{D,m}$ can be expressed as follow:

$$\pi_{D,m} = \pi_{D,b} \exp\left(\frac{-J_w}{k_D}\right) \qquad (5)$$

Similarly, $\pi_{F,i}$ can be expressed as follow:

$$\pi_{F,i} = \pi_{F,b} \exp(K_f J_w) \qquad (6)$$

Where,

k_D = mass transfer coefficient in the draw solution side and

K_f = solute resistivity for diffusion within the porous support layer

Therefore, substituting (5) and (6) in equation (4), water flux through FO dense layer is given by:

$$J_w = A\left[\pi_{D,b} \exp\left(\frac{-J_w}{k_D}\right) - \pi_{F,b} \exp(J_w K)\right] \qquad (7)$$

When the feed solution is in contact with the support layer of the membrane, the mode of filtration is called PRO mode or AL-DS mode and when it is in contact with the active layer of the membrane, the mode of filtration is called FO mode or AL-FS mode. Thus, Eq. (7) is applicable for PRO mode. For FO mode, water flux through FO dense layer is given by:

$$J_w = A\left[\pi_{D,b} \exp(-J_w K_D) - \pi_{F,b} \exp\left(\frac{J_w}{k_f}\right)\right] \qquad (8)$$

k_f = mass transfer coefficient in the feed solution side and

K_D = solute resistivity for diffusion within the porous support layer

Solute resistivity K is defined as:

$$K = \frac{t\tau}{\varepsilon D_s} \qquad (9)$$

Where, t, τ and ε are membrane thickness, tortuosity and porosity, respectively. D_s is the solute diffusion coefficient (K.L et al., 1981) of a single solute. Larger K values are

associated with more severe ICP effect (Cath et al., 2006). S is called the structural constant and is defined as:

$$K\,D_s = \frac{t\tau}{\varepsilon} = S \qquad (10)$$

Obtaining parameters in flux models

Further Leob et. al (Loeb et al., 1997) have derived an equation to determine K:

$$K = \left(\frac{1}{J_w}\right)\ln\frac{B + A\pi_{D,b}}{B + J_w + A\pi_{F,m}} \qquad (10)$$

Where, B is salt permeation coefficient. A and B can be obtain using RO type experiments. A can be obtained from equation (1) and if salt rejection in RO is denotes by R, B is related to R by:

$$B = \frac{A(1-R)(\Delta P - \Delta\pi)}{R} \qquad (11)$$

The parameter K can be obtained from FO type experiments where applied pressure is zero. If pure water is used in feed side $\pi_{F,b}$ is equal to zero. If the osmotic pressure of the draw solution is known, , K can be obtained following equation (K.L et al., 1981):

$$K \sim \frac{A\pi_{D,b} - J_w}{BJ_w} \qquad (12)$$

Mass transfer coefficient k is given by:

$$k = \frac{Sh\,D}{d_h} \qquad (13)$$

Where,

$$Sh = 1.85\left(Re\,Sc\frac{d_h}{L}\right)^{0.33}\ for\ laminar\ flow \qquad (14)$$

And

$$Sh = 0.04Re^{0.75}Sc^{0.33}\ for\ turbulant\ flow \qquad (15)$$

Here Sh, d_h, Re, Sc and L denotes Sherwood number, hydraulic diameter, Reynolds number, Schmidt number and length of the channel, respectively.

All these parameters are explained in the Table 6 below.

Table 6: Experimental methods to compute characteristic parameters of an FO membrane

Parameter	Equation	Experiment
A (water permeability coefficient)	$J_w = A\,(\Delta\pi - \Delta P)$	RO type experiment (with a known applied pressure ΔP)
B (salt permeation coefficient)	$\frac{A(1-R)(\Delta P - \Delta\pi)}{R}$	RO type experiment. R is salt rejection of the membrane and A is known from above experiment
K (Solute resistivity)	$\frac{A\pi_{D,b} - J_w}{BJ_w}$	FO type experiments with no applied pressure. Pure water is used in feed side (therefore, $\pi_{F,b}$ is zero). $\pi_{D,b}$ is the osmotic pressure of the draw solution.
k (Mass transfer coefficient)	$\frac{Sh\,D}{d_h}$	$Sh = 1.85\left(Re\,Sc\,\frac{d_h}{L}\right)^{0.33}$ (for laminar flow) $Sh = 0.04\,Re^{0.75}Sc^{0.33}$ (for turbulence flow)

Where Re - Reynolds number, Sc - Schmidt number, d_h - hydraulic diameter, L - channel length, Sh – Sherwood number.

2.2.1 Applications of FO

Since late 1990s, that is after HTI Innovations (USA) started commercial FO membrane fabrications, FO has been given significant attention and number of lab scale and pilot scale research have started in progress. As per the literature the main factors that needs research attention in FO are:

1. **Selection of a proper draw solution**: which gives higher water flux, lower reverse salt flux (RSF) and easy to regenerate
2. **FO hybrid systems**: applying FO to improve existing processes (such as RO, MD) and/or to increase the applicability of FO system (such as to regenerate draw).

3. **Water flux optimisation through FO**: Varying the process parameters to improve the FO process.

4. **Type of membranes**: Fabrication of novel membranes is given significant attention. Material and the fabrication methods are varying to improve the performance of the membrane

5. Fouling tendency of the FO membrane

These five points will be discussed in detail in the following sections.

2.2.1.1 Selection of a Proper Draw Solution

A draw solution should be having a higher osmotic pressure compared to the feed solution to yield a higher water flux. Also, it should be non-toxic, chemically inert to the membrane, highly soluble in water, and specially it should be easily regenerated and separated from the pure product water. A draw solution having above properties can be organic, inorganic, combination of organic – inorganic nanoparticles or gas and volatile compound (Alejo et al., 2017). Gaseous and volatile compound draw solutions have limited advantages such as lower water flux and limited recyclability. Further RSF is higher. Organic and inorganic solutes give higher water flux since their osmotic pressure is higher, but, regeneration of draw solution is not economical. Recently, magnetic nanoparticles (MNP) have been used as draw solutes in FO for water reuse. Studies prove that the MNPs can be easily recovered from draw solutions by applying a magnetic field (Ling et al., 2010a, Ge et al., 2011). However, water flux is comparatively low when a magnetic field is applied. Despite these finding from this research group, ion aggregation is a disadvantage and the human health and environmental hazards are still under assessment yet.

Table 7 shows the research on types of draw solutions for FO applications. Having same osmotic pressure, NaCl, $MgCl_2$ and NH_4HCO_3 have performed in a different way with the same CTA flat sheet membrane. This is due to the variation in density and viscosity of the draw solution. Even though NaCl shows highest water flux among the three selected draw solutions, it gives the highest RSF as well.

Since the KCl osmotic pressure is significantly high (89.3 atm) it has shown a higher water flux with CTA flat sheet membranes. PEG-$(COOH)_2$-MNPs 250, having nearly same osmotic pressure as KCl has shown only half of the water flux even in PRO mode. As mentioned earlier, MNPs lead to lower flux than inorganic draw solutions at the same osmotic pressures.

Other than the draw solutions mentioned in the Table 7 and in the text, SO_2, Aluminium sulphate, Glucose, Fructose, polymer hydrogels, copper sulphate, magnesium sulphate and citrate-coated magnetic nano-particles have been investigated as draw solutes in FO applications (Li et al., 2011a, Kravath and Davis, 1975, Li et al., 2011b, Na et al., 2014, Alnaizy et al., 2013a, Alnaizy et al., 2013b). However, all of these are having pros and cons.

Table 7: The physicochemical properties and FO water flux of draw solutes used in FO processes. Table adapted from Ref. (Ge et al., 2013). Feed solution was DI water except for Polyglycol copolymer*.

Draw solute(s)	Concentration (M)	Osmotic pressure (atm)	Molecular weight (g/mol)	Water flux (LMH)	Remark	Ref.
NaCl	0.60	28	58.5	9.6	CTA FS membrane FO mode	(Achilli et al., 2010)
$MgCl_2$	0.36	28	95	8.4	CTA FS membrane, FO mode	(Achilli et al., 2010)
KCl	2	89.3	74.6	22.6	CTA FS membrane, FO mode	(Phuntsho et al., 2011)
NH_4HCO_3	0.67	28	79	7.3	CTA FS membrane, FO mode	(Achilli et al., 2010)
Sucrose	1	26.7	342.3	12.9	CA HF, FO mode	(Su et al., 2012)
PAA-Na 1200	0.72 g /mL	44	1200 Da	22	CA HF, PRO mode	(Mathew et al., 1989)
PEG-$(COOH)_2$-MNPs 250	0.065	73	None	13	CTA FS membrane, PRO mode	(Ge et al., 2011)
1,Trimethylimidazolium iodide	1	50	238	13	CTA FS membrane, PRO mode	(Yen et al., 2010a)
Sodium formate	0.68	28	68	9.4	CTA FS membrane, FO mode	(Alejo et al., 2017)
Polyglycol copolymer* (feed = 3.5% NaCl)	30~70%	40~95	>500 Da	≥ 4	CTA FS membrane, FO mode	
Sodium hexa-carboxylatophenoxy phosphazene	0.067	None	1089	6	CTA FS membrane, FO mode	(Ge et al., 2013)

Once the draw solution has extracted pure water from the feed solution, regeneration is a controversial issue. Regeneration is a further process hence it gives extra complexity for the FO process. RO is to be a better regeneration process operating at low pressures depending on the final concentration of draw solutions (Miller et al., 2007), however some researchers suggest Membrane Distillation (MD), Nano Filtration (NF), Ultrafiltration (UF) and evaporation as a replacement to RO since the operating cost for RO is high.

Table 8 shows the current regeneration approaches tested by different research groups. As explained above, RO is an option however, operating cost is high. NF, UF and ED regeneration have relatively low operating costs. MD's recovery rate is higher, however, similar to RO it has high operating costs.

In addition to regeneration, RSF or reverse salt diffusion is an inherent disadvantage in FO applications. This is critical when FO is applied in food and dairy industry as it affects the final quality of the food concentrate or diary product concentrate. In these specific applications, most commonly investigated draw solutions are NaCl, glucose, fructose, sucrose and corn syrups as they are non-toxic.

Table 8: Overview of the existing recovery approaches of draw solutions in FO (Kravath and Davis, 1975, Tularam and Ilahee, 2007, McCutcheon et al., 2006a, McGinnis and Elimelech, 2007, McCutcheon et al., 2006b, Stone et al., 2013, Cath et al., 2010, Yangali-Quintanilla et al., 2011, Bowden et al., 2012, Tan and Ng, 2010, Zhao et al., 2012, Su et al., 2012, Ge and Chung, 2013, Hau et al., 2014, Ge et al., 2012a, Ling and Chung, 2011, Yen et al., 2010b, Guo et al., 2014, Zhao et al., 2014, Wang et al., 2011, Ge et al., 2012b, Xie et al., 2013, Zhang et al., 2014, Zhang et al., 2013, Alnaizy et al., 2013a, Alnaizy et al., 2013b, Li et al., 2011a, Li et al., 2011b, Razmjou et al., 2013b, Ling et al., 2010b, Ge et al., 2011, Phuntsho et al., 2011, Phuntsho et al., 2012, Razmjou et al., 2013a, Cath et al., 2006, Ling and Chung, 2012, Liu et al., 2011, Ou et al., 2013, Duan et al., 2014)

Category	Recovery methods	Draw solutions	Advantages and disadvantages
Thermal separation[1]	Heating or air stripping	SO_2	Easy, but energy intensive, and toxic
	Heating (~60 °C)	NH_3/CO_2	High water recovery rate, energy-efficient, but poor water quality
	Hearting (~60 °C) with bubbling N_2	SPS	Energy-efficient, but poor water quality
Membrane separation	RO	Seawater, organic ionic salts	High water recovery rate, high salt rejection, but high operating cost
	NF	Divalent salts (e.g. $MgSO_4$), sucrose, EDTA sodium salts, hydroacid complexes	High water recovery rate, relatively high salt rejection, relatively low operating cost, but limited to the DSs with multivalent ions
	UF	PSA, modified MNPs	High water recovery rate, low operating cost, but poor salt rejection especially for DSs with low Mws
	MD	2-Methylimidazole-based compounds, NaCl, Na-CQDs, PSA, thermosensitive copolymer	Low capital cost, high water quality, relatively high water recovery rate, less affected by feed salinity, but high operating cost unless using low grade heat
	ED	NaCl	Energy-saving when combined with solar energy, adjusting the salt concentration of product water, but high capital cost, unsuitability for desalination of high saline water
Precipitation for recovery[2]	Precipitation by adding Ca(OH)2	$Al_2(SO4)_3$	Energy-efficient, but costly consumables toxic by-products
	Metathesis precipitation by adding Ba(OH)2	$MgSO_4$, $CuSO_4$	Energy-efficient, but costly consumables, toxic by-products

Stimuli–response for recovery	Response to heat combined with hydraulic pressure	Hydrogels	Relatively energy-efficient, environmental-friendly, but poor liquid water recovery rate, unsuitability for practical applications in a continuous FO process
	Response to sunlight	Composite hydrogels	
	Response to gas pressure	Hydrogels	
	Magnetic separation	Functionalized MNPs	Easy, energy-efficient, environmental-friendly, high water recovery rate, but poor reusability due to agglomeration, poor water quality
	Response to magnetic heating	Magnetic hydrogels	Relatively energy-efficient, environmental-friendly, but poor liquid water recovery rate, unsuitability for practical applications in a continuous FO process
Combined processes for recovery	Precipitation combined with magnetic response	$Al_2(SO4)_3$ combined with $Fe_3O_4@SiO_2$	Energy-efficient, but complicated procedures, toxic by-products
	Integrated electric-field NF system	Surface-dissociated MNPs	High water recovery rate, good reusability but complicated procedures
	Hot ultrafiltration (HUF)	Thermosensitive polyelectrolytes	Easy, high water recovery rate, but relatively high operating cost unless using low grade heat
Direct use for drinks, irrigation, and desert restoration	None	Glucose, fructose, edible saccharide solutions,	No energy input, but not pure water, limited to specific applications
		Fertilizer	No energy input, but not pure water, requiring post treatment for direct irrigation, needing a large storage tank
		NaLS (Sodium lignin sulfonate)	No energy input, but not pure water, limited to specific applications

[1]= G.W. Batchelder, Process for the demineralization of water, US Patent, 1965 and R.L. McGinnis, Osmotic desalination process, US Patent, 2002. [2]= B.S. Frank, Desalination of sea water, US Patent, 1972.

2.2.1.2 FO Hybrid Systems

A few commercial scale FO hybrid applications were launched in 2016, however very little data is available in literature on these (Miller et al., 2007). The hybrid systems mentioned in this section are operating in lab scale or pilot scale plants.

Fertiliser drawn FO desalination (FDFO) has been successfully applied in lab and pilot plant scale to dilute fertilisers while concentrating saline ground water (Phuntsho et al., 2012, Holloway et al., 2015, Mathew et al., 1989). Recent studies are trying to implement FO-RO hybrid systems to reduce the energy costs associated with typical RO plants. This energy saving occurs when feed seawater is diluted using a waste water stream so that diluted seawater needs less pressure during the RO desalting process. Further FO hybrid systems have demonstrated the potential of a combined FO and membrane bioreactor (MBR) hybrid system, known as the osmotic membrane bioreactor (OMBR) system to produce high quality product water with low fouling tendency (Cornelissen et al., 2008, Zhang et al., 2012, Liu and Mi, 2012), however only at lab scale. FO membranes have been used to dilute seawater using secondary wastewater effluent as draw solution, in order to reduce the energy cost associated with desalination (Yangali-Quintanilla et al., 2011). A few studies have been carried out to treat landfill leachate, food industry effluent, and to increase the water recovery of RO (Petrotos et al., 1999, Achilli et al., 2009, Martinetti et al., 2009, Alejo et al., 2017). Table 9 shows the FO hybrid systems used and advantages gained compared to conventional stand-alone FO process.

In general, hybrid systems are energy efficient compared to stand alone systems. For example, in a FO-LPRO hybrid system, energy cost is only 50% (~1.5 kWh/m^3) of that used for high pressure SWRO desalination.

Table 9: FO hybrid systems reported in literature. Table adapted from (Chekli et al., 2016).

Hybrid system	Draw solution	Membrane type(s) for FO process	FO performance	Remarks
FO-heating (~60°C)	NH_4HCO_3	Commercial flat sheet (FS) RO and CTA FO membranes (lab-scale studies) and polyamide (PA) thin-film composite (TFC) FO membrane (pilot-scale study)	Water flux: 7.2 LMH. Reverse salt flux: 18.2 g/m^{2}h at 2.8 MPa (lab-scale studies). Water flux: 2.6LMH, system recovery of 66% and more than 99% total dissolved solids (TDS) removal (Pilot-scale study)	Energy efficient process (i.e. specific energy consumption of the hybrid system is significantly lower than other thermal distillation methods) with high water recovery rate but water quality does not meet the WHO standard for ammonia
FO–MD	2-Methylimidazole-based compounds	Commercial CTA FS FO membrane	Water flux: 0.1–20 LMH (2.0 M DS and DI water as feed). Reverse salt flux: 5–80 g/m^{2}h	A water flux of about 8 LMH was achieved across the MD membrane. ICP effects were higher when using the 2-methylimidazole-based compound with divalent charge. High reverse salt flux and cost of synthesis remains high.
FO–MD	Na+-functionalized carbon quantum dots (Na-CQDs)	Commercial TFC FO membrane	Water flux: about 3.5LMH after the fifth cycle. Almost negligible reverse draw solute permeation.	Better performance compared to NaCl. Inexpensive, chemically inert and biocompatible.
FO-magnetic field	Thermosensitive MNPs	Commercial FS CTA FO membrane	Water flux: < 2 LMH. Performance of MNPs remains stable after 5 cycles.	Separation of MNPs under lower strength magnetic field which significantly decreased their agglomeration. Costly and complex synthesis. No information on permeate water quality.

Functionalised MNPs			Water flux: 10–17LMH (PRO mode) and 7–9LMH (FO mode) with PAA-MNPs at different sizes 3.6 – 21nm and DI water as feed water. 9 and 13 LMH (FO and PRO mode respectively) with 0.065M PEG-$(COOH)_2$ MNPs and DI as feed water. The water flux dropped to 10.3 LMH (PRO mode) after 9 cycles.	Straightforward and energy efficient process, high water recovery rate but slightly drop of water flux due to agglomeration of the MNPs
FO-UF	Modified magnetic nanoparticles (PAA-MNPs)	Commercial CTA flat sheet FO membrane	Water flux (PRO mode): Up to 17 LMH with 0.08mol/L PAA-MNPs and DI water as feed	MNPs remained active even after 5 cycles of UF recovery without any alteration. This hybrid system requires lower energy consumption compared to RO and NF. However, the smaller MNPs pass through the UF membrane and therefore synthesis of MNPs suspension with narrower size distribution is required.
FO-Electric field-NF	Polyelectrolytes (e.g. PAA-Na)	Commercial CTA flat sheet FO membrane	Water flux (PRO mode): 6LMH with 0.72g/mL PAA-Na as DS and seawater as feed.	High water recovery rate. Various molecular weights (MW) and expanded polymer structure allowing DS regeneration via low-pressure UF process. High rejection rate (>99%) for PAA with MW of 1800Da. However, poor salt rejection for DS with low MW.

FO–NF	Hydroxyl acids of citric acid (CAc) (Fe–CAc; Co–CAc and Co2-CAc)	CA, TFC on polyethersulfone supports (TFC–PES) and polybenzimidazole and PES dual layer (PBI–PES) hollow fibre membranes	Water flux: Up to 17.4LMH with 2.0M Fe–CAc as DS and synthetic seawater (i.e. 3.5wt% NaCl) as feed. 90% rejection rate for Fe–CAc by NF membrane.	Low operating pressure (i.e. 10bar), low reverse draw solute and high rejection rate (i.e. more than 90%)
FO-Stimuli to heating combined with hydraulic pressure	Hydrogels	Commercial FS CTA FO membrane	Water flux: 0.30–0.96LMH with 2000ppm NaCl as feed. Very low water recovery rates (i.e. less than 5%).	Environmental-friendly and relatively energy efficient process but low liquid water recovery rate. Unsuitable for applications that require continuous FO process
FO-Stimuli to heating	Semi-interpenetrating network (IPN) – hydrogels	Commercial FS CTA FO membrane	Water flux: Ranging from 0.12 to 0.18LMH after 5h operation which is 1.5–3 times higher than conventional hydrogels. Better performance can be achieved by increasing membrane/hydrogel contact area.	At 40°C, the semi-IPN hydrogels quickly released nearly 100% of the water absorbed during the FO drawing process. Drawing and dewatering cycles are highly reversible. However, very low water flux (i.e. less than 0.5 LMH).
FO-Stimuli response to sunlight	Composite hydrogels reduced graphene oxide	Commercial FS CTA FO membrane	Water flux: Up to 3.1 LMH with 2000ppm NaCl as feed. Water recovery up to 44.3% at 1.0 kW/m^2 with 1h exposure time.	Environmental-friendly and relatively energy efficient process but low liquid water recovery rate and low water flux. Unsuitable for applications that requires continuous FO process

Composite hydrogels light-carbon particles			Commercial flat sheet CTA FO membrane	Water flux: Up to 1.32 LMH with 2000ppm NaCl as feed. Up to 100% water recovery rate when solar light is used with 1h exposure time at a solar irradiation of 1.0kW/m^2.
FO-Stimuli response to gas pressure	Hydrogels	Commercial FS CTA FO membrane		Water flux: Up to 1.5LMH with 2000 ppm NaCl as feed. Gas pressure stimuli worked better for large particles whereas temperature stimuli are more effective with small particles
FO-Stimuli response to magnetic heating	Magnetic hydrogels	Commercial FS CTA FO membrane		Water flux: Up to 1.5 LMH with 2000ppm NaCl as feed. 53% Liquid water recovery via magnetic heating compared to only 7% under convection heating.
FO-Stimuli to heating	Functionalised thermo-responsive microgels	Commercial FS CTA FO membrane	Water flux: Up to 20 LMH after 3 cycles (decrease of 13% compared to initial flux).	A high water flux up to 23.8LMH and high water recovery ability of 72.4% were achieved.
FO–RO	Glucose	Not reported	Not reported	Limited water recovery due to the low osmotic efficiency of glucose which also created high ICP effect due to its large molecular weight.

FO–LPRO	Red seawater	Commercial CTA FS FO membrane	After 10 days of continuous FO operation, 28% of flux decline was observed (initial water flux of 5LMH) but membrane cleaning (hydraulically cleaned) allowed 98.8% water flux recovery.	Energy cost of this hybrid system is only 50% (~1.5kWh/m3) of that used for high pressure SWRO desalination
FO–MSF/MED	Concentrated Brine		No experimental results – modelling studies only	Simulation results showed that FO demonstrates good performance for the removal of divalent ions from feed solution which mitigates the scaling on the surface of heat exchangers. FO-MED system is less energy intensive and has greater recovery rate compared to FO-MSF.
FO–NF	Various DS tested both inorganic and organic salts	Commercial FS CTA FO membrane	Water flux: 10LMH for both FO and NF processes. Salt rejection by FO membrane up to 99.4% for all DS tested.	Water flux of about 10LMH was observed for both FO and NF processes. High salt rejection (i.e. up to 97.9% for NF process) and good quality product water (i.e. meeting the drinking water TDS standard).
FO–NF	Divalent salts ($MgCl_2$, $Na2SO_4$)	Commercial CTA FS FO membrane	Water flux: 8–12LMH (FO and PRO mode tested). Higher fluxes were obtained with PRO mode but flux decline was more pronounced. Salt rejection of the diluted DS: 97.7%.	Lower operating pressure, less flux decline due to membrane fouling, higher flux recovery after cleaning, higher quality of product water compared to standalone RO process.

FO–ED	NaCl	Commercial CTA FS FO membrane	Water flux: Up to 3.5LMH (simulation not experimental) with 1M NaCl as DS and brackish water or wastewater as feed and assuming 130 L/day product water.	Energy efficient process when ED powered by solar energy. High quality produced water meeting potable water standards but high capital cost and unsuitable to desalinate high saline water

In addition to these advantages, one inherent disadvantage of FO process is lower water flux. Since the water flux through the membrane decides the productivity of the whole process, a lot of research is being conducted to optimise water flux through FO. This is being testing in lab scale using (1) changing FO process parameters (cross flow velocity (CFV), pH, Temperature, feed and draw concentrations, sonication, etc), (2) varying membrane modules (flat sheet, hollow fibre, spiral wound, different material of the membrane (CTA, PA, PSf) and (3) different fabrication methods.

2.2.1.3 Water Flux Optimisation Experiments

Several researchers have studied the effect of CFV on water flux when different types of draw solutions are used. Higher CFV should perform better as it reduces the ECP effect. Hawari et al (2016) have investigated the combined influence of temperature and flow rate of feeds on the performance of forward osmosis (Hawari et al., 2016). Results demonstrated that the concentrative internal concentration polarization (CICP) could be mitigated by increasing the feed solution flow rate and using a spacer.

There are number of studies where researchers have tried to change the temperature of either or both of draw and feed solution. In the same study mentioned above, Hawari et al also investigated the increase in water flux when the draw solution temperature increases. On increasing the draw solution (DS) temperature from 20 °C to 26 °C the flux increased linearly and then started decreasing when temperature increased further due to the development of a temperature gradient as shown in Figure 10. Membrane flux increased by 93.3% due to temperature increase from 20 to 26 °C and the flow rate from 1.2 to 3.2 L/min using 0.5 M NaCl as the draw solution and distilled water as the feed solution.

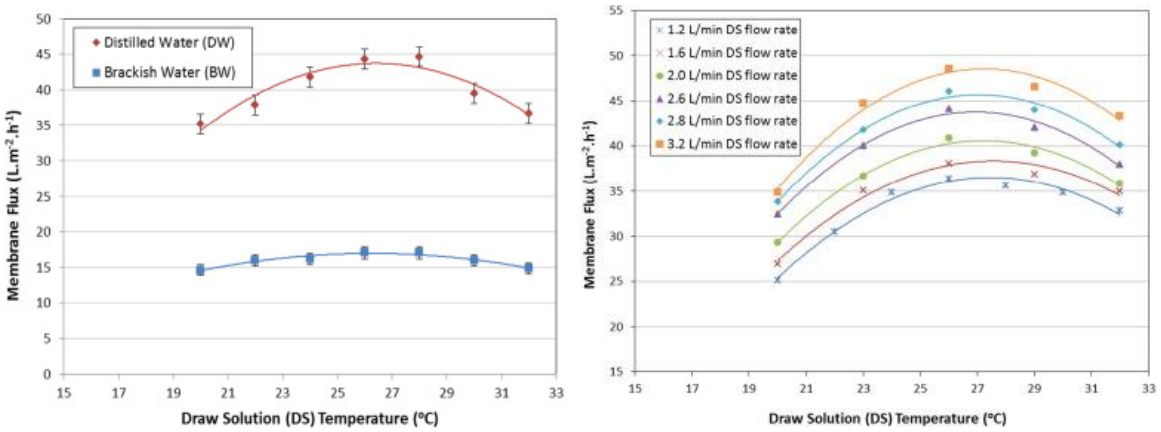

Figure 10: (a) Effect of increasing DS temperature on the membrane flux at a DS and FS flow rate of 2.0 L/min (DS-AL mode, 0.5 M NaCl DS, distilled water or 5 g/L NaCl FS, and 20 °C FS temperature) (b) Effect of increasing the DS temperature with different DS flow rates on the membrane flux (DS-AL mode, 0.5 M NaCl DS, distilled water FS, 20 °C FS temperature, and 1.2 L/min FS flow rate). (Hawari et al., 2016).

In another study by Zhao et al., (Zhao et al., 2016), the performance of forward osmosis (FO) in treating the high-salinity feed water was investigated under different temperatures, membrane orientations and flow cross velocities in terms of water flux, membrane scaling and removal efficiency of Ni (II). They proved that increased cross flow velocity could promote the water flux effectively for treating the high-salinity feed water, however enhanced temperature could not. Further they reported that, for the proposed operation to be energy efficient, the optimum operating conditions would be 35 °C and 10 cm/s.

2.2.1.4 Types of Membranes

Qasim and research group (2015) reviewed the membrane developments since the emergence of FO technology. They categorised the recent membrane developments depending on the method of fabrication (Qasim et al., 2015) as:

1. Thin film composite (TFC) membranes,
2. Chemical modification to the membranes, and
3. Phase inversion-formed membranes.

A summary of their report on TFC and chemically modified membranes is given below (Qasim et al., 2015).

TFC membranes: TFC membranes are available in flat sheet or hollow fibre. Different research groups have used with different polymer materials such as Polyamide (PA) (both flat sheet and hollow fibre available), polymer polyethersulfone (PES) (hollow fibre and flat sheet) sulphonated material in the substrate (flat sheet), PSf (flat sheet), and substrates with different contents of hydrophilic sulphonated poly (etherketone) (SPEK) (flat sheet). ICP effects from employing TFC FO membranes are governed by the porous support layer while the selective active layer governs the salt rejection and reverse salt permeation. To improve FO desalination performance and reduce the ICP effects, the support layer must be highly hydrophilic with low structural constant S (S is explained in theory section 2.2.1). However, almost all the above-mentioned TFC membranes consist of hydrophobic PSf support.

Chemically modified membranes: NF-like FO membranes with polyacrylonitrile (PAN) substrate using polyelectrolyte layer-by-layer (LbL) assembly were fabricated by Tang and research group. However, lower rejection and higher production cost are the limiting factors. Fane and group used chemical modification to fabricate both hollow fiber and flat sheet FO membranes with Torlon® polyamideimide (PAI) substrate prepared by phase inversion (Setiawan et al., 2011, Setiawan et al., 2012, Qiu et al., 2012). The membrane was chemically treated with the polyelectrolyte polyethyleneimine (PEI) to develop a positively charged nanofiltration (NF)-like selective layer. However, FO desalination applications are limited as the salt rejection is lower. Goh et al. (Goh et al., 2013) immobilized multi-walled carbon nanotubes (MWCNT) on PAI hollow fiber substrate by vacuum filtration method. The MWCNT immobilized PAI substrates were then chemically treated with PEI to develop positively charged nanofiltration (NF)-like selective layer. This modification showed higher water flux compared to the membrane without MWCNTs. However, like other surface modifications, RSF has not reduced. Puguan et al. (Puguan et al., 2014) chemically cross-linked polyvinyl alcohol (PVA) nanofibrous substrate formed by electrospinning. PVA can provide a very hydrophilic support, hence would reduce ICP and increase the water flux. The cross-linking was performed using acid catalyzed glutaraldehyde in acetone solution. Subsequently, polyamide active layer was formed by interfacial polymerization. Water flux was 7-8 times higher compared to well-known commercial HTI membranes, due to low structural parameter value.

Water flux through TFC hollow fibre membranes were compared in a study conducted by Shibuya et. al (Shibuya et al., 2017). The TFC hollow fibre membranes showed better performances in terms of water fluxes compared to previously reported hollow fibre membranes. Some of their results are shown in Figure 11. With the same draw and feed concentrations (1 and 0.5 M) flat sheet membranes gave lower water fluxes compared hollow fibre modules. However, as mentioned by Shibuya et.al, to pass through the hollow fibre coupons, extra pressure needs to be applied. Therefore, performance comparison with flat sheets may give opposite results in terms of economics.

In another study by Xiong and his research group, novel TFC FO membranes were fabricated (Xiong et al., 2016) and gave water flux up to 10 LMH when DI water and 0.5 M NaCl were used as feed and draw solution, as shown in Figure 12.

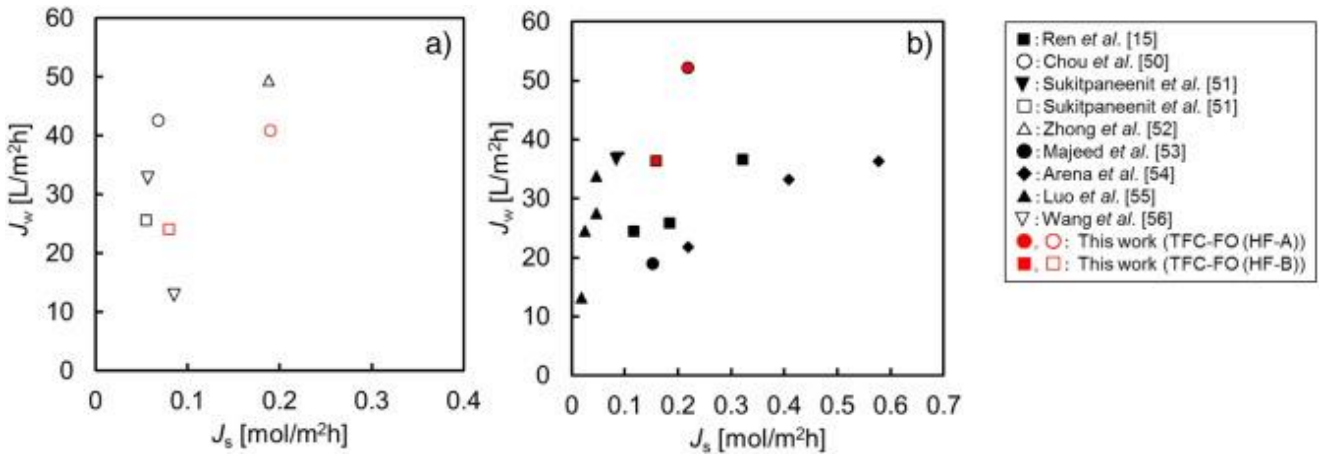

Figure 11: Relationship between water flux and reverse salt flux of TFC-FO-HF membranes. All data were obtained in AL-DS orientation; a): C_{DS} = 0.5 M, b): C_{DS} = 1.0 M (Shibuya et al., 2017).

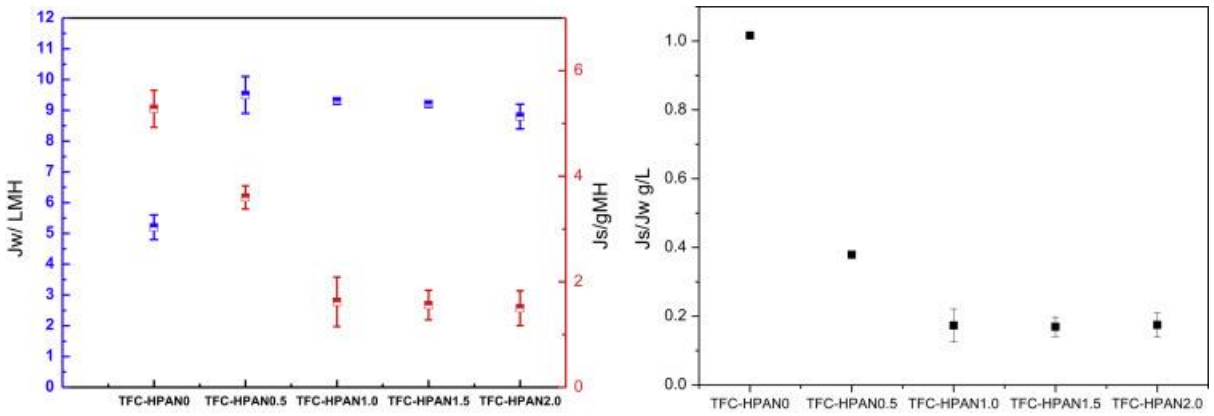

Figure 12: FO performance of TFC membranes prepared with different PAN substrates. (feed solution: DI water; draw solution: 0.5 M NaCl; flow rate: 0.3 L/min; temperature: 20 °C; FO mode.) (Xiong et al., 2016).

2.2.1.5 Fouling of FO membranes

In addition to water flux optimisation experiments, fouling tendency of FO membrane for different applications as investigated in some studies. All these studies have been conducted with synthetic foulants such as gypsum, silica, organic and inorganic compounds, salts, colloids, and microorganisms. In general, it has been shown that at lower CFV FO membrane is less susceptible to fouling as the fouling layer is thin and loose. However, in some applications where the CFV and water flux is high, there is a high potential for a membrane fouling. As reported by Kim et at (2017), feed pressure could be considered as an indicator of fouling occurrence (Kim et al., 2017). Combination of osmotic backwash and physical cleaning used in their study was reported as effective for cleaning both CTA and TFC membrane modules. Figure 13 shows the reduction in feed inlet pressure after proposed cleaning process in this particular study. However, as per the reported results, proposed cleaning process failed to recover the flux completely.

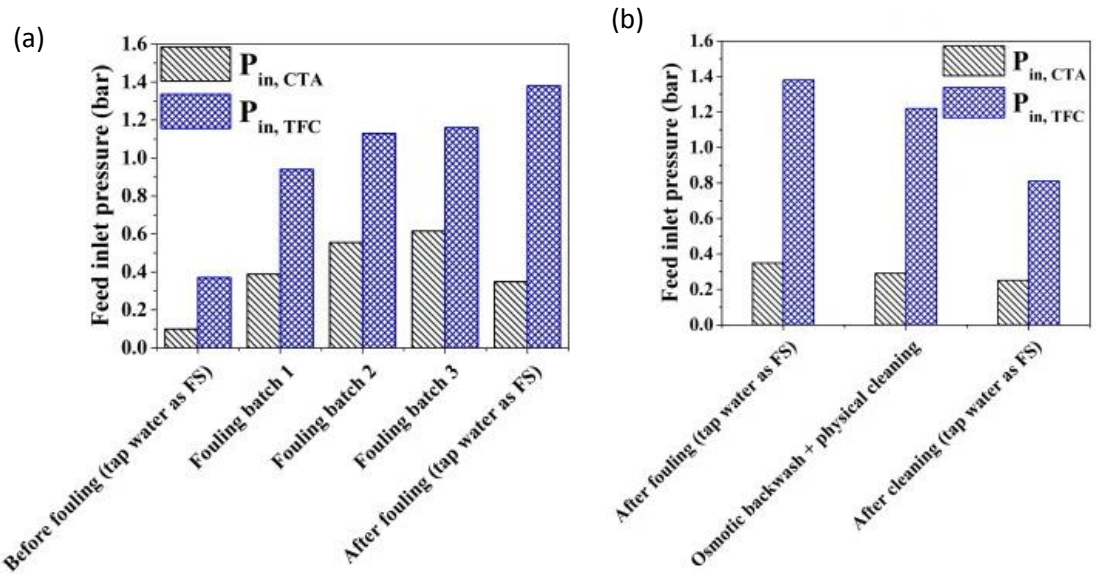

Figure 13: (a) Feed inlet pressure change with CTA and TFC modules. Fouling experiments were conducted using 35 g/L RSS as DS and feed fouling solution prepared by addition of 1.2 g/L RSS, 0.22 g/L $CaCl_2$, 0.2 g/L alginate, 0.2 g/L humic acid

(b) Effect of osmotic backwash and physical cleaning on the feed inlet pressure recovery. Physical cleaning with maximum feed cross-flow velocity of 0.44 and 0.91 m/s for CTA and TFC, respectively was performed for 5 min using tap water (Kim et al., 2017).

Silica scaling has proven to be the most dominant inorganic causing fouling in real FO desalination applications (Li et al., 2012b, Kim et al., 2015). Organic and inorganic (gypsum scaling) fouling, was investigated by some research groups. (Elimelech and his coworkers (Mi and Elimelech, 2008, Baoxia and Elimelech, 2010), Lee et al. and Kim et.al (Lee et al., 2010a, Kim et al., 2014)). For all of these fouling was highly reversible as the observed fouling layers were loosely packed. Water flux was completely recovered by periodic rinsing, interestingly without the addition of any chemicals. In addition to these studies, when actual brackish lake water was used as feed water, TFC FO membrane showed a 65% water flux drop in 24 hrs, however, similar to previous study, DI water flushing fully recovered the water flux without any chemicals (Chun et al., 2015).

In summary, all the literature available concludes that both organic and inorganic fouling in FO is highly reversible. This is due to the lower pressure applied during FO operation and hence the fouled layer formed is readily removable through frequent rinsing and flushing.

2.2.2 Summary

Despite the amount of literature available, this technology is still at laboratory scale and pilot scale plants due to the disadvantages mentioned in this section such as significantly lower flux, higher reverse salt flux, and complexity of regeneration of draw solution from product water flux (Arkhangelsky et al., 2012, McCormick et al., 2008). Therefore, numerous researchers are working on application of FO in SWRO and this is a very achieve research area to date in the field of desalination. Further, there is a theoretical lag in the FO flux prediction models. Much research is being conducted to investigate the factors affecting the water flux performance in FO and developing mathematical models to predict flux performance precisely (McCutcheon and Elimelech, 2006, K.L et al., 1981, Tan and Ng, 2008, Cath et al., 2013a, Gray et al., 2006, Zhao and Zou, 2011, Yong et al., 2012) and to characterise the FO membrane in terms of diffusion, solute resistivity and mass transfer.

Therefore, in this study, FO was applied in SWRO process to aid the reduction of pre-treatment sludge volume and a novel RO-FO hybrid system was proposed. Next chapter (Chapter 3) explains the experimental protocol and the materials used. Then the following chapters will detail the results, discussion and the conclusions made at each stage of the research.

Chapter 3: Materials and Methods

3.1 Introduction

This chapter describes the materials, experimental set-ups and methods, and analytical methods used in this sturdy.

3.2 Materials

3.2.1 Membranes

Flat sheet cellulose tri-acetate (CTA) membranes were purchased from Hydration Technology Innovations (HTI) USA. Support layer of the flat sheet membrane is made up of polyester mesh and average pore diameter is 0.74 nm (Xie et al., 2012). Scanning Electron Microscopy (SEM) images of the flat sheet CTA membrane given in Figure 14. As Figure 14(a) shows, the membrane is on an embedded screen support. Figure 14(b) shows the support layer and the embedded mesh and the Figure 14(c) is the active layer where water permeation happens.

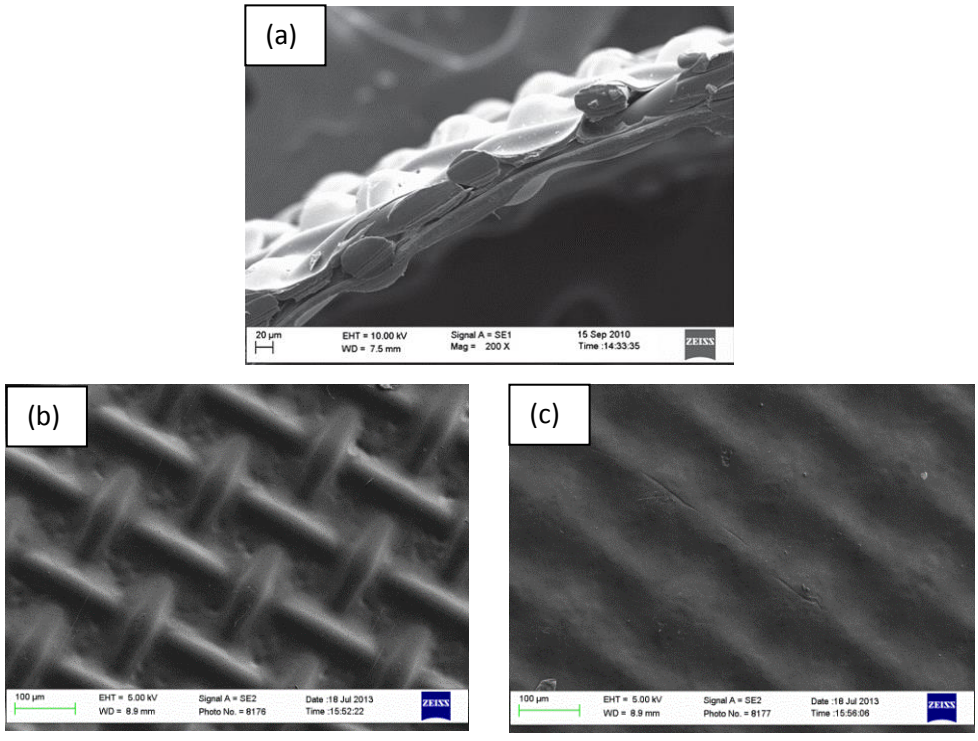

Figure 14: SEM images of hydrophilic Cellulose Triacetate (CTA) membrane on embedded polyester screen support (a) cross section (Gao, 2013) (b) Support side (c) active side.

Hollow fibre polyamide (PA) membranes used were fabricated at Samsung Cheil Industries Inc., Korea and consist of a Sulphonated Polysulphone (SPSf) support layer (Majeed, 2014).

SEM images of the hollow fibre PA membrane are given in Figure 15. Figure 15(a) shows the lumens and the Figure 15(b) shows the thickness of the lumens with pores. CTA and PA membranes used were hydrophilic and hydrophobic, respectively.

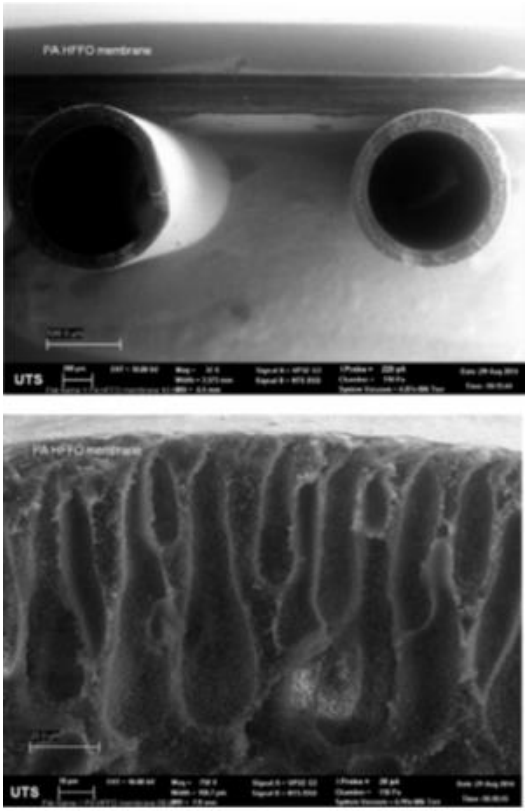

Figure 15: SEM images of hydrophobic Polyamide (PA) membranes (Lotfi et al., 2015). Active layer is inside surface of the hollow fibre and the support layer is outside surface of the fibres.

3.2.2 Draw solutions

For the initial water flux optimisation experiments, selected salt solutions were used as draw solution. The used salt solutions were NaCl, $MgCl_2$, $CaCl_2$, Na_2SO_4, $MgSO_4$, and $CaSO_4$ as they were the most commonly used draw solutions in literature considering osmotic pressure and economic benefits. In addition, these salts are the major elements available in SWRO brine as shown in the Table 10 .

Table 10: Major ion compositions of seawater. Selected anions and cations are shown in red colour.

	Typical Seawater	Eastern Mediterranean	Arabian Gulf at Kuwait	Red Sea at Jeddah
Chloride (Cl^-)	18,980	21,200	23,000	22,219
Sodium (Na^+)	10,556	11,800	15,850	14,255
Sulphate (SO_4^{2-})	2,649	2,950	3,200	3,078
Magnesium (Mg^{2+})	1,262	1,403	1,765	742
Calcium (Ca^{2+})	400	423	500	225
Potassium (K^+)	380	463	460	210
Bicarbonate(HCO_3^-)	140	-	142	146
Strontium (Sr^{2+})	13	-	-	-
Bromide (Br^-)	65	155	80	72
Borate (BO_3^{3-})	26	72	-	-
Fluoride (F^-)	1	-	-	-
Silicate (SiO_3^{2-})	1	-	1,5	-
Iodide (I^-)	<1	2	-	-
Others	-	-	-	-
Total dissolved solids (TDS)	34,483	38,600	45,000	41,000

Ref: (https://www.lenntech.com/composition-seawater.htm)

Other than these salt solutions, RO concentrate was used as the draw solution for the FO experiments. These brine samples were prepared following the process shown in Figure 16. Seawater collected from Geelong, Australia, was pre- filtered to remove large suspended particles such as seaweeds. Optimum $FeCl_3$ coagulant (i.e. 5 mg/L which was obtained at lab scale and given in the appendix section) added seawater was then passed through a cylindrical dual media filter (DMF) at a rate of 7.6 m/h where DMF diameter, sand media bed depth and anthracite media bed depth are 50, 400 and 300 mm, respectively. Further details on DMF can be found in the appendix section. After 4 h of filtration, filter media bed was backwashed for 2 min using tap water. The pH, total organic carbon (TOC), electrical conductivity (EC) and turbidity of the seawater and filtered seawater were determined. Furthermore, particle size distribution of backwashed sludge was analysed using Malvern Mastersizer. Particle size distribution of backwashed sludge (named as Lab sludge) is given in Figure 17 . Properties of brine solution are given in Table 12. The seawater used and filtered seawater properties are also shown in the same Table.

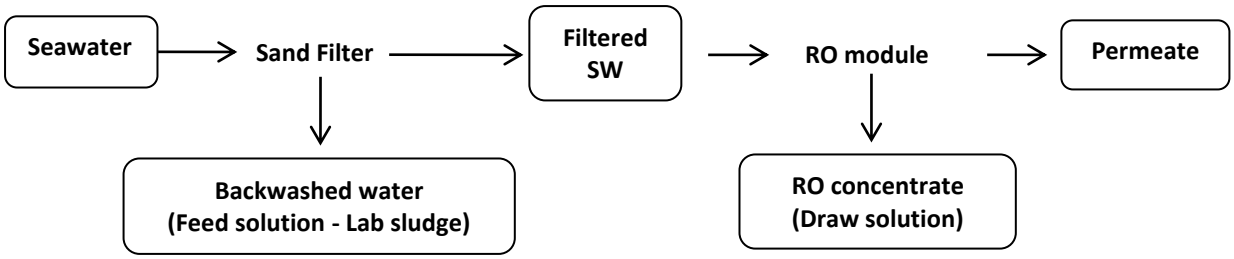

Figure 16: Draw solution preparation procedure followed at lab scale. Seawater passed through the sand filtration and then subjected to RO to produce the ROC used as draw.

3.2.3 Feed solutions

Industrial $Fe(OH)_3$ sludge was received from the Perth Seawater Desalination Plant (PSDP), Perth, Australia, in addition to the backwash sludge prepared according to previous section (refer Figure 16). Therefore, there were two types of feed solutions/sludge solutions used in the study *viz*. (1) PSDP sludge and (2) lab scale prepared sludge denoted as Lab sludge. However, for some water flux optimisation experiments MilliQ water was used as feed solution. Properties of feed sludge used in this study are given in Table 11 and Table 12. Since the received sludge contained 25% TS content (the solids content before sending to landfill), filtered seawater (prepared following the process explained in Section 3.2.2) was used to reduce the solids content to ~4%. This backwash sludge which comes from media filtration contains around 4% TS. Particle size distribution of $Fe(OH)_3$ sludge (PSDP sludge and Lab sludge) was analysed using Malvern Mastersizer and given in Figure 17. The used seawater and filtered seawater properties are shown in the Table 11 and Table 12.

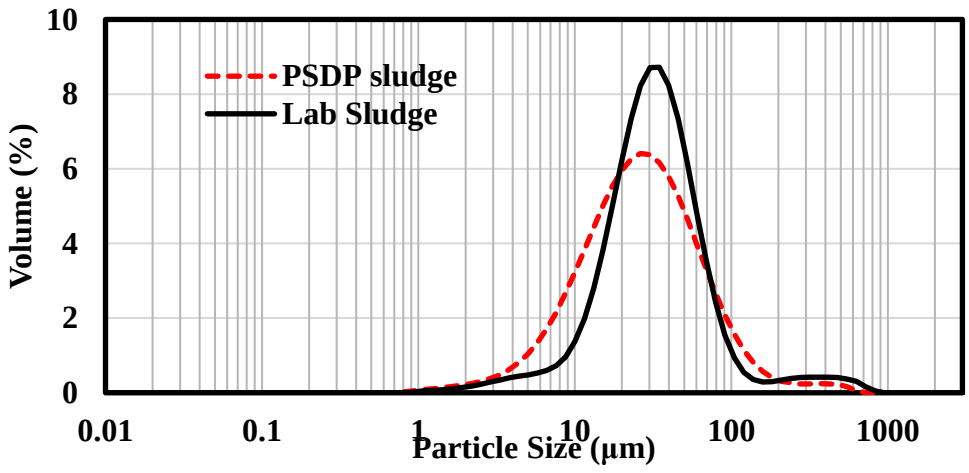

Figure 17: particle size distribution of PSDP sludge and lab sludge

Table 11: Major anions and cations concentrations of feed and draw solutions used in this study. Cations were identified using Atomic Absorption Spectrometry (AAS) and anion concentrations were recognised through *Merk*® test kits.

		PSDP sludge (mg/L)	RO concentrate (mg/L)	Seawater (mg/L)	Lab sludge (mg/L)
Cations	Ca^{2+}	454	1,101	457	20
(Filtered)	Na^{+}	14,724	19,130	8,773	3,713
	Mg^{2+}	2,607	2,947	469	-
	K^{+}	626	815	414	274
	Fe^{3+}	0.4	ND*	ND*	0.1
Anions	Cl^{-}	16,500	36,000	22,300	5,700
	SO_4^{2-}	1,800	4,400	2,200	695
	NO_3 as N	2.3	0.4	1.2	0.5

*ND - not detected

Table 12: Properties of feed and draw solution used in this study.

Property	Seawater	Filtered seawater	Draw solution - ROC	Feed solution - PSDP Sludge	Feed solution - Lab Sludge
pH	8.42	7.68	7.77	8.69	-
Turbidity (NTU)	29.1	0.45	-	-	-
EC (mS/m)	4,450	4,470	7,300	5,150	-
TOC (mg/L)	1.71	0.73	3.10	-	1.944
Alkalinity – mg/L as $CaCO_3$	110	45	68	102	30
Hardness (EDTA)-mg/L as $CaCO_3$	4,600	6,200	9,550	4,500	0
Solids content (% TS)	-	-	-	4.04	1.01
Specific gravity	-	-	-	1.01	1.00

3.3 Experimental Procedure

3.3.1 Characterising the flat sheet FO membrane: Prediction of effective diffusion coefficient of flat sheet FO membrane (Chapter 4)

Feed (MilliQ water) and draw solutions (K_2SO_4, Na_2SO_4, NaCl, $MgCl_2$, diluted ROC and diluted seawater) were passed through the membrane at 0.50 ms^{-1} cross flow velocity in co-current flow configuration. Active layer of the flat sheet FO membrane was facing the feed solution. Schematic diagram and a picture of the experimental set up are given in Figure 19. Average temperature of the feed and draw solutions was 12 ^{o}C (room temperature) with a coefficient of variation of 0.1. Change in the weight of the draw solution was programmed to

be stored in a data logger at one-minute time intervals. Experimental water flux ($J_{w,e}$) was determined by:

$$J_{w,e} = \frac{\text{change in weight in time } \Delta t}{\text{density of water } \times \text{ effective membrane area } \times \Delta t} \qquad (16)$$

After one hour of filtration, properties of the feed and draw solutions were measured. A new FO membrane coupon was used for each new salt solution.

3.3.2 Optimising the water flux through flat sheet FO membrane (Chapter 5)

Effect of cross flow velocity

Feed ($Fe(OH)_3$ sludge) and draw solutions (NaCl and $MgCl_2$) were passed through the membrane at 0.25, 0.50 and 1.00 ms^{-1} cross flow velocities in counter current flow configuration. Sludge was circulated on the porous side of the membrane and stirred at a constant rate during the experiment to eliminate settling of particles. Experimental set up used is given in Figure 18 and Figure 19. Average temperature of the solutions was maintained at 22 ^oC with a coefficient of variation of 0.1. Change in the weight of the draw solution was programmed to be stored in a data logger at one minute time intervals. Experimental water flux ($J_{w,e}$) was determined by equation (16) mentioned in Section 3.3.1. After 3 hours of filtration, properties of the feed and draw solutions were measured. Membrane was cleaned by backwashing with 0.5M NaCl and DI water in the opposite mode prior to each experiment for 30 min. Theoretical water flux ($J_{w,t}$) was calculated and compared with that of experimental value.

Figure 18: FO experimental setup used. Flat sheet FO module's membrane area is 33.54 cm^2.

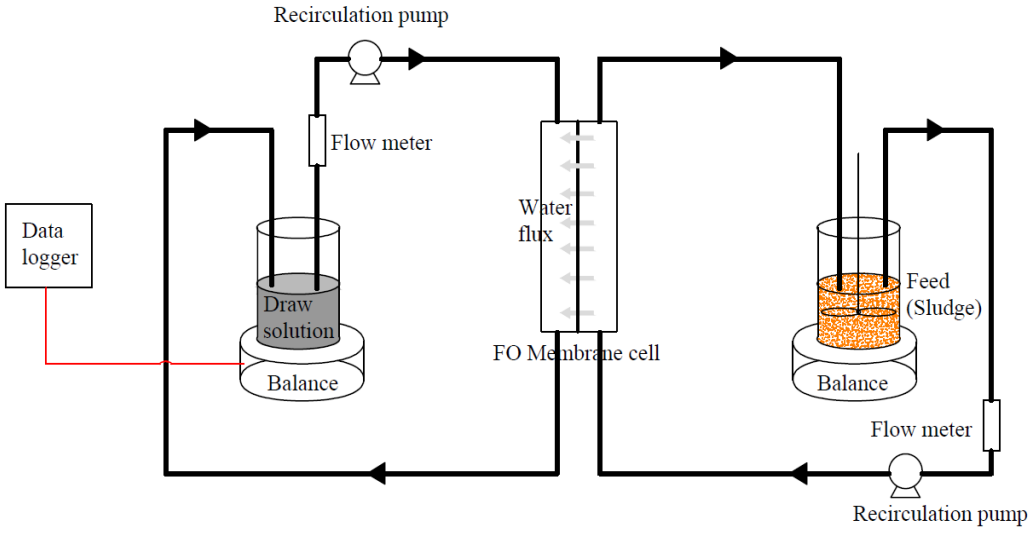

Figure 19: Schematic diagram of the FO set up used in this study. Flat sheet FO module's membrane area is 33.54 cm^2.

Effect of pH, temperature and membrane orientation

Feed (sludge prepared in the laboratory by dual media filtration as shown Figure 16 in or actual sludge received from PSDP) and draw solutions were passed through the membrane at 0.25 ms^{-1} cross flow velocity in counter current flow configuration. Feed was circulated on the porous side (active layer facing draw solution – ALDS mode) as well as on the active layer side (active layer facing feed solution – ALFS) of the membrane and stirred at a constant rate during the experiment to eliminate settling of particles. Feed temperature was varied to 20, 30 and 40°C and feed pH was varied to 6, 7 and 8. A new membrane coupon with an effective area of 33.54 cm^2 was used for each experiment. Change in the weight of the draw solution with filtration time was programmed to be stored in a data logger at 15 min time intervals. Experimental water flux ($J_{w,e}$) was determined by equation (16) in Section 3.3.1. Properties of the feed and draw solutions were measured at every 15 min for 2 h of filtration.

3.3.3 Optimising the water flux through hollow fibre FO membrane (Chapter 6)

Feed (either MilliQ water or $Fe(OH)_3$ sludge) and draw solutions (NaCl, $MgCl_2$, $CaCl_2$, Na_2SO_4, $MgSO_4$, and $CaSO_4$) were passed through the membrane at different feed/draw Reynolds number (Re) ratios. Re ratios were varied by changing the velocity of the feed and draw solutions. Sludge/MilliQ water was circulated outside the hollow fibre membrane and the draw solution through the lumens. Since the inside surface of the hollow fibre is the active layer, the experiments were run in AL-DS mode. Experimental set up shown in Figure 20 was used.

Figure 20(a) shows the hollow fiber PA membrane module used. There were 5 numbers of lumens with 1.2 mm outer diameter in the module giving an overall effective membrane area of 25.45 cm^2. Change in the weight of the draw solution was programmed to be stored in a data logger at one minute time intervals. Experimental water flux ($J_{w,e}$) was determined by the equation (16) mentioned in section 3.3.1. After 1 hour of filtration, properties of the feed and draw solutions were measured. Membrane was cleaned using MilliQ water by passing 500 mL of MilliQ water in the both sides for 30 min at 0.5 l/min water prior to each experiment. Water flux before and after cleaning was obtained using 0.5 M NaCl as draw and MilliQ water as feed solution. This will ensure how far membrane has cleaned.

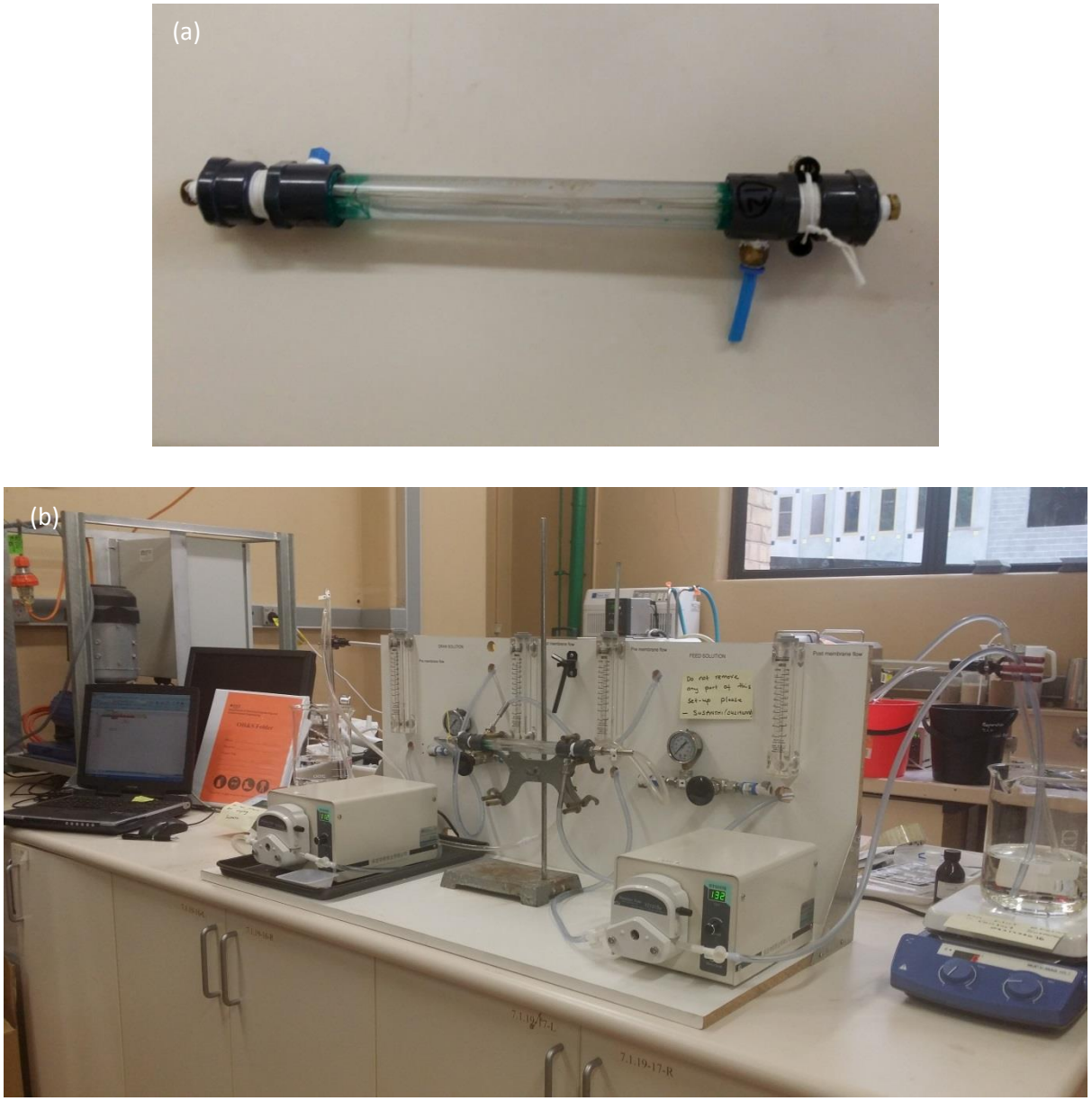

Figure 20: Hollow fibre membrane (a) module (b) experimental set up used in this study. Effective membrane area is 25.45 cm^2.

3.3.4 Fouling behaviour of the flat sheet FO membrane (Chapter 7)

Feed ($Fe(OH)_3$ sludge) and draw (RO brine) solutions were passed through the membrane at 0.04 m/s cross flow velocity (Liu and Mi, 2012, Yoon et al., 2013, Li et al., 2012a) in counter current flow configuration for 1, 2, 4 and 8 weeks with no cleaning in between. Sludge was circulated on the support side of the membrane and stirred continually during the experiment to eliminate settling of particles. Three consecutive experimental runs

using rigs (similar to Figure 19) conducted with feed pH of ~ 8, at ambient temperature and 0.04 m/s cross flow velocity. All the experiments were run in semi-batch mode as the experiments are long term runs, following Li et. al (2012) (Li et al., 2012a). That is, when the draw solution has extracted 30% of water from the feed (300 mL), both draw and feed solutions will be replaced with fresh 1L solutions.

Change in the weight of the draw solution was programmed to be stored in a data logger at 5 min time intervals. Experimental water flux ($J_{w,e}$) was determined by equation (16) mentioned in section 3.3.1. Water flux, conductivity and pH of each set up were recorded continuously using a data logger, EC meter and pH meter, respectively.

3.3.5 Mathematical Modelling (Chapter 8)

A novel hybrid RO/FO system was proposed that will improve both water recovery and reduce the volume of pre-treatment sludge. Three options were proposed and are detailed in Chapter 8. Mass and salt balance calculations were applied to each proposed system in order to evaluate their feasibility. Mass balance calculations were based on both large scale and small scale desalination plant conditions.

3.4 Analytical Method

3.4.1 Basic water quality analysis

The pH, total organic carbon (TOC), electrical conductivity (EC) and turbidity of the seawater and filtered seawater, feed sludge, RO brine and single salt solutions were determined using Hach ® pH meter, TOC analyser, Hach® EC meter and a Hach® turbidity meter , respectively. Major cations in the seawater, filtered seawater, feed sludge (lab and industrial scale) and RO brine were identified using Atomic Absorption Spectroscopy (AAS). The concentrations of the major anions of the same samples were obtained through Merck® test kits. Furthermore, particle size distribution of backwashed sludge was analysed using Malvern® Mastersizer. Total organic carbon (TOC) in the draw and feed solutions were measured using Organic Carbon analyser.

3.4.2 Membrane surface analysis

Membrane surfaces after each filtration experiments were scanned through a Zeiss Supra 55VP scanning electron microscope (SEM) at an accelerating voltage of 5 kV. In addition, to measure the amount of foulants on the membrane surface, foulant layer on the surface was extracted through centrifuging to MilliQ water and TOC concentration in the extracted solution was measured. Since the centrifuged membrane area is known, TOC was calculated per cm^2.

All the FO filtration experiments were run in duplicate, and fouling experiments were run in triplicate in order to verify the reproducibility of the experimental data. Error bars determined from these multiple runs have been displayed in the results and analysis sections.

3.4.3 Mass and energy balance calculations

These calculations were done using Microsoft excel software and sample calculation is given in appendix section. Details of mass balance equations are discussed in Chapter 8.

Chapter 4: Characterising the FO Membrane: Prediction of Effective Diffusion Coefficient of FO Membrane

4.1 Introduction

Forward osmosis (FO) is a novel emerging membrane process which can be used to concentrate a dilute aqueous stream through the use of a concentrated stream obtained from another process such as reverse osmosis (RO). When those two liquid streams are separated by an FO membrane, the osmotic pressure difference between two liquids will allow water to diffuse through the membrane from the diluted stream to the concentrated stream (Cath et al., 2006). However, the amount of water diffused depends on the orientation of the membrane. When the active and the support layers of the membrane face the diluted (or feed) stream and the concentrated (or draw) stream respectively, the mode of the orientation is called AL-FS (active layer facing feed stream). When it is the other way around, the configuration is called to be in AL-DS (active layer facing draw stream) mode. In addition to the desired water flux, there is an undesirable solute diffusion (known as reverse salt flux - RSF) due to the concentration gradient between feed and draw solution will also occur which would lower the performance of the membrane process significantly (Touati and Tadeo, 2016).

Diffusion is the dominant solute transport mechanism through a porous membrane layer. Therefore, to understand the solute transport through a porous FO membrane material, the diffusion coefficient (D) of solutes were experimentally determined. However, when the solutes transport through a tortuous path, effective diffusion coefficient, D_{eff}, is always less than the theoretical D, which is given by Fick's Law. The value of D_{eff} depends on the tortuous path it travels and therefore depends on the porosity (ϵ) and tortuosity (τ) as well as the thickness of the membrane (t).

$$D_{eff} = \frac{t\tau}{\epsilon K} \qquad (1)$$

Where, parameter *K* defines the solute resistivity for diffusion within the porous support layer of the membrane. The value of *K* is a measure of how easily a solute can diffuse through the support layer and thus is a measure of the severity of ICP (McCutcheon et al., 2006b, McCutcheon and Elimelech, 2006). The more severe the ICP, the lower the water flux through FO membrane. Therefore, it is important to study how K varies with different solutes.

The literature has well explained theories to predict the effective diffusion coefficient, D_{eff}, in the presence of a single salt (Tan and Ng, 2008, Loeb et al., 1997, Cath et al., 2006). When multiple salts are present, the effective diffusivity is completely different due to mutual diffusion, ionic size, charge of the solute and properties of the porous media (Miller et al., 2007, Mathew et al., 1989, Holloway et al., 2015). Therefore, this study is carried out to evaluate the value of D_{eff} in the presence of multiple solutes. The D_{eff} will be calculated for different selected salt mixtures, with the help of experimental and theoretical data. A semi-empirical relationship of D_{eff} with water flux will be obtained. The solute resistivity, K, and the structural constant, KD_{eff}, for each selected salt will be described.

4.2 Model Development

The literature has well documented procedures on how to model the flux through the FO membrane (Lee et al., 1981, Tan and Ng, 2008, Tang et al., 2010). Mathematical models proposed by various researchers consider the solute flux through the membrane in order to compute the effective osmotic pressure which is the driving factor in the FO process (McCutcheon and Elimelech, 2006). Models for predicting the water flux across an asymmetric FO membrane have been developed to take into account both external and internal concentration polarization (CP) effects. The following models were obtained based on the literature (Cath et al., 2006, McCutcheon and Elimelech, 2006, McCutcheon et al., 2006b, Tan and Ng, 2008, Gray et al., 2006, Loeb et al., 1997).

For AL-FS mode:

The water flux, J_w is given by,

$$J_w = A\sigma\left(\pi_{F,i} - \pi_{F,m}\right) \quad (2)$$

Where, A is the permeability coefficient, σ is the reflection coefficient, $\pi_{F,i}$ and $\pi_{F,m}$ are osmotic pressures at the membrane interface and the membrane surface that is facing the feed stream, respectively.

$$\pi_{F,m} = \pi_{F,b}\exp(-\frac{J_w}{k_f}) \quad (3)$$

Where, $\pi_{F,b}$ is the osmotic pressure of the bulk feed stream and k_f is the mass transfer coefficient of solute from the bulk feed stream to the surface of the membrane. Similarly, $\pi_{F,i}$ can be related to the osmotic pressure of the bulk draw solution, $\pi_{D,b}$ as below:

$$\pi_{F,i} = \pi_{D,b}\exp(-J_w K_D) \quad (4)$$

Where, K_D is the solute resistivity. Thus, equation (2) can be rearranged to:

$$J_w = A\sigma[\pi_{D,b}\exp(-J_w K_D) - \pi_{F,b}\exp(-\frac{J_w}{k_f})] \quad (5)$$

Similarly, for AL-DS mode, J_w can be given by:

$$J_w = A\sigma\left[\pi_{D,b}\exp\left(-\frac{J_w}{k_d}\right) - \pi_{F,b}\exp(-J_w K_F)\right] \quad (6)$$

Where, k_d *is* the mass transfer coefficient of solute from the membrane to the bulk draw stream. K_D and K_F are solute resistivity values for AL-DS and AL-FS modes, respectively, and can be obtained from the following equations:

$$K_D = \left(\frac{1}{J_w}\right) ln\left[\frac{B+A\pi_{D,b}}{B+J_w+A\pi_{F,m}}\right] \quad (7)$$

$$K_F = \left(\frac{1}{J_w}\right) ln\left[\frac{B+A\pi_{D,b}-J_w}{B+J_w+A\pi_{F,m}}\right] \quad (8)$$

Where, B is the salt permeability coefficient. When de-ionized water and brine solutions are used as feed and draw solutions, respectively, equations (5) and (6) can be simplified to the following forms:

AL-FS mode: $J_w = A\pi_{D,b}\ exp(-J_w K_D)$ (9)

AL-DS mode: $J_w = A\pi_{D,b} exp(-J_w/k_d)$ (10)

While equation (10) will allow computing the mass transfer coefficient k_d using the experimental flux, equation (9) will help to compute the solute resistivity, K_D. By using the k_d, the effective diffusion coefficient, D_{eff} of solutes present in the brine solution can be estimated. Similarly, computing $K_D D_{eff}$ will help to find the structural constant of the FO membrane using the equation (1). In this approach, values of solute rejection, R, and the salt permeability coefficient, B, are not required to compute K_D and D_{eff}.

4.4 Forward Osmosis Experiments

Flat sheet CTA membranes with a woven, embedded support backing and average pore diameter of 0.74 nm (Xie et al., 2012) were purchased from Hydration Technologies Inc (HTI), USA. Prior to the membrane separation, pH, temperature and electrical conductivity (EC) of feed (de-ionized water) and draw solutions (K_2SO_4, Na_2SO_4, NaCl, $MgCl_2$, K_2SO_4 + $MgCl_2$ + Na_2SO_4, K_2SO_4 + $MgCl_2$, K_2SO_4 + Na_2SO_4, $MgCl_2$ + Na_2SO_4, diluted brine solutions and diluted seawater solutions) were measured. All the single, dual and triple salt solutions' final concentrations were fixed to be 30 g/L which is in the range of seawater salinity. Mixed concentrations, according to the equivalent molar ratio of each salt, are given in Table 13.

Further, brine and seawater solutions were diluted to 0, 25, 50, 75 and 100% using de-ionized water in order to have a range of salt concentrations.

Table 13: Salt solution mixing ratios

Salt solution	Final concentration (g/L)	Mixing ratio (g/L)
K_2SO_4	30	30
$MgCl_2$	30	30
Na_2SO_4	30	30
K_2SO_4 + $MgCl_2$ + Na_2SO_4	30	7.4 + 13.5 + 9.1
K_2SO_4 + $MgCl_2$	30	10.6 + 19.4
K_2SO_4 + Na_2SO_4	30	13.5 + 16.5
$MgCl_2$ + Na_2SO_4	30	18.0 + 12.0
NaCl	30	30

Feed and draw solutions were passed through the membrane at ambient temperature (20 ^oC) at a rate of 0.50 m/s cross flow velocity in counter current flow configuration. Change in the weight of the draw solution was programmed to be stored in a data logger at one minute time intervals. Experimental water flux ($J_{w,e}$) was calculated. During 1 hour of membrane filtration, properties of the feed and draw solutions (pH, EC and temperature) were measured at every 10 min. Experiments were run in both AL-DS and AL-FS modes to aid structural parameter calculations. A new membrane coupon was used for each salt solution. Density, viscosity and osmotic pressure of each salt solution and salt mixture were obtained using the OLI® stream analyzer and reported in Table 14. With the help of experimental and theoretical data, effective diffusion coefficients of draw solutions were calculated.

Table 14: Properties of draw solutions prior to membrane filtration

Draw solution	Conductivity, EC (mS/cm)	Density, ρ (kg/m^3)	Viscosity,μ (Pa·s)	Osmotic pressure $P_{D,b}$ (bar)
1. Seawater				
100% dilution	28.55	1024.2656	0.001027	14.27
75% dilution	32.40	1024.2656	0.001027	16.19
50% dilution	37.13	1023.6881	0.000981	18.54
25% dilution	42.60	1023.6881	0.000981	21.32
0% dilution	52.95	1023.6881	0.000981	26.10
2. RO concentrate				
100% dilution	36.90	1024.2656	0.001027	17.96
75% dilution	43.45	1023.9808	0.001004	20.18
50% dilution	45.75	1023.9808	0.001004	23.27
25% dilution	55.43	1024.2656	0.001027	26.53
0% dilution	67.33	1023.9808	0.001004	33.03
3. Salt solution				
$K_2 SO_4$	30.40	1023.19	0.001266	8.53
$MgCl_2$	45.70	1025.13	0.001390	22.11
Na_2SO_4	29.50	1026.53	0.001335	10.25
$K_2 SO_4 + MgCl_2 + Na_2SO_4$	34.90	1024.29	0.001343	14.17
$K_2 SO_4 + MgCl_2$	41.60	1019.43	0.001317	12.10
$K_2 SO_4 + Na_2SO_4$	28.80	1026.05	0.001307	8.85
$MgCl_2 + Na_2SO_4$	38.60	1025.26	0.001370	16.78
NaCl	45.70	1021.04	0.001278	22.38

4.5 Results and Discussion

4.5.1 FO Experiments Results

Concentraton polarisation (CP) effects on the draw solution sides are dilutive external concentration polarization (DECP) (in AL-DS mode) and combined DECP and dilutive internal concentration polarization (DICP) (in ALFS mode). Since de-ionized water was used as feed, concentrative external concentration polarization (CECP) and concentrative internal concentration polarization (CICP) effects on the feed solution sides were minimized (or negligible) in these experiments.

Experimental water flux at each mode was calculated and is shown in Figure 21. Higher water flux was observed under AL-DS mode compared to AL-FS mode, as expected (Zhao et al.,

2011), for all 3 types of draw solutions. Zhao et al (Zhao et al., 2011) reports that membrane orientation is basically influenced by the feed solution composition and the concentration degree (i.e., concentration factor or water recovery). Further, AL-DS mode is preferable when using the solutions with low salinity feed. Since the feed solution is DI water in this study, AL-DS mode showed better performance with regards to the water flux.

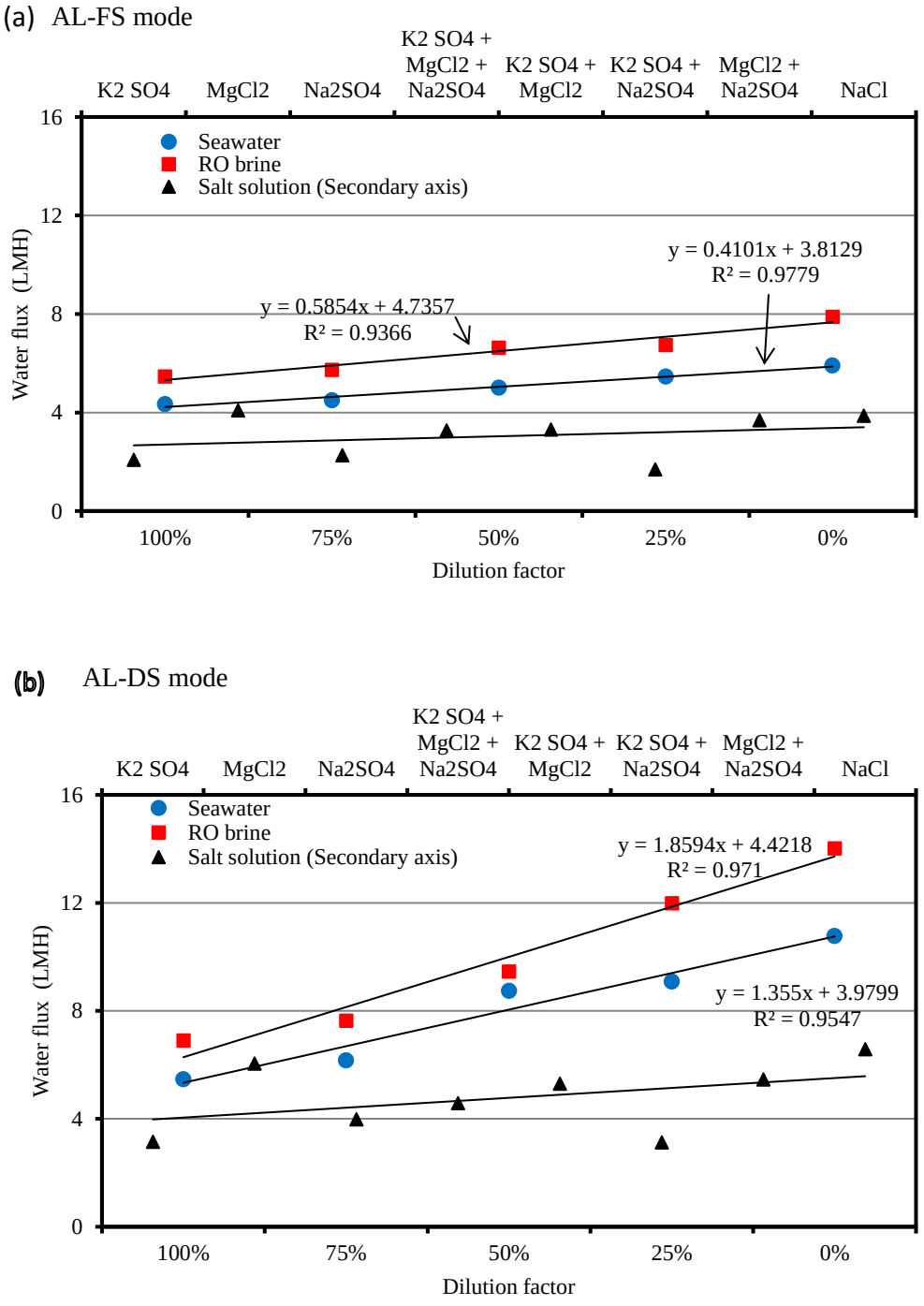

Figure 21: Water flux obtained at (a) AL-FS and (b) AL-DS configurations.

Further, in AL-FS mode, ICP is severe as all the draw solutes are passing through porous side of the membrane. This gives a lower water flux in AL-FS mode compared to AL-DS. The rate of increase in water flux when brine and seawater concentration increase, is lower in AL-FS mode. This is evidenced as the gradient of increase in water flux with draw solution concentration at AL-FS and AL-DS modes are 0.58 and 1.86, respectively for RO brine and 0.41 and 1.35 for Seawater, respectively. Overall, AL-FS mode gradient is one third of the gradient as AL-DS mode. Even though a correlation cannot be obtained for single, dual and triple salt solutions, similar to the previous two types of draw solutions, AL-DS mode flux is higher compared to AL-FS mode. Higher number salts in the draw solution gives higher flux compared to single salt draw solutions.

4.5.2 Prediction of Effective Diffusion Coefficient

The pure K_2SO_4 (30 g/L) data were chosen from Tables 13 and 14 and step by step specimen calculations are given in the appendix section. Similarly, effective diffusion coefficient for each salt solution was calculated. The calculated effective diffusion coefficient, solute resistivity, mass transfer coefficient, Reynolds number, and structural coefficients are given in Table 15.

Calculated D_{eff} values were plotted for each salt solution and given in Figure 22. The D_{eff} for single, dual and triple salt solutions is significantly lower compared to those for seawater and brine solutions. Higher number of salts in the mixture and higher concentration leads to a higher D_{eff} value. The 0%, 25%, 50% diluted brine showed up to 4.5×10^{-6} cm^2/s and 0%, 25% diluted seawater showed up to 3×10^{-6} cm^2/s D_{eff} values. When the concentration of salt mixtures is low, the D_{eff} is lower.

Table 15: Calculated effective diffusion coefficients and structural constants for each salt solution.

Draw solution	Solute resistivity, K_D (s/m)	Mass transfer coefficient, k_d (m/s)	Reynolds number, *Re*	Effective diffusion coefficient, D_{eff} (cm^2/s)	Structural coefficient, $K_D D_{eff}$ (m)
1. Seawater					
100% (dilution)	7.13E+05	2.40E-06	1558.4	8.15E-07	5.81E-05
75% (dilution)	7.63E+05	2.69E-06	1558.4	9.69E-07	7.39E-05
50% (dilution)	7.06E+05	5.73E-06	1630.5	3.00E-06	2.11E-04
25% (dilution)	6.83E+05	4.81E-06	1630.5	2.31E-06	1.57E-04
0% (dilution)	7.03E+05	5.38E-06	1630.5	2.72E-06	1.92E-04
2. RO concentrate					
100% (dilution)	5.68E+05	3.05E-06	1558.4	1.17E-06	6.63E-05
75% (dilution)	5.84E+05	3.30E-06	1593.6	1.31E-06	7.67E-05
50% (dilution)	5.02E+05	4.60E-06	1593.6	2.16E-06	1.08E-04
25% (dilution)	5.56E+05	7.14E-06	1558.4	4.16E-06	2.31E-04
0% (dilution)	5.04E+05	7.37E-06	1593.6	4.36E-06	2.20E-04
3. Salt solution					
$K_2 SO_4$	1.87E+06	1.31E-06	324.8	4.30E-07	8.03E-05
$MgCl_2$	1.20E+06	1.73E-06	296.3	6.54E-07	7.83E-05
Na_2SO_4	1.88E+06	1.79E-06	309.1	6.84E-07	1.29E-04
$K_2 SO_4 + MgCl_2 + Na_2SO_4$	1.25E+06	1.59E-06	306.6	5.73E-07	7.15E-05
$K_2 SO_4 + MgCl_2$	1.05E+06	2.97E-06	311.2	1.46E-06	1.53E-04
$K_2 SO_4 + Na_2SO_4$	2.82E+06	1.22E-06	315.6	3.86E-07	1.09E-04
$MgCl_2 + Na_2SO_4$	1.16E+06	1.91E-06	300.8	7.54E-07	8.74E-05
NaCl	1.33E+06	2.04E-06	321.0	8.32E-07	1.10E-04

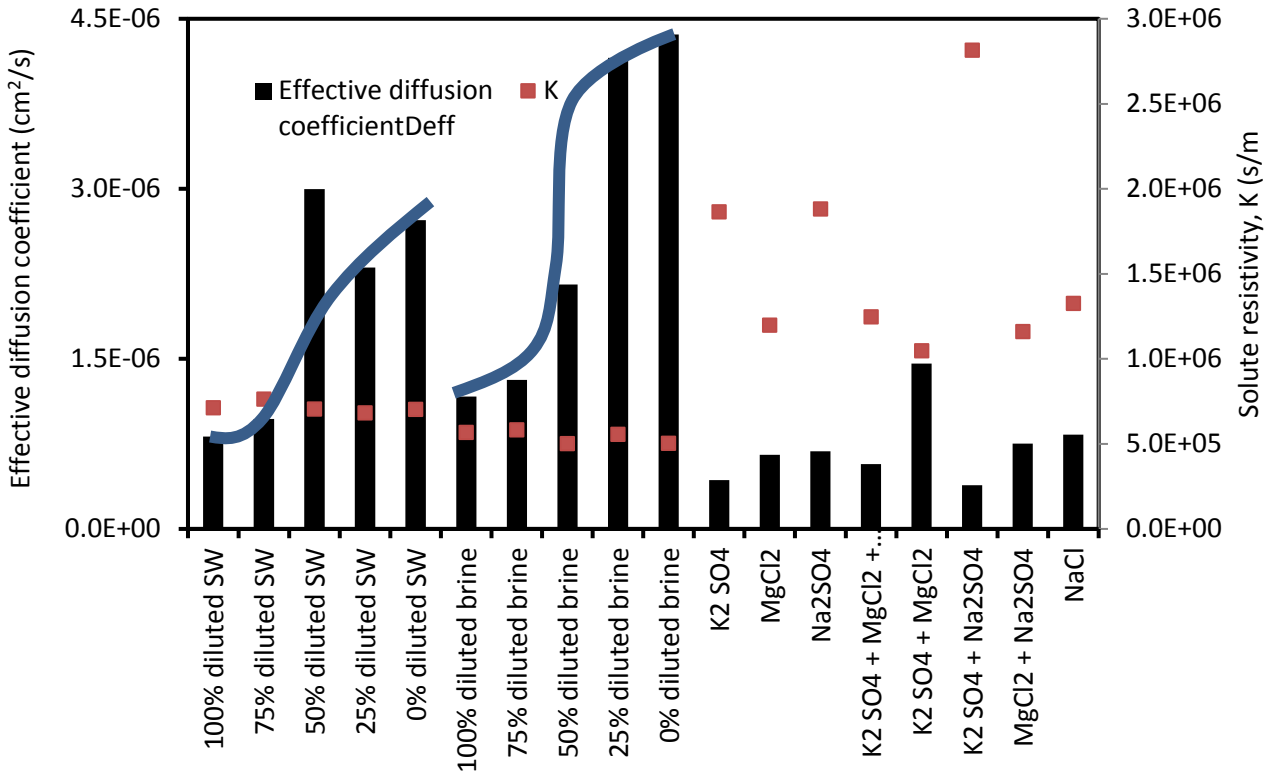

Figure 22: Effect of salt on Deff with corresponding solute resistivities.

Irrespective of salt combinations, a relationship of D_{eff} with water flux was developed. Change in water flux is plotted against the effective diffusion coefficient in AL-FS and AL-DS modes (Figure 23). At higher effective diffusion coefficient values, a higher water flux was observed in both modes. The correlation of water flux and D_{eff} is given by the two trend lines displayed in Figure 23.

Figure 23(a) shows the AL-FS mode results. The logarithmic semi-empirical relationship of water flux (J_w) and effective diffusion coefficient (D_{eff}), displayed using dotted line, has the coefficient of determination, R^2, value of 0.7753 and is given below.

$$J_w = 1.995\, ln\left(D_{eff}\right) + 31.72 \qquad (11)$$

As the semi-empirical relationship predicts, at lower D_{eff} values lower fluxes could be observed. However, when D_{eff} is higher, the rate of increase in water flux is low. This could be due to higher reverse salt flux as D_{eff} is higher.

Figure 23(b) shows the AL-DS mode results and its semi-empirical relationship is given in equation (12). AL-DS mode shows a better fit in logarithmic mode compared to AL-FS mode with a R^2 value of 0.8843. However, similar to ALFS mode, as D_{eff} gets higher, increase in rate of water flux becomes lower.

$$J_w = 3.784\, ln\left(D_{eff}\right) + 58.67 \qquad (12)$$

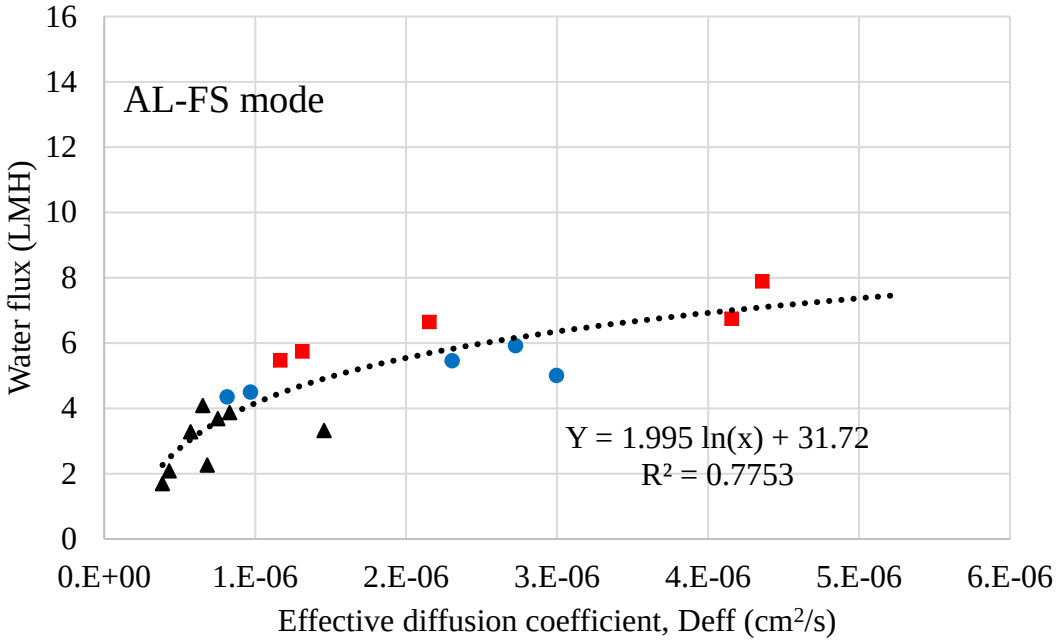

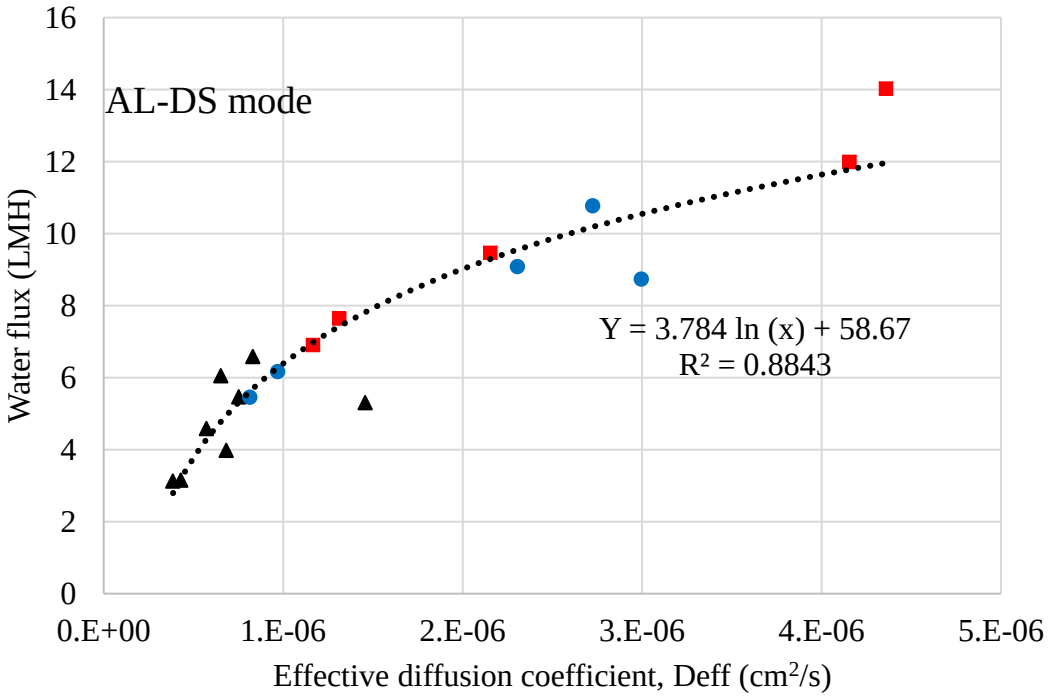

Figure 23: Correlation of (a) AL-FS mode and (b) AL-DS mode water flux and effective diffusion coefficient. ▲- salt solution ■ - RO brine and ●- seawater.

Semi-empirically obtained solute resistivity values were plotted and given in Figure 24. SO_4^{2-} solutions (either single or dual) show higher solute resistivity than Cl^- solutions. This higher resistivity would have reduced the ICP effect and therefore higher water flux can be obtained. However, in this study as final weight concentrations were kept constant, due to the variation in osmotic pressure of draw solutions this phenomenon cannot be seen in the results. A separate study with similar osmotic pressure draw solutions will help to understand this clearly.

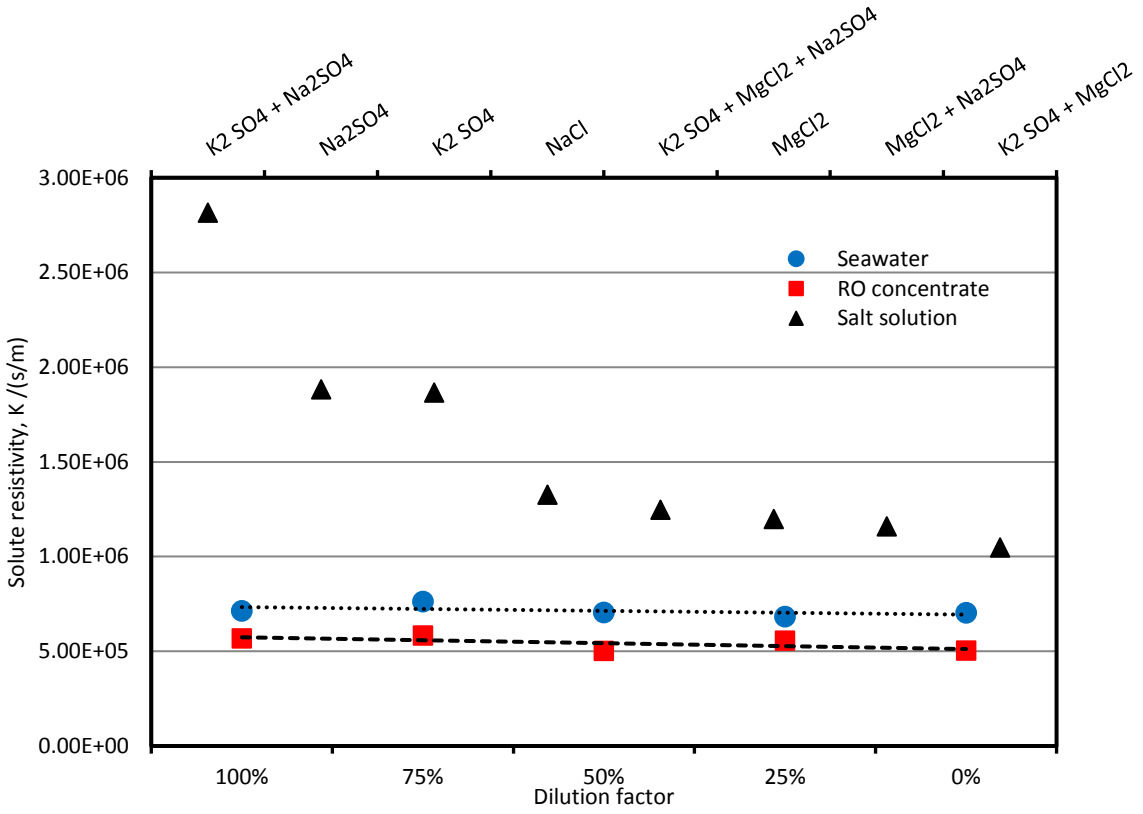

Figure 24: Solute resistivity of seawater, RO concentrate and salt solutions.

However, blending SO_4^{2-} with Cl^- reduced the solute resistivity. Ionic size of SO_4^{2-} and Cl^- are 0.149 and 0.181 nm, respectively. Since lower ionic sizes provide higher water and salt flux (Touati and Tadeo, 2016) SO_4^{2-} should have shown better performance than Cl^-. As shown in Figure 21, water flux increases when higher Cl^- ions are blended with smaller SO_4^{2-}ions.

The structural coefficient of the FO membrane $K_D D_{eff}$ ($= t\tau/\varepsilon$) can vary with the concentration of the solutes as τ and ε can be altered according to those concentrations. The porosity and the tortuosity can be varied with filtration time depending on the sizes of the solute ions. Therefore, we cannot expect the structural coefficient to be constant for any salt solution. As Figure 25 shows, the higher number of salts as well as higher concentrations (0% and 25% diluted brine) showed the highest $K_D D_{eff}$ values ($> 2\times10^{-4}$ m) compared to other salt solutions. Further, 0% diluted seawater also has a higher $K_D D_{eff}$ value, i.e., 1.92×10^{-4} m. the single, dual and triple salt solutions show comparatively lower structural coefficients.

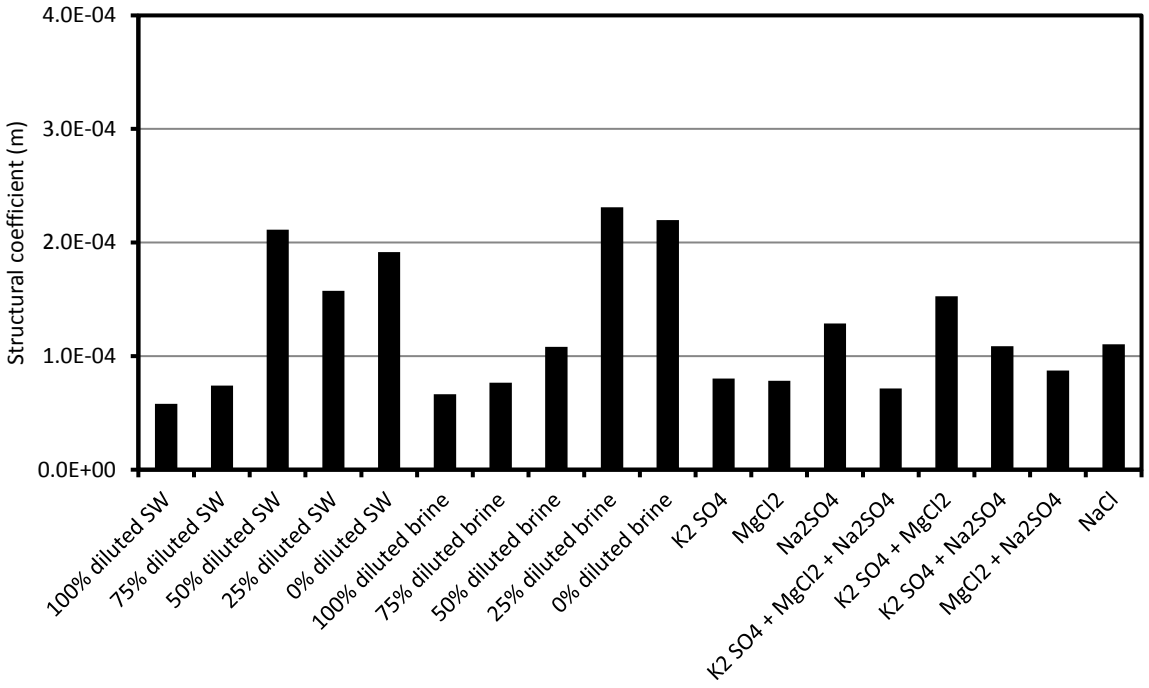

Figure 25: Structural coefficient of different salt solutions

4.6 Conclusions

FO membrane was characterised in this part of study. A semi empirical relationship to predict the effective diffusion coefficient of FO membrane was proposed. Following conclusions were made through this part of study.

1. Regardless of salt combination, a relationship of D_{eff} versus water flux was obtained at AL-FS and AL-DS modes.
2. Higher solute concentrations and higher number of solutes in draw solution showed higher effective diffusion coefficient values.
3. Solute resistivity of SO_4^{2-} ions lowered when it is blended with lower molecular size Cl^- ions.
4. The semi-empirical results showed that the structural coefficient, $K_D D_{eff}$, varies depending on the type of the salt as well as its concentration.

Chapter 5: Optimising the Water Flux through Flat Sheet FO Membrane

5.1 Effect of Cross Flow Velocity

Corresponding publication: Liyanaarachchi, S., V. Jegatheesan, L. Shu, S. Muthukumaran and K. Baskaran (2014). A preliminary study on the volume reduction of pre-treatment sludge in seawater desalination by forward osmosis, Desalination and Water Treatment 52(4-6): 556-563 (Liyanaarachchi et al., 2014b).

5.1.1 Introduction

Pre-treatment is one of the most important processes in a seawater desalination process. Seawater is pre-treated to remove suspended particles, organic matter and microorganisms. However, more research and development is needed in this area as current desalination facilities experience various practical issues. Generation of high volume of sludge is the major practical issue associated with the available pre-treatment methods. Sludge undergoes centrifugal process during which high amount of energy is consumed to reduce its volume before being discharged. Furthermore, disposal and transportation of sludge accounts for more than 90% of the total operation and maintenance cost. Therefore, reduced sludge volume undoubtedly reduces the associated expense of pre-treatment and hence the total operational cost.

The osmotically driven membrane process, Forward Osmosis (FO) or pressure retarded Osmosis (PRO), is believed to be a promising emerging technology to reduce the volume of pre-treatment sludge. Fertiliser drawn FO desalination (FDFO) has been successfully applied at lab scale to dilute fertilisers while concentrating saline ground water (Phuntsho et al., 2012). FO membranes have been used to dilute seawater using secondary wastewater effluent as draw solution, in order to reduce the energy cost associated with desalination (Yangali-Quintanilla et al., 2011). A few studies have been carried out to treat landfill leachate, food industry effluent, and to increase the water recovery of RO (Petrotos et al., 1999, Achilli et al., 2009, Martinetti et al., 2009). FO has been given significant attention over the past few years due its superior characteristics such as high feed water recoveries (~ up to 85%), operates at low or no hydraulic pressure with a lower electrical consumption (~0.25 kWh/m^3 of product water) and lower membrane fouling tendency compared to other membrane treatments (McGinnis and Elimelech, 2007, Lee et al., 2010b, McCutcheon et al., 2005). However, this technology is still in the development stage either in bench scale or pilot plant scale (Elimelech, 2007, Cath et al.,

2006). In the literature, there were no reports which evaluated the capability of FO to reduce the volume of pre-treatment sludge of seawater reverse osmosis (SWRO) process.

Therefore, the effect of concentration of draw solution in the reduction of volume of the $Fe(OH)_3$ sludge generated in the pre-treatment for the SWRO process, and the effect of cross flow velocity on water flux were investigated in this study. Furthermore, experimental and theoretical water fluxes were compared using available literature.

5.1.2 Materials and Methods

Flat sheet CTA membranes detailed in Section 3.1 were used. Feed solutions were $Fe(OH)_3$ sludge (~ 25% TS) from the Perth Seawater Desalination Plant (PSDP), Australia. NaCl and $MgCl_2$ were selected as draw solutions and their properties are summarized in the Figure 26. Seawater (Table 14) was used to dilute the $Fe(OH)_3$ feed from ~ 25% TS to ~ 4% TS. Feed and draw solutions were passed through the membrane at 0.25, 0.50 and 1.00 ms^{-1} cross flow velocities in counter current flow configuration as it provides constant osmotic pressure difference ($\Delta\pi$) along the membrane cell. Sludge was circulated on the porous side of the membrane and stirred at a constant rate during the experiment to eliminate settling of particles. FO experimental set up detailed in Section 3.2 (Figure 19) was used.

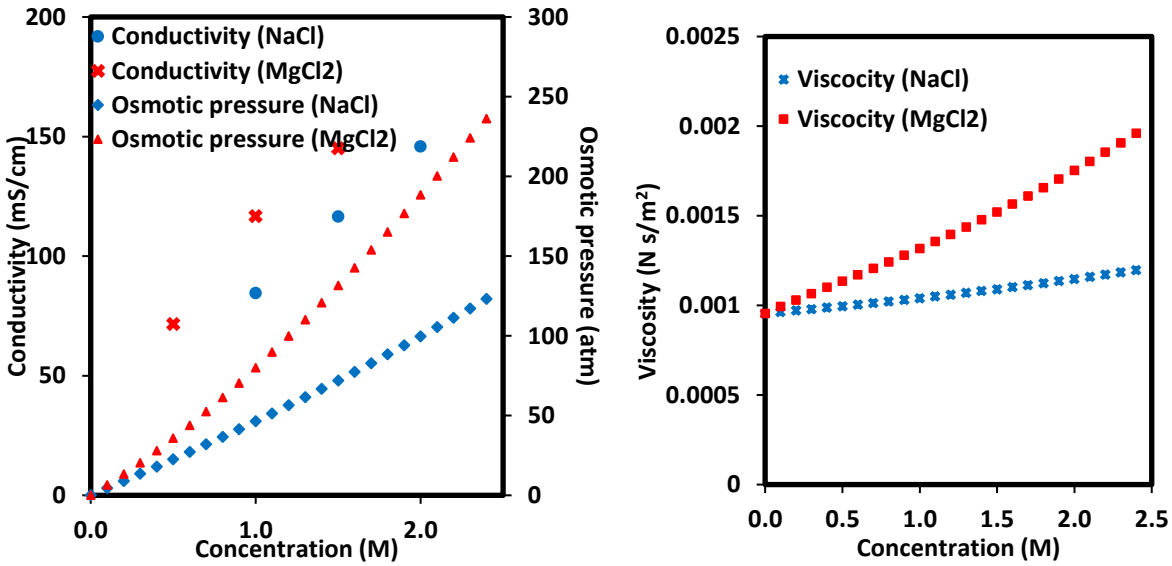

Figure 26: (a) Variation of conductivity (experimental data) and osmotic pressure (OLI Stream Analyser software data) and (b) viscosity (OLI Stream Analyser software data) of selected draw solutions with corresponding molar concentrations

5.1.3 Theoretical Water Flux Calculation

The driving force for the water permeation is osmotic pressure difference of two solutions; hence theoretical water flux through membrane can be calculated using equation (2) where, A, $\pi_{D,b}$, and $\pi_{F,b}$ are water permeability coefficient, bulk osmotic pressure of draw solution and bulk osmotic pressure of feed solution, respectively, as explained in Section 2.2.1.

$$J_{w,t} = A\left[\pi_{D,b} - \pi_{F,b}\right] \qquad (2)$$

However, in an osmotic process, on the feed side the polarised layer is more concentrated than bulk solution (with feed solutes). On the other side the polarised layer is less dense than the bulk draw solution (with draw solutes). This polarisation effect governs the overall water flux through membrane. Therefore, in the presence of concentration polarisation (CP), equation (2) can be modified as follows, where k_D and K are mass transfer coefficient in the draw solution side and solute resistivity for diffusion within the porous support layer, respectively.

$$J_{w,t} = A\left[\pi_{D,b}\exp\left(\frac{-J_{w,t}}{k_D}\right) - \pi_{F,b}\exp\left(J_{w,t}K\right)\right] \qquad (7)$$

This equation has proved in Section 2.2.1. First term in equation (7) accounts for the dilutive external concentration polarisation (ECP) on the active layer of the membrane and the second term accounts for the concentrative internal concentration polarisation (ICP) within the porous support layer. As noted earlier, when the feed solution is in contact with the support layer of the membrane, the mode of filtration is called active layer facing draw solution mode (AL-DS) mode and when it is in contact with the active layer of the membrane, the mode of filtration is called active layer facing feed solution mode (AL-FS) mode. Thus, equation (7) is applicable for AL-DS mode.

5.1.4. Results and Discussion

Effect of cross flow velocity on flux behaviour

Change in the water flux with elapsed time is given in Figure 27. There was a significant flux decline during 3 hours of filtration despite the change in cross flow velocity or draw solution concentration. When cross flow velocity of feed and draw solutions were maintained at 0.25 ms^{-1}, water flux with 1.0, 1.5 and 2.0 M NaCl draw solutions decreased after 3 hours by 18, 28 and 15%, respectively. At 0.5 ms^{-1} of cross flow velocity, water flux fluctuated significantly with time for both the draw solutions.

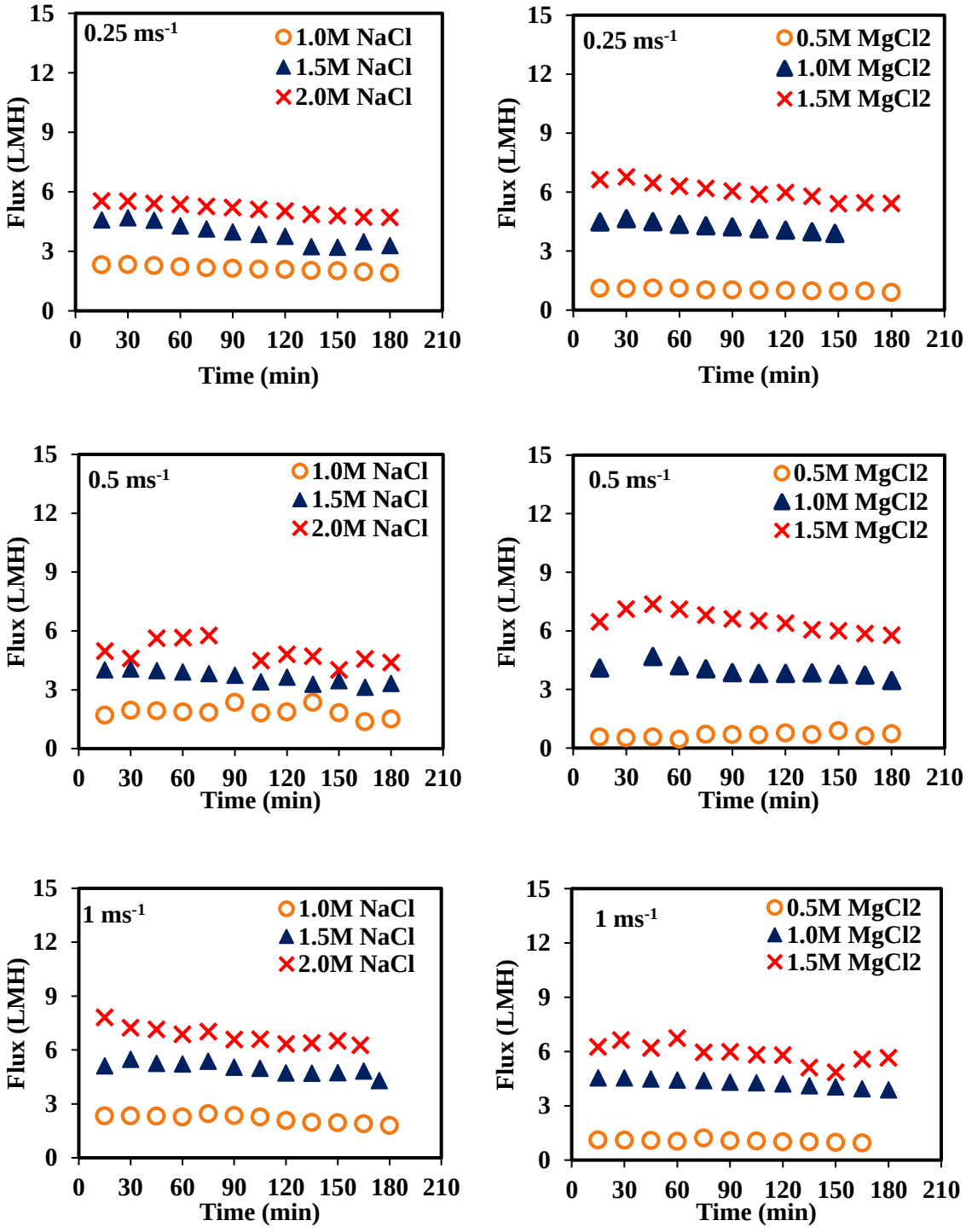

Figure 27: Change in water flux with filtration time at different concentrations of draw solution and different cross flow velocities

Average fluxes were calculated at corresponding cross flow velocity and draw solution concentration as shown in Figure 28. When the cross flow velocity increased from 0.25 ms^{-1} to 0.5 ms^{-1}, there was no significant change in the flux. However, there was a marginal increase in the water flux, when the cross flow velocity was increased to 1 ms^{-1}. Increase in the cross

flow velocity could reduce the dilutive ECP of the membrane due to increase in turbulence along the membrane active layer surface. However, the effect of cross flow velocity on the dilutive external CP is not significant due to inherent lower water flux in FO membrane (Cath et al., 2006). The marginal increase in water flux could be due to this phenomenon. This was observed at each concentration of draw solution. At the lowest concentrations of the draw solutions (0.5M $MgCl_2$ and 1M NaCl) the flux increased only by 4% and 2%, respectively, when cross flow velocity increased from 0.25 to 1 ms^{-1}. However, water flux increased from 5.13 LMH to 6.80 LMH (i.e. 33% increase) with the increase in cross flow velocity from 0.25 ms^{-1} to 1 ms^{-1} at highest concentration of the draw solution (2M NaCl).

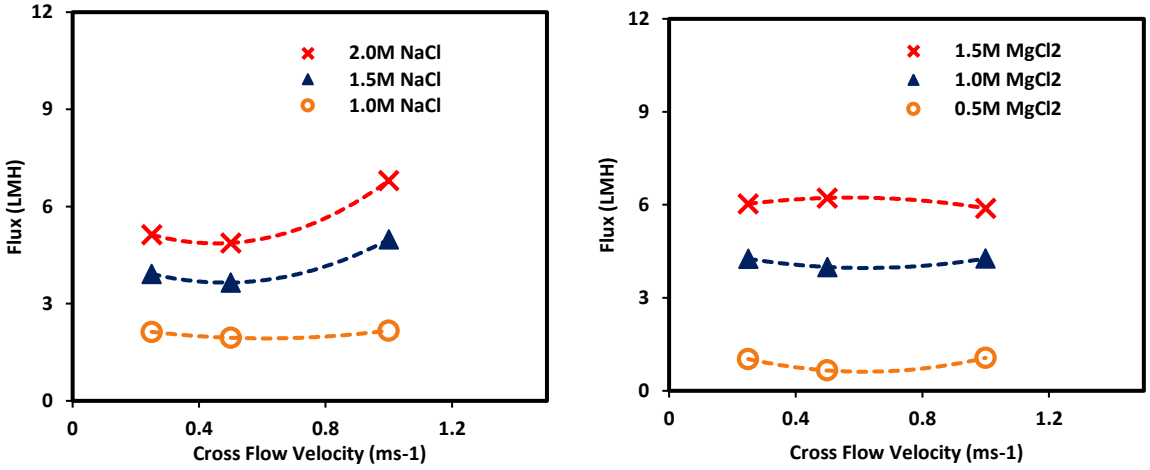

Figure 28: Average water flux as a function of cross flow velocity at different concentrations of draw solution.

A higher concentration of draw solution could draw a higher flux. However, the effect of dilutive ECP along the dense side of the membrane will become higher when the flux is higher which in turn will reduce the flux. A lower than expected flux at higher concentration of draw solution is explained by this phenomenon. Thus, it is evident that effect of cross flow velocity is not significant to change the water flux from the feed that contained $Fe(OH)_3$ sludge. Altering ECP by changing cross flow velocity may affect the solute flux through the FO membrane (Hancock and Cath, 2009). However, solute flux was not examined in this preliminary study.

Effect of internal concentration polarisation on water flux

The higher the concentration of draw solution, the higher the flux obtained. Due to the higher osmotic pressure of $MgCl_2$ solution than NaCl solution at the same molar concentration, higher flux was expected from former draw solution. However, there was no significant increase in

the flux. Higher draw solution concentrations generate higher osmotic driving forces and hence produce more water flux. However, higher water fluxes increase the severity of concentrative ICP as interface of porous support layer and dense layer of the membrane gets more concentrated (McCutcheon et al., 2006b). Therefore, significant increase in flux could not be obtained with increasing osmotic pressure. In order to evaluate the flux behaviour in the presence of concentrative ICP, water flux was plotted as a function of normalised driving force, as shown in Figure 29. The logarithmic water flux trend in the plot implies that higher normalized driving forces caused by higher draw solution concentrations reduce the increment in water flux. This could be due to increase in severity of concentrative ICP with increase in water flux. Furthermore, viscosity of the draw solution and diffusivity of the solutes controls the water flux through membrane (Hancock and Cath, 2009). The viscosity of the $MgCl_2$ solution is higher than NaCl solution at a specific molar concentration (Figure 26b), and the diffusivity of $MgCl_2$ (1.05×10^{-9} m^2/s) is lower than NaCl (1.48×10^{-9} m^2/s). This could result in a CP effect that would reduce the permeate water flux through the membrane (Hancock and Cath, 2009, Achilli et al., 2010, Cath et al., 2013b). In a study on FO mode conducted by Hankok and Cath (2009), the lower diffusion coefficient of magnesium compared to sodium (as draw solution) increased the severity of ICP and the higher viscosity of $MgCl_2$ (at the same osmotic pressure) increased the severity of ECP. As reported elsewhere, one of the major negative impacts for further development of osmotically driven membrane process is the ICP (Cath et al., 2013b).

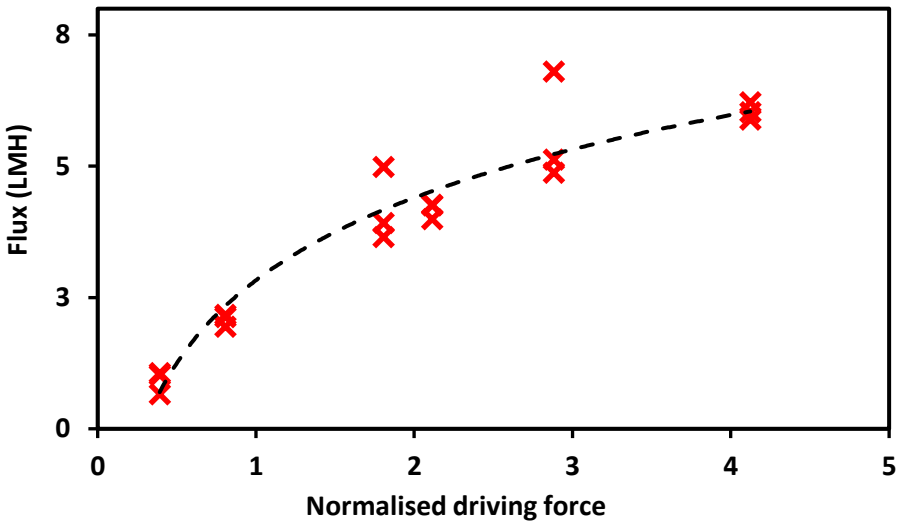

Figure 29: Permeate flux as a function of normalised driving force, $\frac{\pi_{D,b}-\pi_{F,b}}{\pi_{F,b}}$, where $\pi_{D,b}$ and $\pi_{F,b}$ are bulk osmotic pressure of the draw and the feed solution, respectively.

Comparison of experimental flux data with theoretical values

Theoretical flux was calculated using equation (2) (Table 16) Performance ratio declines with increase in draw solution concentration despite the change in cross flow velocity. Equation (2) over predicts the flux as it does not consider the concentration polarisation effect and hence lower performance ratio. However, when equation (7) is used to compute the flux we were unable to find a solution. Our laboratory experiments produced the value for water permeability coefficient (A) as 2.3015×10^{-7} m /s atm which did not allow the flux value to converge while solving equation (7). When lower values were used for A, equation (7) converged to obtain a value for the flux. This needs further investigation. The values used to solve equation (7) are shown in Table 17.

Table 16: Osmotic pressure, theoretical and experimental flux and performance ratio of each draw solution

Concentration of draw solution (M)		Cross flow velocity, V (m/s)	Bulk π of draw solution (atm)	Bulk π difference ($\boldsymbol{\pi_{D,b} - \pi_{f,b}}$) (atm)	Normalised driving force $\frac{(\boldsymbol{\pi_{D,b} - \pi_{f,b}})}{\boldsymbol{\pi_{f,b}}}$	Flux, $\boldsymbol{J_{w,e}}$ (expt) (LMH)	Flux, $\boldsymbol{J_{w,t}}$ (equation (**2**)) (LMH)	Performance ratio
NaCl	1.0	0.25	46.39	20.5	0.79	2.13	17.00	0.13
	1.5	0.25	72.03	46.2	1.78	3.92	38.24	0.10
	2.0	0.25	99.64	73.8	2.85	5.13	61.11	0.08
	1.0	0.50	46.39	20.5	0.79	1.95	17.00	0.11
	1.5	0.50	72.03	46.2	1.78	3.65	38.24	0.10
	2.0	0.50	99.64	73.8	2.85	4.88	61.11	0.08
	1.0	1.00	46.39	20.5	0.79	2.17	17.00	0.13
	1.5	1.00	72.03	46.2	1.78	4.99	38.24	0.13
	2.0	1.00	99.64	73.8	2.85	6.80	61.11	0.11
$MgCl_2$	0.5	0.25	35.72	9.9	0.38	1.02	8.16	0.13
	1.0	0.25	79.93	54.1	2.09	4.26	44.78	0.10
	1.5	0.25	131.55	105.7	4.08	6.03	87.54	0.07
	0.5	0.50	35.72	9.9	0.38	0.66	8.16	0.08
	1.0	0.50	79.93	54.1	2.09	3.99	44.78	0.09
	1.5	0.50	131.55	105.7	4.08	6.22	87.54	0.07
	0.5	1.00	35.72	9.9	0.38	1.06	8.16	0.13
	1.0	1.00	79.93	54.1	2.09	4.27	44.78	0.10
	1.5	1.00	131.55	105.7	4.08	5.89	87.54	0.07

$\pi_{D,b}$ and $\pi_{F,b}$ are bulk osmotic pressures of draw and feed solutions, respectively. Normalised driving force = ($\frac{\pi_{D,b}-\pi_{F,b}}{\pi_{F,b}}$). Theoritical flux was calculated using equation (2). Perforemance ratio is the ratio between experimental flux and theoritical flux. Feed solution (sludge) bulk osmotic pressure ($\pi_{f,b}$) is assumed to be 25.9 atm.

Table 17: Coefficients used to solve equation (7)

	Draw solution concentration (M)				
	0.5	1.0	1.5	2.0	
k_D- Mass transfer coefficient in the $MgCl_2$ draw solution side ($\times 10^{-5}$ ms^{-1})					
At 0.25 ms^{-1}	1.1918	1.1918	1.1918		
At 0.50 ms^{-1}	1.4981	1.4981	1.4981		
At 1.00 ms^{-1}	4.9497*	4.6700*	4.3840*		
k_D- Mass transfer coefficient in the NaCl draw solution side ($\times 10^{-5}$ ms^{-1})					
At 0.25 ms^{-1}		1.5818	1.5818	1.5818	
At 0.50 ms^{-1}		1.9883	1.9883	1.9883	
At 1.00 ms^{-1}		7.1516*	7.0762*	6.9920*	
A- Water permeability coefficient at 22 ^oC ($\times 10^{-7}$ m/s.atm)					2.3015
K- Solute resistivity for diffusion within porous layer ($MgCl_2$) ($\times 10^5$ s/m)					2.8381
K- Solute resistivity for diffusion within porous layer (sludge) ($\times 10^5$ s/m)					2.0135

Note that all the experiments were run in PRO mode.

* turbulent flow.

5.1.5 Summary of this part of study

This section of the study investigated the effect of the concentration of two draw solutions ($MgCl_2$ and NaCl) in the reduction of $Fe(OH)_3$ sludge volume and the effect of cross flow velocity on flux through FO membrane. The higher the concentration of NaCl and $MgCl_2$, the higher the water flux observed. However, the percentage increase was not significant due to the occurrence of internal concentration polarisation (ICP). $MgCl_2$ draws marginally increased water flux than NaCl, when the conditions of feed and draw solutions were similar. Increase in cross flow velocity (from 0.25 to 1.0 ms^{-1}) marginally changed the flux with both draw solutions as higher cross flow velocities were unproductive to beat the external concentration polarisation (ECP) effect along the membrane surface. However, at 1 ms^{-1}, highest fluxes were obtained for both draw solutions.

Therefore, following conclusions were drawn after this preliminary study.

1. Increase in cross flow velocity (from 0.25 to 1.0 m/s) could not significantly reduce the presence of ECP, hence marginal increase in flux observed with increase in cross flow velocity.
2. Higher the concentration of draw solution higher the water flux obtained from the FO process.
3. Although $MgCl_2$ has a higher osmotic pressure than NaCl at the same molar concentration, there were no significant differences in water fluxes when $MgCl_2$ and NaCl were used as draw solutions. Higher viscosity of $MgCl_2$ (draw) solution and lower diffusivity of $MgCl_2$ (draw) solute control the water flux through membrane as both increase the severity of internal as well as external CP.

5.2 Effect of Temperature and Membrane Orientation

Corresponding publication: Liyanaarachchi, S, V. Jegatheesan, I. Obagbemi, S. Muthukumaran and L. Shu. Effect of feed temperature and membrane orientation on pre-treatment sludge volume reduction through forward osmosis. Desalination and Water Treatment,2015. 54(4-5): p. 838-844. (Liyanaarachchi et al., 2015).

5.2.1 Introduction

Seawater desalination process has significantly moved towards membrane technology during last decade. Seawater reverse osmosis (SWRO) in general is the most common process due to higher water recovery (~ up to 80 %) and lower energy consumption (~ 3- 4 kW h/m^3 of product water) compared to other desalination processes (Nooijen and Wouters, 1992, Ebrahim and Abdel-Jawad, 1994, Abou Rayan and Khaled, 2003, Misdan et al., 2012, Semiat, 2008). However, the greatest challenge in SWRO is to achieve higher water recoveries while minimizing operational costs associated with waste (*i.e.* pre-treatment sludge and brine) management.

Therefore, as stated earlier, this study focuses on brine management while reducing the volume of pre-treatment sludge from the SWRO process using forward osmosis (FO) technology. Figure 30 shows a typical existing SWRO system with main waste streams mentioned above. At present generated pre-treatment sludge (Q_1) undergoes centrifugation following a settling tank and brine (Q_2 and Q_3) discharged to sea or are get blended in the sewer lines thus diluting it before discharging to sea (Sadhwani et al., 2005, Greenlee et al., 2009).

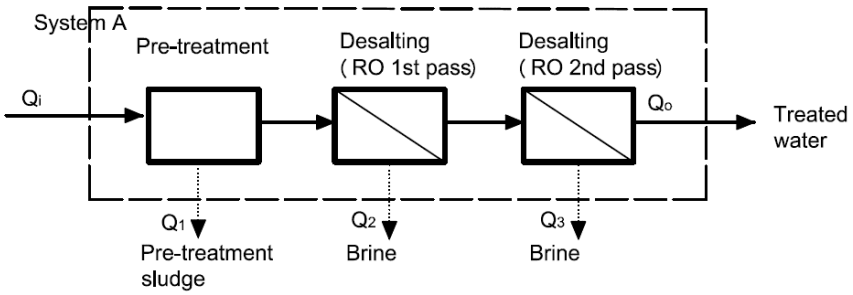

Figure 30: Schematic diagram of a typical existing SWRO system. Dotted lines show the waste streams during desalination process.

Previous Section (Section 5.1) showed that FO can be applied to dewater pre-treatment sludge (Liyanaarachchi et al., 2014b). However, regeneration of draw solution was an issue (NaCl and $MgCl_2$). Therefore in this section of the study brine was proposed as the draw solution since it has following advantages: (1) Diluted brine can be sent back to desalting process to increase the overall water recovery or (2) if brine is discharged back to sea, dilution is an added advantage as many brine disposal regulations are based on concentrations but not on volume (Ahmed et al., 2001). However, depending on the pre-treatment sludge generation method (backwashing of media filters are done using filtered seawater or RO reject), dewatering volume of sludge may vary as water permeation through FO depends on the concentration gradient of draw and feed solutions.

Therefore, two types of sludge at different concentrations were used as feed solutions in this study. Optimum feed temperature and effect of membrane orientation in the reduction of pre-treatment sludge volume using the proposed system was investigated.

5.2.2 Materials and Methods

The two types of pre-treatment sludge used as feed solutions were Laboratory prepared sludge (preparation process explained in Chapter 3) and actual industrial sludge obtained from Perth seawater desalination plant (PSDP sludge). RO brine which was prepared as explained in the Chapter 3 was used as draw solution.

FO experiments

FO experiments were run with flat sheet cellulose triacetate (CTA) membranes. Feed (Lab sludge or PSDP sludge) and draw solutions were passed through the membrane at 0.25 ms^{-1} cross flow velocities in counter current flow configuration. Feed was circulated on the porous side (AL-DS mode) as well as on the active layer side (AL-FS mode) of the membrane and stirred at a constant rate during the experiment to eliminate settling of particles. Feed temperature was varied from 20, 30 and to 40 ^{o}C and a new membrane sheet with an effective area of 33.54 cm^2 was used for each experiment. Change in the weight of the draw solution with filtration time was programmed to be stored in a data logger at 15 min time intervals. Experimental water flux ($J_{w,e}$) was determined by using equation (16). Properties of the feed and draw solutions were measured at every 15 minutes for 2 hours of filtration.

5.2.3 Results and Discussion

Properties of initial seawater, pre-treated seawater, DMF backwash water (Lab sludge), RO permeate, and RO concentrate are given in Figure 31. Backwashed water (Lab sludge) contains 1% of total solids with a marginally higher TOC compared to initial seawater (from 1.71 to 1.94 mg/L). However, filtered seawater contains significantly lower amount of TOC (0.73 mg/L) with 98% turbidity reduction (from 29.1 to 0.45 NTU). Since DMF removes dissolved organics and suspended solids, the EC of initial and filtered seawater was practically unchanged, i.e., 44.5 and 44.7 mS/cm, respectively. However, after passing through the spiral wound RO system, conductivity of RO reject (concentrate) increased to 73.0 mS/cm. The TOC of the concentrate became four times higher than that of the filtered water.

Particle size distributions of Lab sludge and PSDP sludge are shown in Chapter 3. Distribution of PSDP sludge particles is wider compared to Lab sludge. Majority of PSDP sludge contains 24.8 - 33.6 µm particles whereas Lab sludge contains 34.7 -39.8 µm particles. Temperature of Lab sludge and PSDP sludge were changed from 20, 30 to 40 ^{o}C. Change in water flux with elapsed time is given in Figure 32. There was a significant flux decline during 2 hours of filtration despite the change in temperature or orientation of membrane. Average water fluxes were calculated at corresponding temperatures and given in Figure 33. Results for each mode will be discussed in the following sections separately.

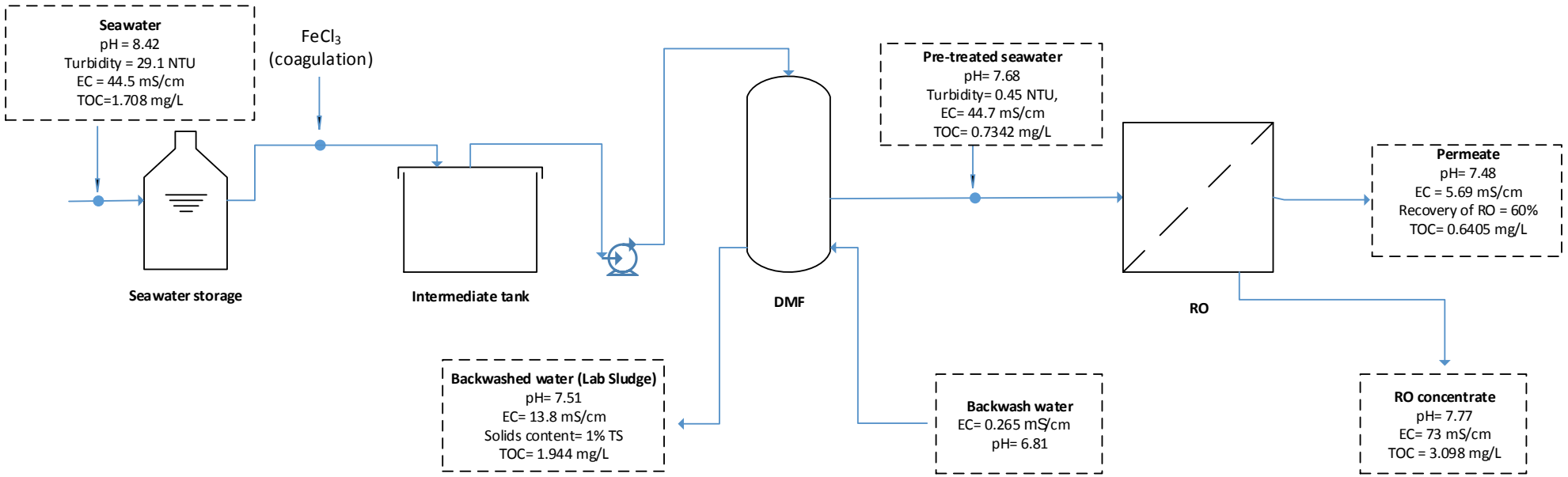

Figure 31: Properties of initial seawater, pre-treated seawater and pre-treatment sludge prepared at lab scale. TOC and EC denote for Total Organic Carbon and Electrical Conductivity, respectively. All the samples were prepared as batches.

Water flux in AL-DS mode

Water flux for PSDP and Lab sludge were approximately similar at 20 ^{o}C. However, there was a significant increase in water flux with increased temperature for Lab sludge. When temperature of feed solution was increased from 20 to 40 ^{o}C, water flux was 3 times greater at higher temperature (Figure 32). Decreased viscosity at elevated temperatures would have enhanced the water flux through the membrane. However, on the contrary, there was no significant change in water flux at increased feed temperatures for PSDP sludge. Even though both Lab sludge and PSDP sludge contain $Fe(OH)_3$, PSDP sludge contains more constituents such as coagulant aids, process control chemicals (pH controllers, anti-scalants, sodium metabisulphite etc) (VOLLPRECHT, 2013). Furthermore, increase in temperature would have increased the mobility of ions in the feed solution. These dissolved ions may have increased the severity of the internal concentration polarisation (ICP) effect at higher temperatures (since feed solution was facing the porous support layer), hence no significant increase in flux resulted.

When experiments were conducted at elevated temperatures (40 ^{o}C) of feed solution (both lab and PSDP sludge), the temperature of the draw solution was initially kept at 20 ± 2 ^{o}C. During experiments, the temperature of the draw solution increased by 8 ^{o}C over a period of 2 hours and the volume of the draw solution increased due to ~30 mL of water permeate. Thus, the increase in the osmotic pressure on the draw side was negligible. While the osmotic pressure of the feed would have increased at higher temperatures, the viscosity will have reduced. Increase in flux at higher temperatures for lab sludge as feed indicates that the effect of viscosity is dominant over the effect of osmotic pressure. This should be the same for the PSDP sludge as feed. However, the flux did not increase when the temperature of the PSDP sludge was increased. It may be mainly due to the fouling of PSDP sludge.

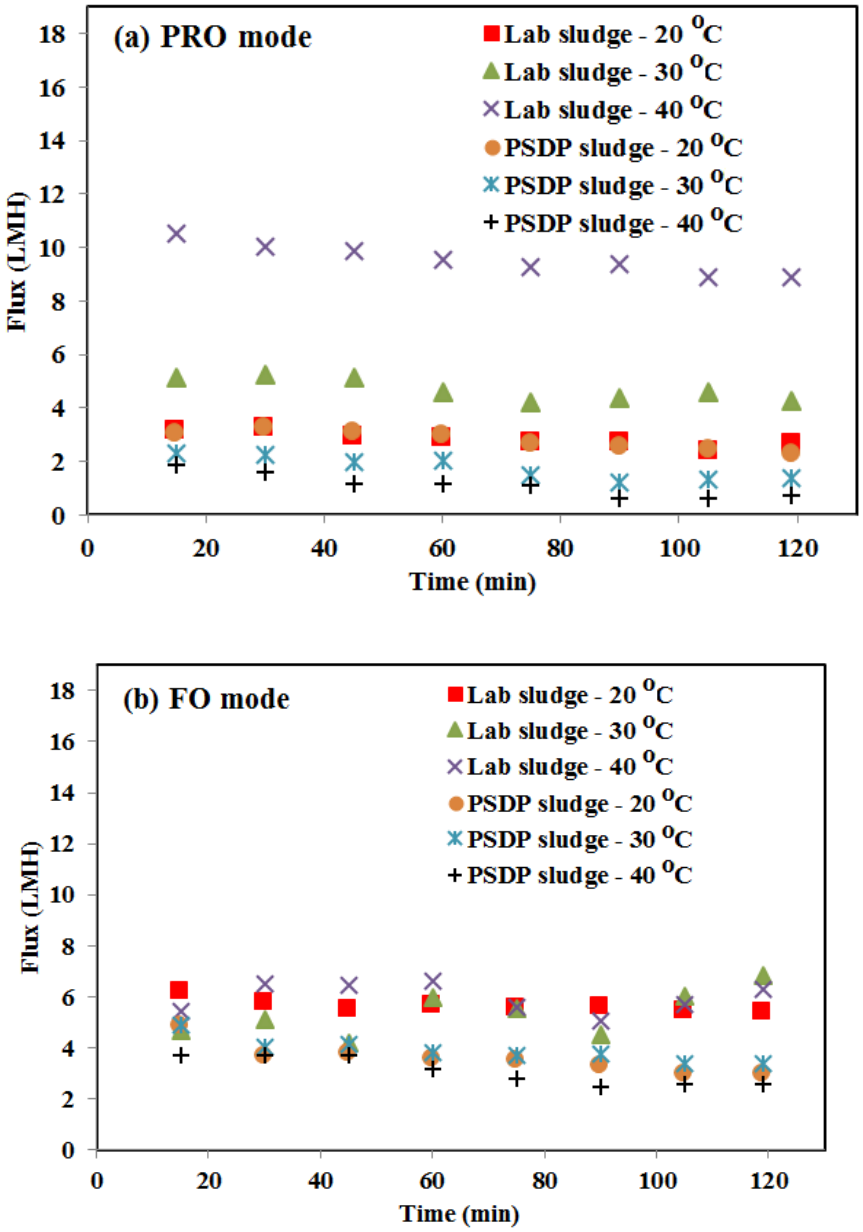

Figure 32: Averaged water flux versus elapsed time at different feed temperatures with error bars in (a) AL-DS mode (feed solution facing porous support layer) (b) AL-FS mode (draw solution facing porous support layer).

Water flux in AL-FS mode

There was no significant change in water flux with increase in temperature for Lab sludge. At 20, 30 and 40 ^{o}C averaged water fluxes were, 5.72, 5.36 and 5.96 LMH, respectively. However, water flux is higher in AL-FS mode than in AL-DS mode at 20 ^{o}C. Zhao et. al reported AL-FS

mode is more favourable when feed solution concentration and degree of concentration is higher (Zhao et al., 2011). Comparable results were achieved only with the lowest temperature (20^{o}C). When temperature increased, the water flux in AL-DS mode was significantly higher than AL-FS mode for Lab sludge as shown in Figure 33. At 40 ^{o}C water flux was 10.22 LMH in PRO mode whereas in AL-FS mode flux it was only 5.96 LMH. Similar to Lab sludge, there was no significant change in water flux with increase in temperature for PSDP sludge. However, flux was marginally higher than AL-DS mode.

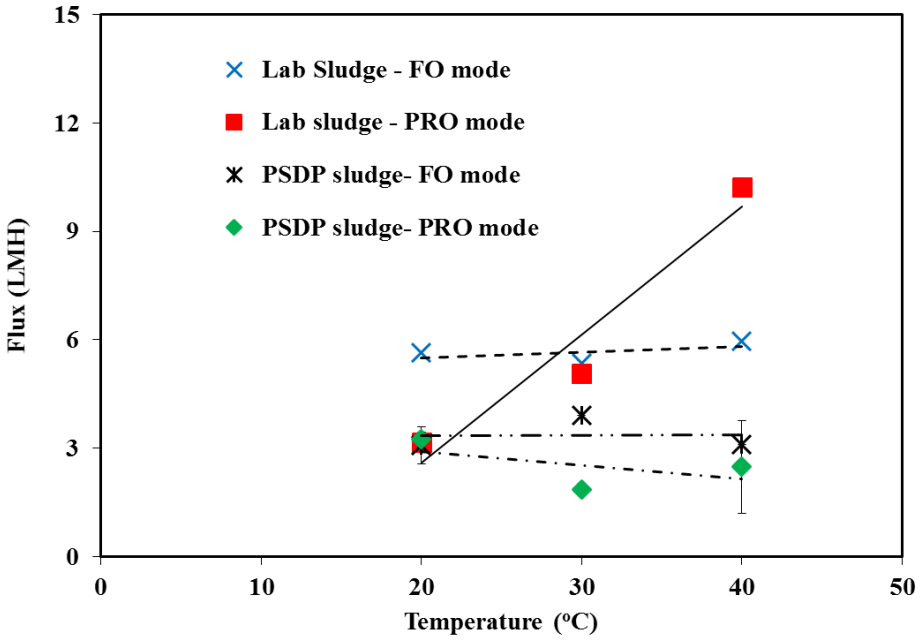

Figure 33: Effect of membrane orientation on water flux. AL-FS mode and AL-DS mode stand for draw solution facing porous support layer and feed solution facing porous support layer, respectively.

5.2.4 Conclusions

This part of the study focused on volume reduction of pre-treatment sludge as well as on dilution of reverse osmosis (RO) concentrate through emerging forward osmosis (FO) technology where RO concentrate draws water from the pre-treatment sludge (feed solution) in order to reduce pre-treatment sludge volume and increase the RO water recovery. Experiments were carried out using two different types of sludge i.e. (1) synthetic pre-treatment

sludge (Lab sludge) which has lower salinity and (2) actual sludge from Perth Seawater Desalination Plant, Australia (PSDP sludge) which has higher salinity. Effect of membrane orientation (AL-FS and AL-DS modes) and temperature of pre-treatment sludge on permeate water flux was investigated. There was a significant increase in water flux from 3.2 to 10.2 LMH (i.e. ~ 3 times higher) when temperature increased from 20 to 40 ^{o}C for Lab sludge in AL-DS mode. However, there is no significant effect of temperature on water flux in AL-FS mode for Lab sludge. On contrary, for PSPD sludge, there was no effect on water flux with increase in temperature at AL-DS mode. Dissolved ions in the porous side increased the severity of concentrative internal concentration polarisation (CICP), hence it could reduce the flux. There was no significant change in water flux when temperature increased from 20 to 40 ^{o}C for PSDP sludge in AL-FS mode. However, higher amount of water has permeated from Lab sludge compared to PSDP sludge in AL-FS mode.

Following conclusions were made from this part of study.

1. At elevated temperatures, AL-DS mode is more favourable for pre-treatment sludge solutions which have low constituents (lab sludge where the concentration of dissolved ions was low). However, AL-FS mode performed to be appropriate at lower temperatures for the lab sludge.AL-FS mode is favourable for pre-treatment sludge solutions which have high constituents (PSDP sludge where the concentration of dissolved ions was high).
2. In AL-DS mode, dissolved ions in the PSDP sludge solution in the porous side could have increased the severity of CICP resulting in lower water flux compared to AL-FS mode.
3. All proposed systems are capable in reducing the volume of pre-treatment sludge with further optimised process conditions.

Chapter 6: Optimising Water Flux through Hollow Fibre Membranes

6.1 Introduction

Forward osmosis technology is becoming a promising application in wastewater and water purification applications, dairy industry and fruit juice concentration, however it has been used mostly at laboratory or pilot plant scale with only very few applications at industrial scale [Poriferra- http://www.poriferanano.com/]. Its limitation to lab scale is due to inherent lower water permeation, reverse salt flux (RSF), selection of proper draw solution and complexity in regeneration of draw solution. The latter disadvantage is mainly due to footprint and economic aspects as regeneration of draw solution needs reverse osmosis applications. The first two mentioned drawbacks are being addressed by introducing new membranes fabricated with different polymer materials and membrane type. Flat sheet membranes available to date are showing low water fluxes. For example the best available flat sheet membranes to date, CTA membranes manufactured by HTI innovations USA gives a maximum water flux of 9.6 LMH when DI water and 0.6 M NaCl salt solution is used as feed and draw solution, respectively (Miller et al., 2007).

However, when sludge and brine are passed through flat sheet membranes, the maximum water flux obtained was ~ 3 LMH when brine and sludge conductivities were 45 ms/cm and 72 mS/cm, respectively (Chapter 5). This is significantly lower than other applications available in literature. But, having waste sludge on one side of the membrane, due to fouling and concentration polarisation effect, the maximum flux obtained is still acceptable. Having higher water flux would improve the performance of the proposed FO/RO system especially in terms of operational expenditure (OPEX). Hollow fiber membranes are believed to perform better than flat sheet membranes considering higher water flux as well as lower reverse salt flux (Wang et al., 2010, Su et al., 2010, Sivertsen et al., 2012). Therefore, in this study the applicability of hollow fiber membranes for sludge dewatering when brine is used as draw solution was investigated. Since the water diffusion through the FO membrane depends on density (ρ), viscosity (μ), cross flow velocity, and the channel thickness, the effect of these factors on water flux through hollow fibre membranes was examined. All these parameters are function of the Reynolds number (Re) of a solution which is given by:

$$Re = \frac{\rho v d}{\mu}$$

where v is the velocity of a fluid and d is the channel equivalent diameter. Therefore, the Re of the draw and feed solution were varied and the effect on water flux and RSF was analysed. Further, at the optimum Re of draw and feed, the sludge dewatering capacity at different sludge solids content was investigated.

6.2 Materials and Methods

Feed (either MilliQ water or $Fe(OH)_3$ sludge) and draw solutions (NaCl, Na_2SO_4, $MgCl_2$ $CaCl_2$ and RO brine-ROC) were passed through the membrane at different feed:draw Reynolds number (Re) ratios. The properties of draw and feed solutions used to calculate Re are given in Table 18, Table 19 and Table 20. Re was varied by changing the velocity of the feed and draw solutions. Sludge/MilliQ water was circulated outside the hollow fibre membranes and the draw solution through the lumens. Since the inside surface of the hollow fibre is the active layer, the experiments were run in AL-DS mode. Experimental set up is shown in Figure 20. Change in the weight of the draw solution was programmed to be stored in a data logger at one-minute time intervals. Experimental water flux ($J_{w,e}$) was determined by the equation (16) mentioned in section 3.3.1. After 1 hour of filtration, properties of the feed and draw solutions were measured. Membrane was cleaned using MilliQ water prior to each experiment. Theoretical water flux ($J_{w,t}$) was calculated and compared with that of experimental value.

Table 18: Properties of draw solution used in this study.

Draw solution	Density, ρ (kg/m^3)	Viscosity, μ (Pa·s)	Conductivity*, EC (mS/cm)
NaCl	1037.00	0.001080	81.1
Na_2SO_4	1557.00	0.001120	81.9
$MgCl_2$	1072.40	0.001490	96.7
$CaCl_2$	1085.20	0.001330	108.6
ROC	1023.98	0.001004	72.3

Note: Density and viscosity was obtained from OLI ® stream analyser, and *conductivity from experimental values.

Table 19: Major anions and cations concentrations of feed and draw solutions used in this study

		PSDP sludge (mg/L)	ROC (mg/L)	Seawater (mg/L)
Cations	Ca^{2+}	454	1,101	457
(Filtered)	Na^{+}	14,724	19,130	8,773
	Mg^{2+}	2,607	2,947	469
	K^{+}	626	815	414
	Fe^{3+}	0.4	ND*	ND*
Anions	Cl^{-}	16,500	18,000	22,300
	SO_4^{2-}	1,800	2,200	2,200
	NO_3 as N	2.3	0.4	1.2

*ND - not detected

Cations were identified using Atomic Absorption Spectrometry (AAS) and anion concentrations were recognised through *Merk*® test kits.

Table 20: Properties of feed and draw solution used in this study.

Property	Seawater	Filtered seawater	Draw solution - ROC	Feed solution - PSDP $Fe(OH)_3$ Sludge
pH	8.42	7.68	7.77	8.69
Turbidity (NTU)	29.1	0.45	-	-
EC (mS/m)	4,450	4,470	7,300	5,150
TOC (mg/L)	1.71	0.73	3.10	17.06
Alkalinity – mg/L as $CaCO_3$	110	45	68	102
Hardness (EDTA)-mg/L as $CaCO_3$	4,600	6,200	9,550	4,500
Solids content (% TS)	-	-	-	4.04
Specific gravity	-	-	-	1.01

6.3 Results and Discussion

Effect of Re on the water flux

Figure 34 shows the water flux through hollow fiber FO membranes when DI water and salt solutions were used as feed and draw solutions, respectively.

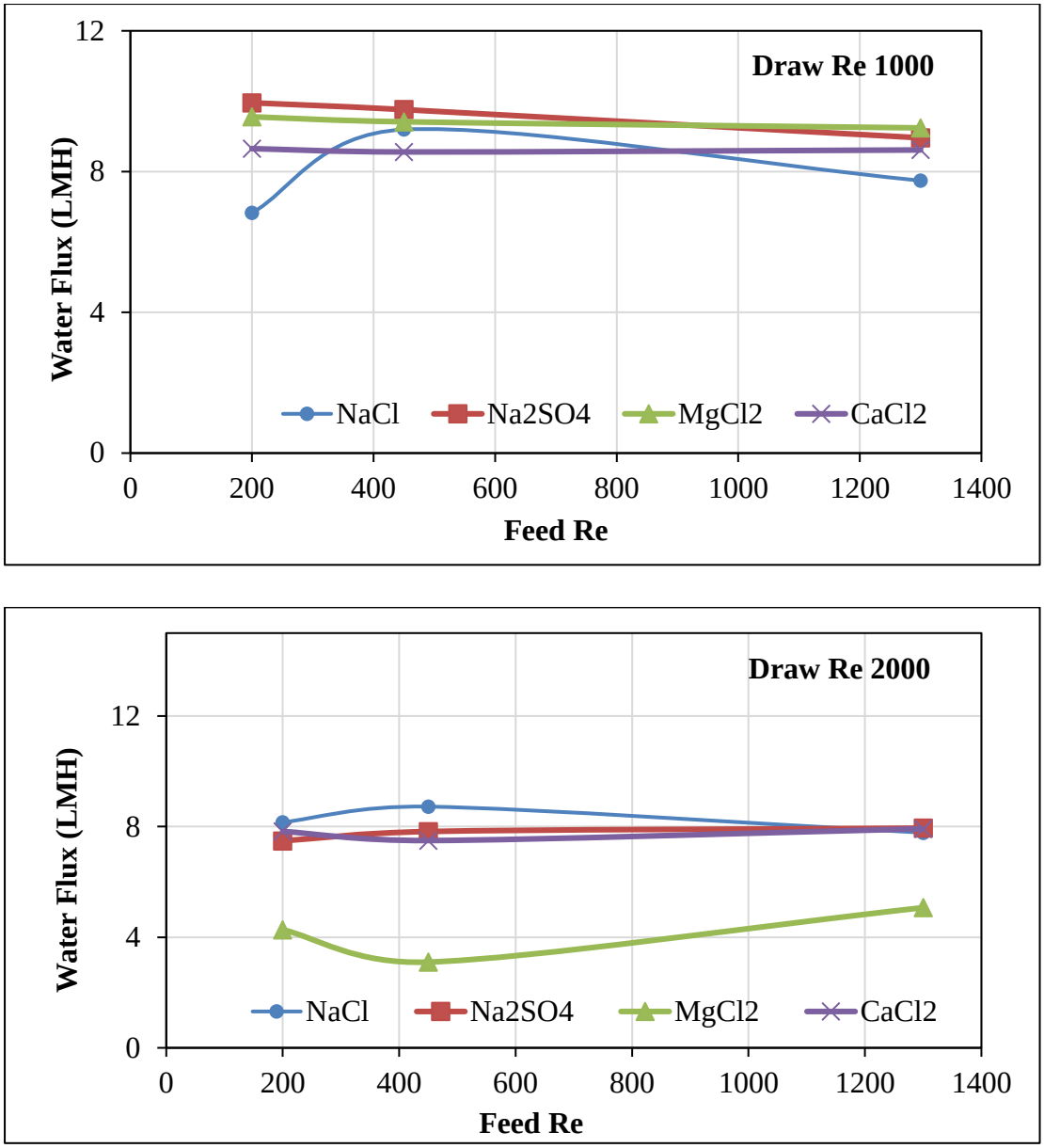

Figure 34: Water flux through hollow fiber membranes when draw solution Re was (a) 1000 and (b) 2000. Note that the experiments were run in AL-DS mode to compare the results with sludge dewatering experiments.

Draw Re was varied to 1000 and 2000 while feed Re was kept at 200, 450 and 1200. When draw solution flowed in laminar condition (Re = 1000) a water flux of up to 10 LMH was observed while Na_2SO_4 gave the highest performance, similar to $MgCl_2$. This is interesting as $MgCl_2$ at 1 M has the highest osmotic pressure; however, when the Re is similar 1M Na_2SO_4 shows similar performance even though its osmotic pressure is lower. Further, when draw solution Re was increased to become near turbulent (Re is 2000), all three draw solutions

showed better performance compared to $MgCl_2$. $MgCl_2$ drew a maximum of 5.07 LMH when the feed Re was highest (1200). Therefore, it is evident that, when selecting a draw solution, not only its osmotic pressure, but also its viscosity, density and the crossflow velocity affect the performance in terms of water flux.

Despite the type of solution 200 Re feed and 1000 Re draw gave the best performance in terms of water flux. Therefore, sludge dewatering experiments (detailed in the following Section) were run at 200:1000 feed to draw Re ratio.

Reverse salt flux of the membrane was determined by measuring the EC value of the feed solution. Since feed was DI water the change in EC was obviously due to the ions transported through the membrane from the draw solution. Figure 35 shows the RSF (or EC values of the feed) for each draw solution. NaCl shows the highest increase in RSF with time. Despite the Re, RSF is increasing with the filtration time. $CaCl_2$ shows the lowest RSF (below 5 µS/cm). $MgCl_2$ which showed lower water fluxes compared to the other salt solutions shows lower RSF, however, higher than for $CaCl_2$. Comparing these values with literature, it is evident that RSF in hollow fiber is higher that of flat sheet FO membranes.

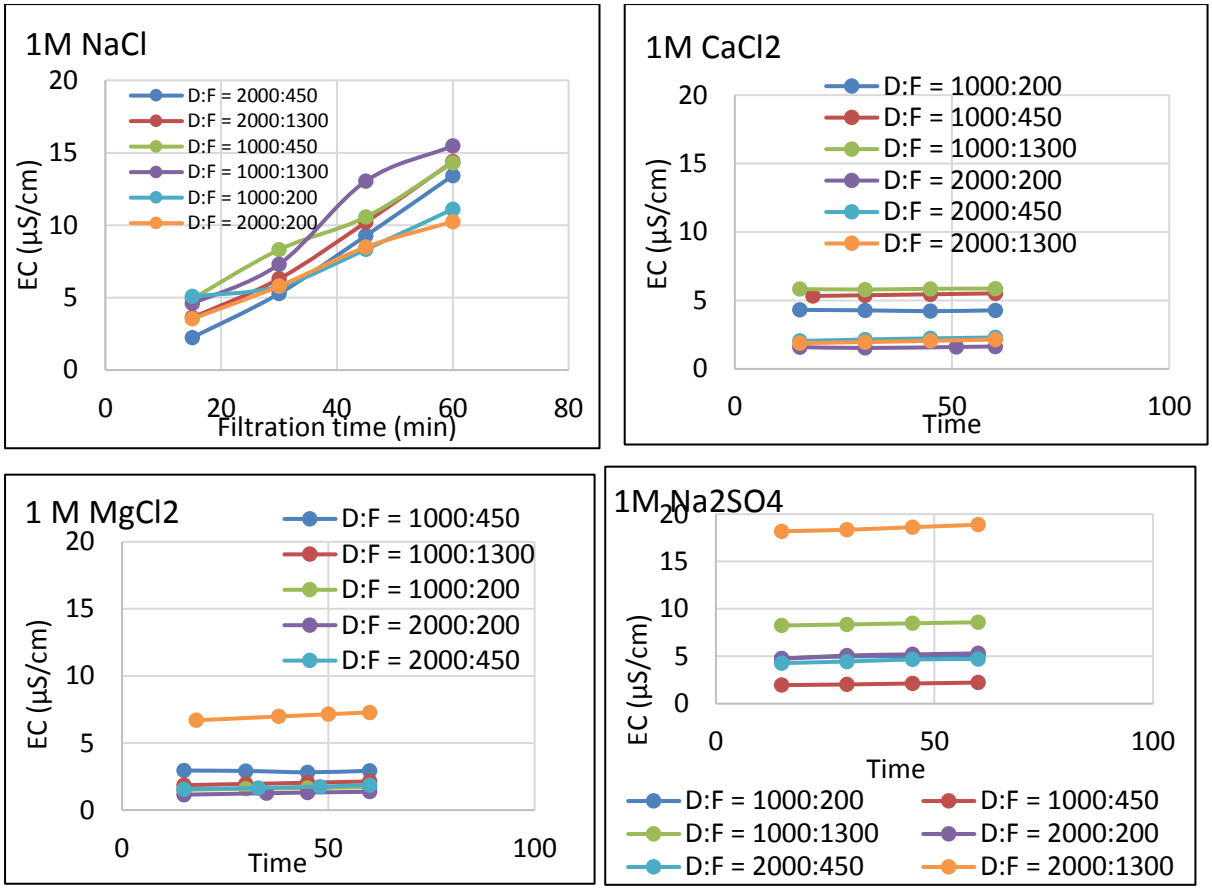

Figure 35: RSF measurements during filtration

Effect of sludge solids content

In this part of study, draw and feed solutions were ROC and pre-treatment sludge, respectively. Pre-treatment sludge solids content was varied from 2 to 8 % TS. As there are two types of pre-treatment sludge (when media filters backwashed using pre-treated seawater or RO reject) total solids content of each sludge type is different. The sludge available in the lab was 15% TS industrial sludge as received from PSDP. Therefore, to obtain required TS contents of each sludge type, 15% TS sludge was diluted using pre-treated seawater (named as High EC, EC = 45 mS/cm) and with DI water (named as low EC, EC = 1.5 mS/cm). Reduced solids contents are shown in Figure 36.

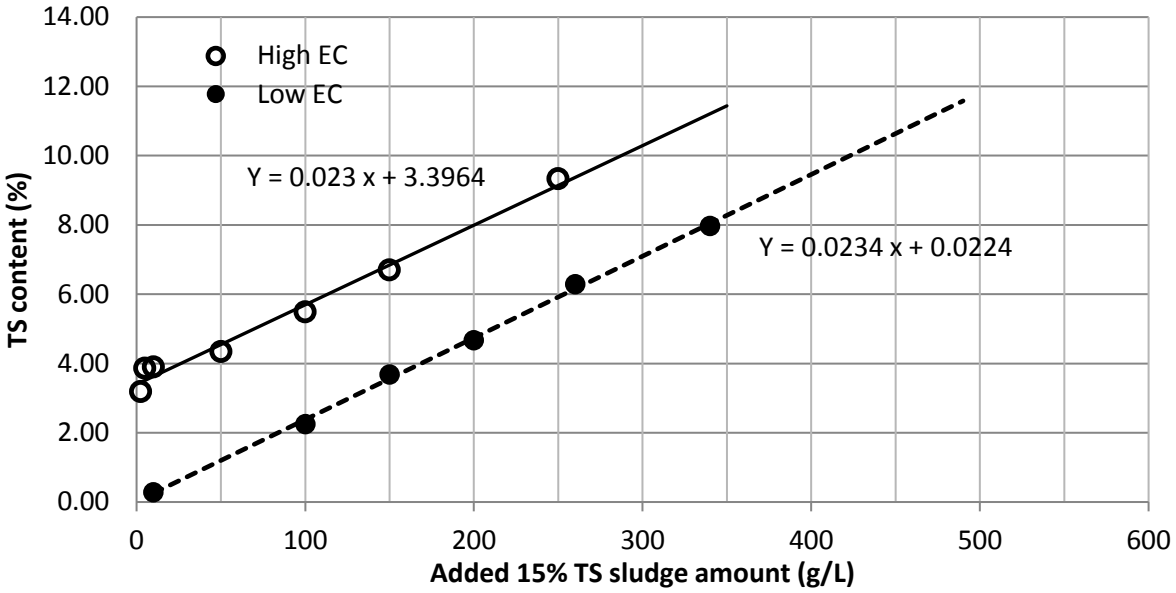

Figure 36: Average TS content of High and Low EC sludge prepared at lab scale starting from 15% TS industrial sludge.

Since seawater and DI water were used for dilution, the gap of the gradients of the two graphs should be the TS content of seawater. Therefore, (3.3964 - 0.0224) = 3.37 TS% is the TS content of pre-treated seawater used. Since TDS of seawater is 30-35 g/L the 3.374 TS% appears acceptable. For FO dewatering applications through hollow fiber membranes, Low EC sludge samples were chosen assuming lower EC (hence higher EC difference between feed and draw) would give better performance with the membrane.

Since the same membrane coupon was used for each experiment (after cleaning); before and after the two-hour sludge dewatering, baseline experiments were run with 0.5 M NaCl and DI water as draw and feed solutions respectively. This was to check whether the membrane coupon had returned to the initial condition after cleaning. The results are shown in Figure 37.

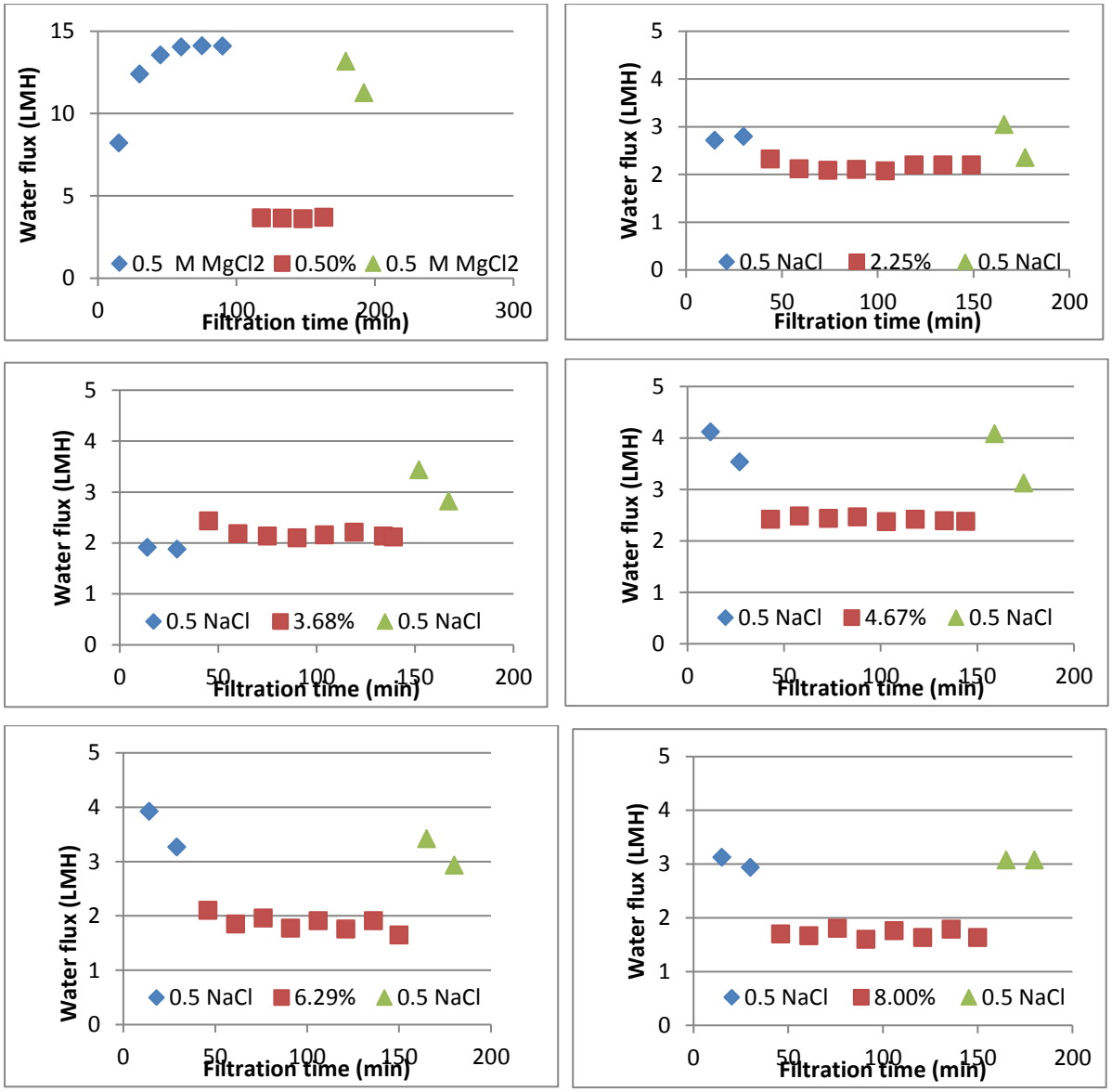

Figure 37: Water flux at each sludge solids content are given in ■. ♦: before sludge dewatering and ▲: after sludge dewatering and cleaning of the membrane.

As Figure 37 illustrates, cleaning has taken the membrane back to the original condition. This means since the sludge dewatering time was only 2 hours, the membrane was either not fouled or the fouling is nearly to 100% reversible. However, to compare the water flux at each sludge solids content, averaged water fluxes were plotted in on one graph (Figure 38).

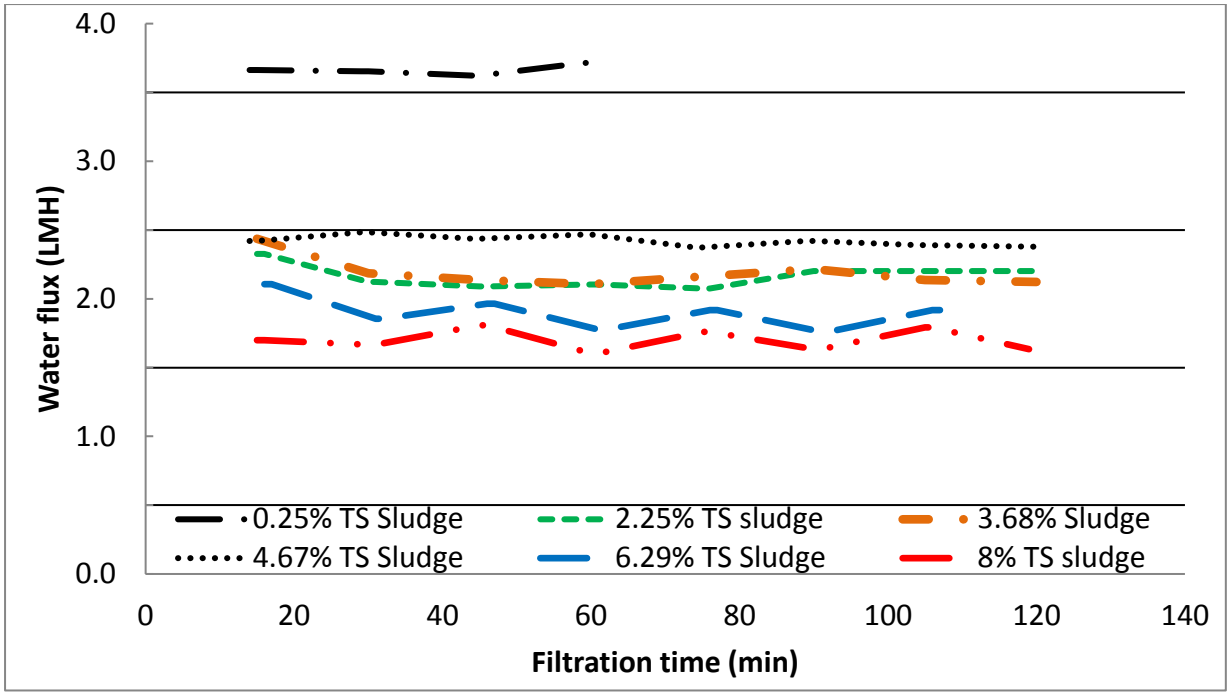

Figure 38: Comparison of water flux at each sludge solids condition.

As Figure 38 shows, the lowest sludge solids content led to the highest water flux, i.e., 3.6 LMH, whereas all the other sludge types showed flux of 1.5 - 2.5 LMH. When sludge solids content increased there was a slight drop in water flux. With increase in solids content the viscosity and the density of the sludge increases. Higher viscosity means lower Re, and higher density means higher Re, however, the combination of higher viscosity and higher density led to lower water permeation through the hollow fibre membranes. The effect of higher amount of solids content was dominant and this would have increased the CP effect as sludge passed through the porous side of the membrane leading to lower water flux.

6.4 Conclusions

In this part of the study, membrane type was varied to hollow fiber PA membrane (instead of flat sheet) and the water flux was compared with the flat sheet CTA membranes. Draw and feed solutions' Re was varied to enhance the water flux through membrane. Lower feed and draw Re solutions perform better compared to higher Re solutions. At the best Reynolds Number (Re) numbers pre-treatment sludge and ROC showed averaged water flux of 2.1 LMH when sludge solids content is 3.68% (as is sludge solids content). With the same conditions

(same temperature, TS content and pH, and PRO mode), flat sheet CTA membranes showed 1.5 times higher water flux compared to hollow fibre membranes. Therefore, for sludge dewatering flat sheet membranes can be recommended.

Chapter 7: Performance Evaluation of Flat Sheet FO Membrane through fouling study.

7.1 Introduction

Bio-fouling is due to unwanted growth and deposition of biofilms which leads to higher operating pressure, lower recovery, more frequent chemical cleaning, and shorter membrane life (Matin et al., 2011). The major three factors affecting the adhesion of microorganisms' (such as plankton, bacteria, fungi, algae) to membrane surfaces are (Nguyen et al., 2012) ;

(i) Properties of membrane surface (chemical composition, surface charge, surface tension, hydrophobicity, conditioning film, roughness, porosity etc),
(ii) Microorganisms (species, population density, their nutrient status, hydrophobicity, charges, physiological responses etc) and
(iii) Characteristics of feed seawater (temperature, pH, dissolved organic matter, dissolved organics, suspended matter, viscosity, shear forces, boundary layer, flux etc).

Compared to RO bio-fouling in FO can easily be removed by increasing cross flow velocities without any cleaning agents (Yoon et al., 2013). This is due to zero/low hydraulic pressure applied during FO process whereas RO is conducted at high pressure (~ 70 bar).

However, there are very few studies on bio-fouling in FO available in literature. Further, the available studies were conducted with synthetic solutions. In this part of the study all the FO experiments were conducted with actual seawater and pre-treatment sludge. The fouling tendency of FO when pre-treatment sludge and brine are used as the feed and draw solutions, respectively, was investigated. Growth and development of bio-film with filtration time and its effect on water recovery was also examined.

7.2 Experimental Procedure

Flat sheet CTA membranes with a woven, embedded support backing (explained in Chapter 3) were used. Feed (pre-treatment sludge) and draw (RO brine) solutions were passed through the membrane at 0.04 m/s cross flow velocity (Liu and Mi, 2012, Yoon et al., 2013) in counter current flow configuration. Sludge was circulated on the support side of the membrane (FO

mode) and stirred at a constant rate during the experiment to eliminate settling of particles. Experimental set up was similar to that in Figure 19. Experiments were run at 20 ± 2 ^{o}C and triplicated at each operating condition. Change in the weight of the draw solution was programmed to be stored in a data logger at 5 min time intervals. Three consecutive experimental setups (similar to Figure 19) were run. Fouling behaviour on the FO membrane was examined after 1 day, 4 days, 1 week and 5 weeks. One experiment was run until the membrane was fully fouled (i.e., until no water flux observed). Water flux, conductivity, TOC and pH of each set up were monitored continuously using a data logger, EC meter, TOC analyser and pH meter, respectively.

All the fouling experiments were run in semi-batch mode as the experiments were long term runs, following experimental procedure of Li *et.* al (2012), i.e., when the draw solution had extracted 15 % of water from the feed (150 mL), both draw and feed solutions were replaced with fresh 1L tank. Replaced feed and draw tanks', TOC, pH, temperature, and EC were measured. Prior to each new experiment, 3 experimental setups were thoroughly cleaned to remove trace organic matter using the following procedure (Jeong et al., 2013).

Cleaning of FO set-up to remove trace organic impurities prior to each fouling test:

1. Recirculation of 0.5% sodium hypochlorite for 2 h.
2. Removal of trace organic matter by recirculating 5 mM ethylene di-amine tetra-acetic acid (EDTA) at pH 11 for 30 min.
3. Additional removal of trace organic matter by recirculating 2 mM sodium dodecyl sulphate (SDS) at pH 11 for 30 min.
4. Sterilisation of the unit by recirculating 95% ethanol for 1 hour.
5. Rinsing the unit with DI water (several times) to eliminate ethanol residue.

Once the filtration was complete a known area of membrane was selected for analysis for cell count, SEM, TOC, ATP and live/dead cell count analysis (Figure 39).

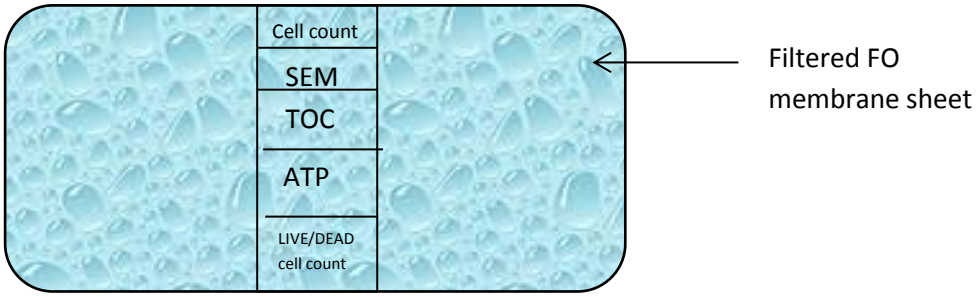

Figure 39: Fouled membrane analytical method protocol

7.3 Results and Discussion

Change in water flux

The water flux pattern with time is shown in Figure 40. Flux declined with filtration time due to two reasons (1) fouling and (2) dilution of the draw solution as draw solution was recirculated. However, flux increased when the draw and feed solutions were replaced with fresh solution. This increased flux was lower than the initial flux of the previous batch due to fouling on the membrane. Flux decline due to fouling is shown in red dashed lines in Figure 40. After one week of filtration, the flux declined further in Figure 40c due to the thickened fouling layer deposited on the membrane. The layer may have contained microorganisms and salt deposits as both draw and feed solutions contain salt ions.

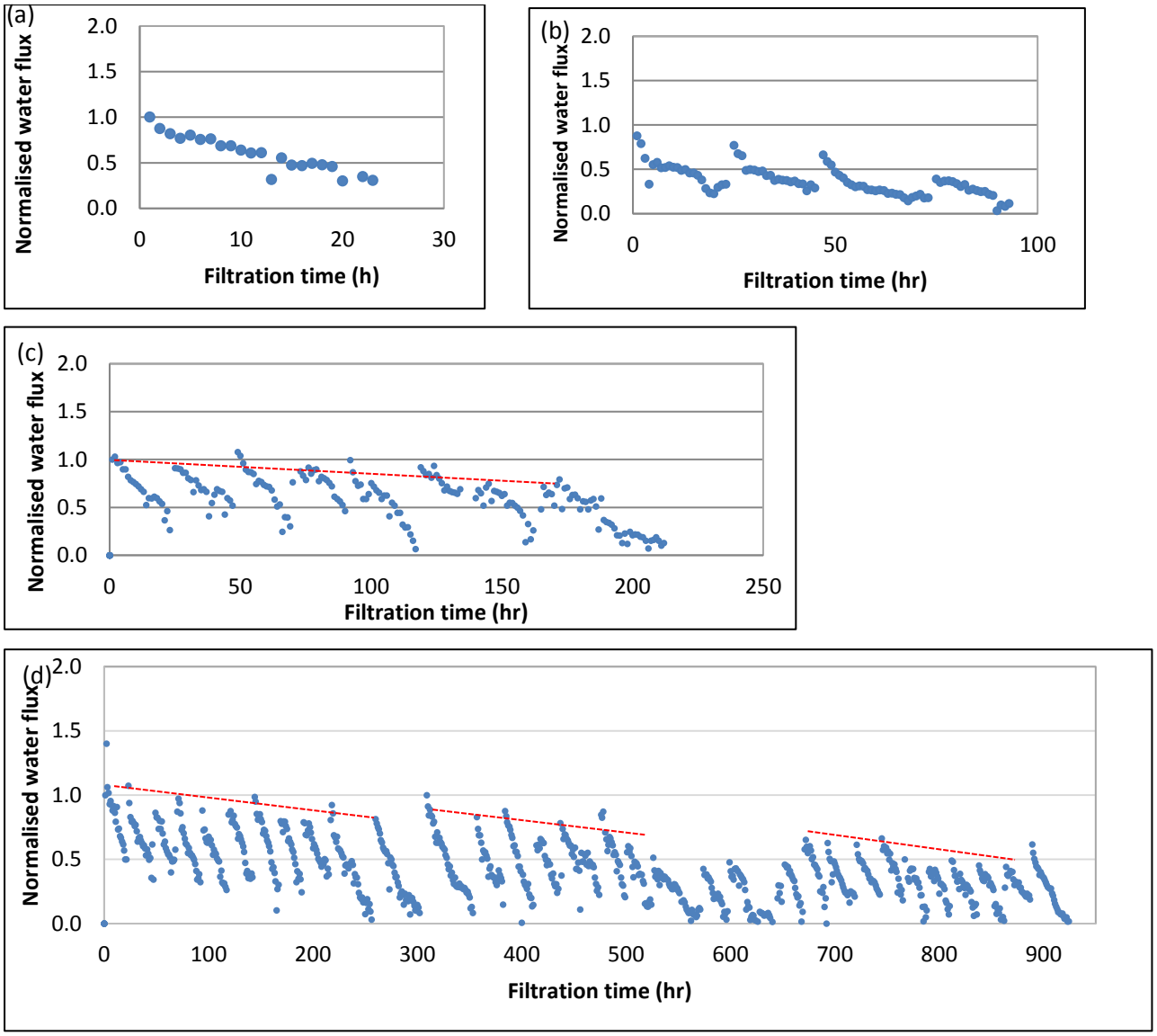

Figure 40: Water flux through FO membrane during long term filtration (a) 1 day (b) 4 days (c) 1 week and (d) 5 weeks.

However, as the EDX spectrum shows in Figure 41, after 1 week of continuous filtration, the FO system showed only salt deposits. This fouling could easily be removed by providing regular flushes at high cross flow velocities as deposited layers were thin and loose.

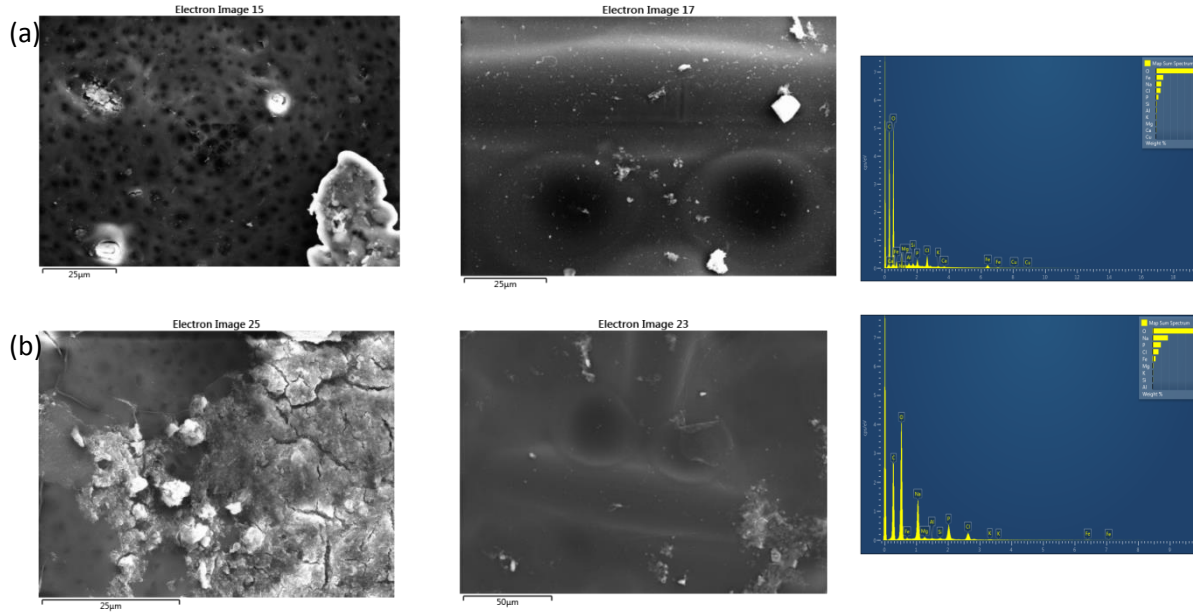

Dense sides | Support sides | Dense side EDXs

Figure 41: SEM images and EDX spectra of the membrane surfaces after (a) 1 week and (b) 5 weeks of filtration.

Interestingly, as Figure 40(d) shows, after 300 hours (about 2 weeks) the flux was increased once more; however, it was less than the start-up water flux. This was repeated after about 650 hours (around 4 weeks). After about 2 weeks the loose salt deposit layer had formed and when its thickness increased, part of the loose layer could be readily removed by the increased process cross flow velocity (because when thickness reduces velocity increases, as shown in Figure 42).

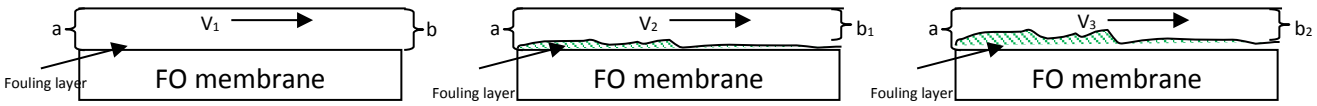

a = channel thickness
b = actual channel thickness = a
V_1= cross flow velocity

(a) Initial membrane

a = channel thickness
b_1 = actual channel thickness < a
V_2= cross flow velocity

(b) Membrane during two weeks

a = channel thickness
b_2 = actual channel thickness < b_1<a
V_3= cross flow velocity >V_1

(c) Membrane after about two weeks

Figure 42: Schematic diagram of the FO membrane surface with filtration time. Fouling layer increased with filtration time and so does the cross velocity.

Longer runs were conducted to confirm this behaviour. That is, filtration was conducted until there was no water flux through the membrane. After eight weeks of filtration there was no evidence of water flux, therefore filtration was stopped, and the membrane surface was analysed by SEM to check evidence for no water flux. Water flux and SEM images are shown in Figure 43 and Figure 44, respectively. In Figure 43, after 5 weeks of filtration higher water flux fluctuations can be observed. This may be due to uneven membrane surfaces on both feed and draw side due to deposits. EDX membrane images supports this suggestion as it shows a spread of salt and silica deposits on the feed side and salt depositions on the draw side (and more EDX images can be found in the appendices section). Further, TOC results show the same behaviour as shown in Figure 45 . Up till 5 weeks, there was an increase in TOC from ~5 to ~7 ppm. However, after 5 weeks, the TOC dropped again. This may be due to clearance of the fouling layer after 5 weeks of filtration.

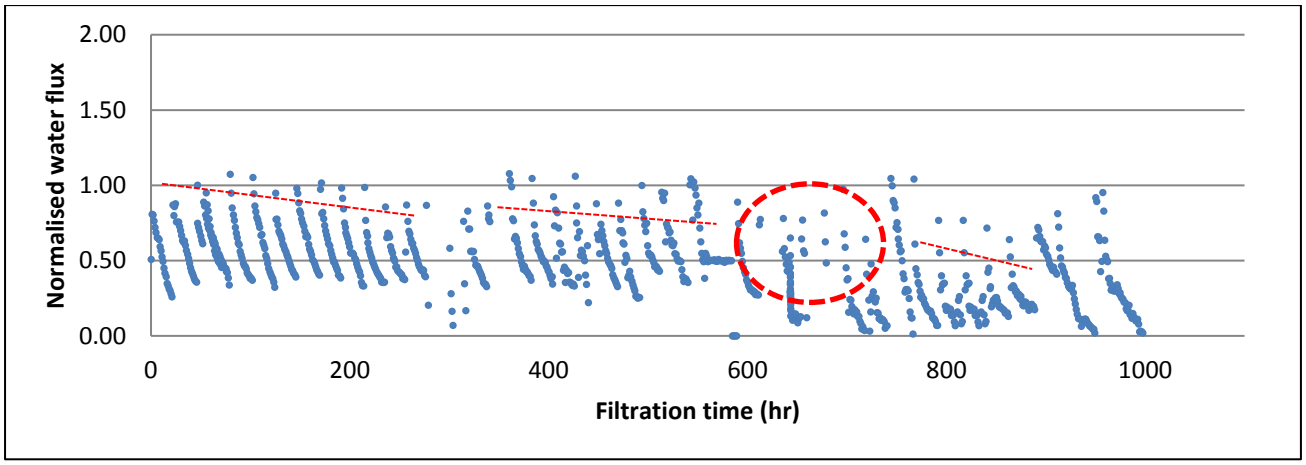

Figure 43: Normalised water flux with respect to filtration time.

TOC results

Draw and feed solutions were replaced with fresh draw and feed samples every 24 hours. The used feed and draw solution TOC values were measured daily. Eight weeks of TOC results are

reported in Figure 45. The remaining TOC results can be found in the appendices section. During 8 weeks of filtration, TOC of the feed and draw solutions fluctuated. Once the 1day, 4-day, 1 week, 5 week and 8 weeks filtration runs were completed, a known area of membrane was selected (as shown in Figure 39) and vortexed with DI water to extract the deposited fouling layer.

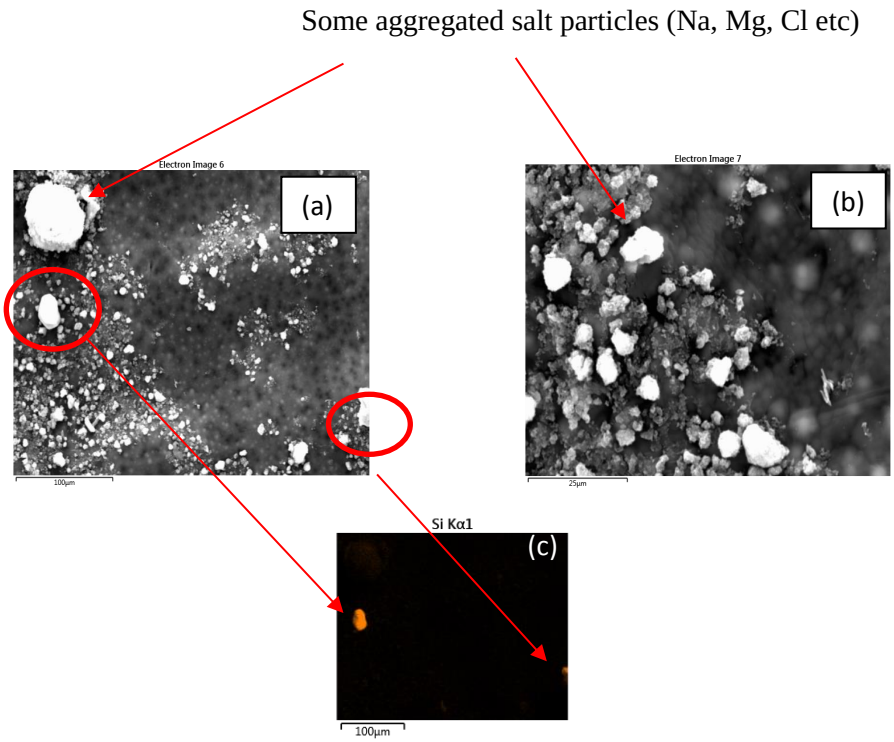

Figure 44: SEM images of the fouled membrane (a) Feed side (b) draw side (c) elemental analysis corresponding to (a) obtained through EDX. Remaining EDX images of both feed and draw sides can be found in the appendices section.

The extracted liquid was used to analyse the TOC content per unit of membrane area (Figure 46). TOC on the membrane surface has increased 10 mg/cm^2 when the filtration time increased from 1 day to 5 weeks. In addition, microorganisms started to grow on the membrane surface after 1 week of continuous filtration. As shown in Figure 46 live and dead cells were propagated over the membrane surface which then led to reduction of water flux. Therefore, membrane may be need at least a once weekly cleaning cycle to avoid this.

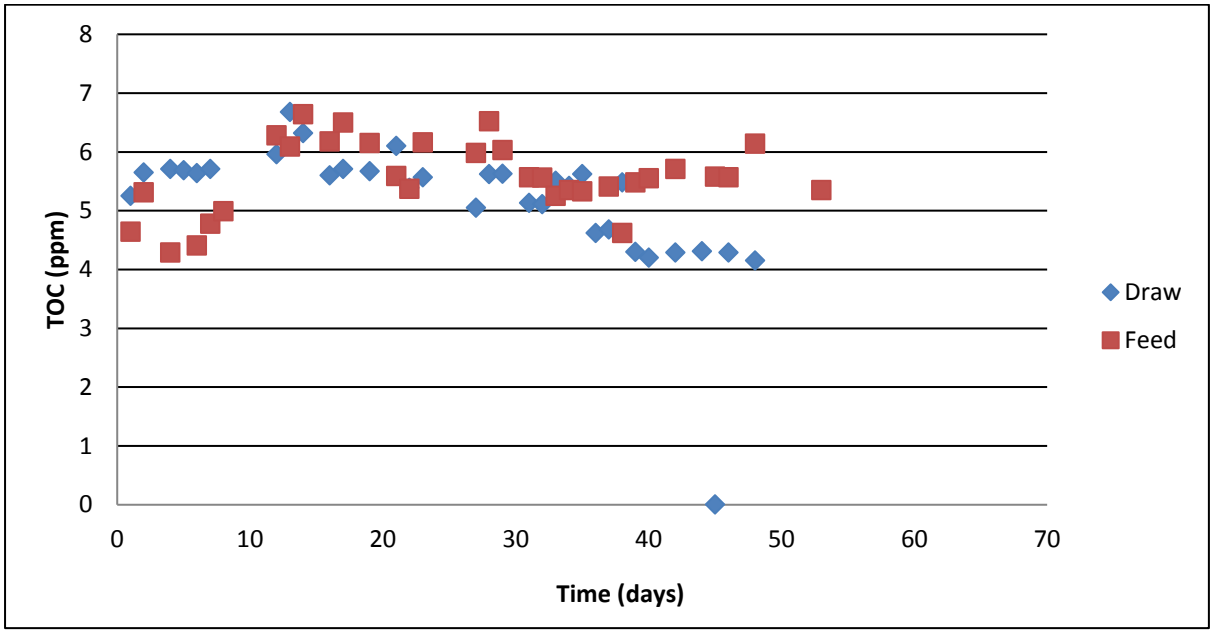

Figure 45: Daily TOC results of the feed and draw solution.

In the 8 weeks filtration trial the TOC value was significantly low (only 10 mg/cm^2), which is hard to explain why. All the experiments other than 8 weeks filtration trail were triplicated. Therefore, another duplicate experiment for 8 weeks trial would be required to confirm the TOC results.

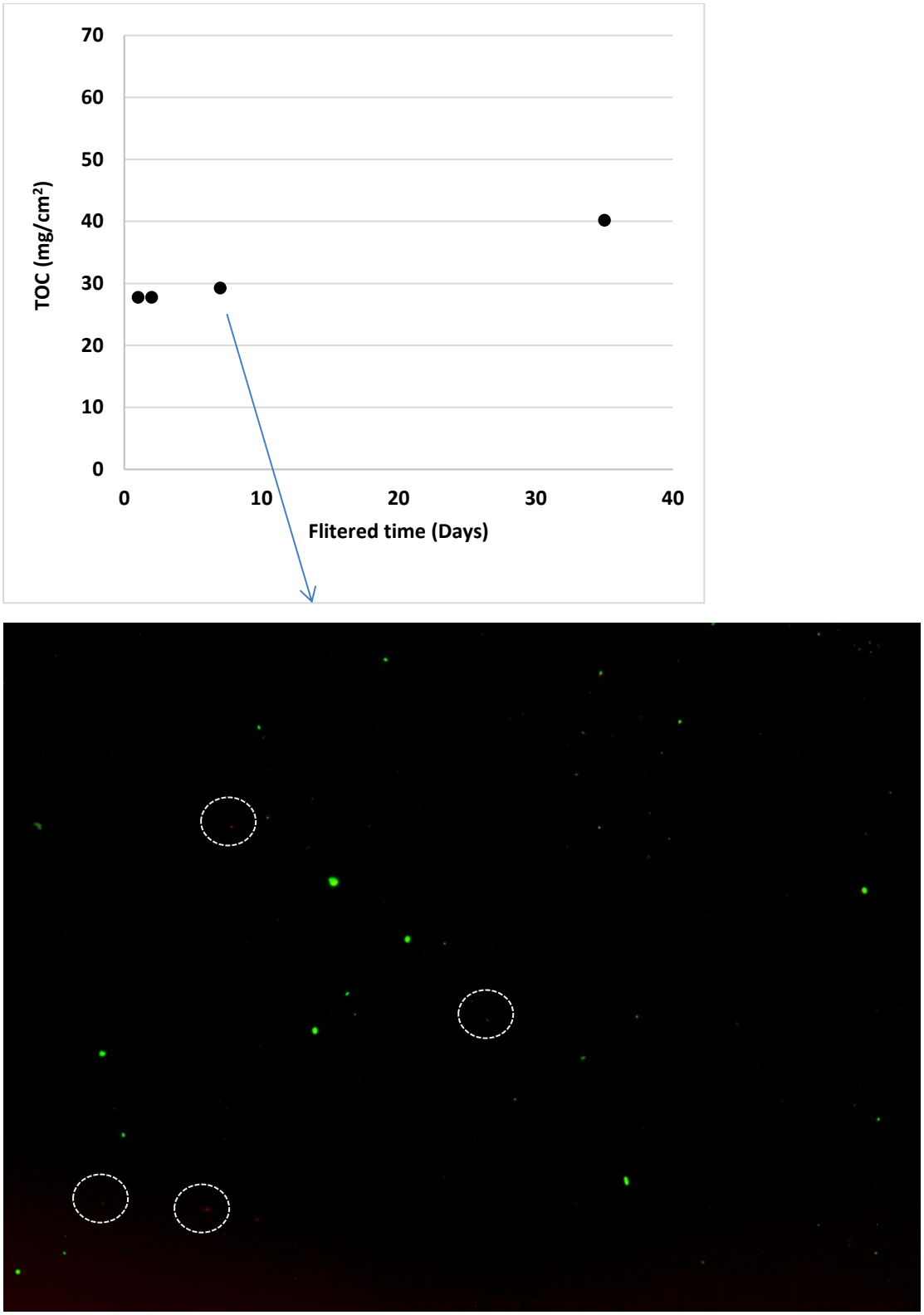

Figure 46: TOC of the filtered membrane and live and dead cells on the membrane. Green - live cells and Red- dead cells (dead cells are circled with white dashed line)

7.4 Conclusions

A ~50% reduction in water flux was observed due to fouling during five weeks of continuous filtration, without cleaning in between. This is mainly due to deposition of metals. After eight weeks of filtration, there was no water permeation. Salt deposition on the FO membrane coupon filtered for eight weeks was higher compared to the FO membrane coupon filtered for five weeks. With frequent cleaning with water, water flux can be brought back to initial value as fouling in FO membrane is reversible. Once a week cleaning cycle may be required for longer runs as live (and dead) cells were observed after one week of filtration on the membrane surface.

Chapter 8: Mass and Energy Balance Calculations

Corresponding Publication: Liyanaarachchi, S., Jegatheesan, V., Muthukumaran, S., Gray, Stephen, Shu, L., S., (2016). Mass balance for a novel RO/FO hybrid system in seawater desalination, Journal of Membrane Science 501: 199-208 (Liyanaarachchi et al., 2016).

8.1 Introduction

It is well-known that the demand for fresh water is increasing and its reserves are depleting. Desalination of seawater has come to aid the demand for fresh water. Desalination processes have evolved from multi-stage flash (MSF) and multi-effect distillation (MED) to reverse osmosis (RO). Approximately 40-50% of the seawater treated by reverse osmosis (SWRO) is converted in to fresh water (Jamaly et al., 2014, J.E.Miller). SWRO has three major draw backs: (i) high volumes of concentrate due to low water recovery, (ii) significant amounts of pre-treatment sludge that needs treatment and disposal and (iii) high energy consumption due to the use of high pressures to overcome the osmotic pressure of concentrated seawater (VOLLPRECHT, 2013, Blank et al., 2007b, NCED, 2010, Latorre, 2005, Ahmed et al., 2001). Although the last draw back has been addressed well by the introduction of energy recovery devices (Fritzmann et al., 2007, Elimelech and Phillip, 2011), the first two draw backs still need solutions. Application of forward osmosis (FO) may be able to provide a solution to those two draw backs.

A novel hybrid RO/FO system is proposed that will improve both water recovery and reduce the volume of pre-treatment sludge. In a typical pre-treatment sludge treatment process, clarified backwash sludge gets mechanically treated until the solids content meets the required landfill conditions. However, this process yields high operation and maintenance (O&M) costs (VOLLPRECHT, 2013). Table 21 shows the O&M cost for a sludge treatment process where daily sludge generation is 275 m^3/day.

Transportation and disposal of sludge costs $465 and $1,978 AU$/day, respectively, which is a significantly high cost. Figure 47 shows an existing treatment process (System E) for pre-treatment of sludge in a seawater desalination plant, where a centrifuge increases the sludge solids content from 2-4% to 25% (VOLLPRECHT, 2013)). The final sludge solids content is an important factor to be considered when proposing a FO system for sludge dewatering, as solids contents similar to those currently achieved or higher are required. However, existing

FO membranes are incapable of producing solids contents of up to 25%, so the FO system considered was to be installed between the clarifier and centrifuge.

Table 21: Operating and maintenance cost of sludge treatment when 275 m^3/day of sludge volume generated from pre-treatment process (VOLLPRECHT, 2013)

Item	Daily cost (AUD/day)
Chemicals	47
Power	35
Transportation	465
Disposal	1,978
Total	2,525

The FO system increases the solids content to a designated extent following which the sludge is centrifuged until solids content reaches 25%. This may reduce the power requirement (Chu et al., 2005), as the FO system uses comparatively less energy to function and maintain than a centrifuge. FO system consumes merely 17.3 kW h/day of power to increase sludge content from 3% to 10% as shown in the following calculations. Further, the volume of filtrate from the centrifuge, which is known as centrate, will be reduced which generally needs treatment before discharge.

Assumed pre-treatment sludge flow rate = 275 m^3/day

Maximum permeate through a proposed FO system,

when sludge content increases from 3 to 10 % = 72 m^3/day

Power consumption of a FO system = 0.24 kW h/m^3 of water produce, (Semiat, 2008, McGinnis and Elimelech, 2007)

∴ Power requirement for the FO system = 0.24 ×72 kW h/day

= <u>17.3 kW h /day</u>

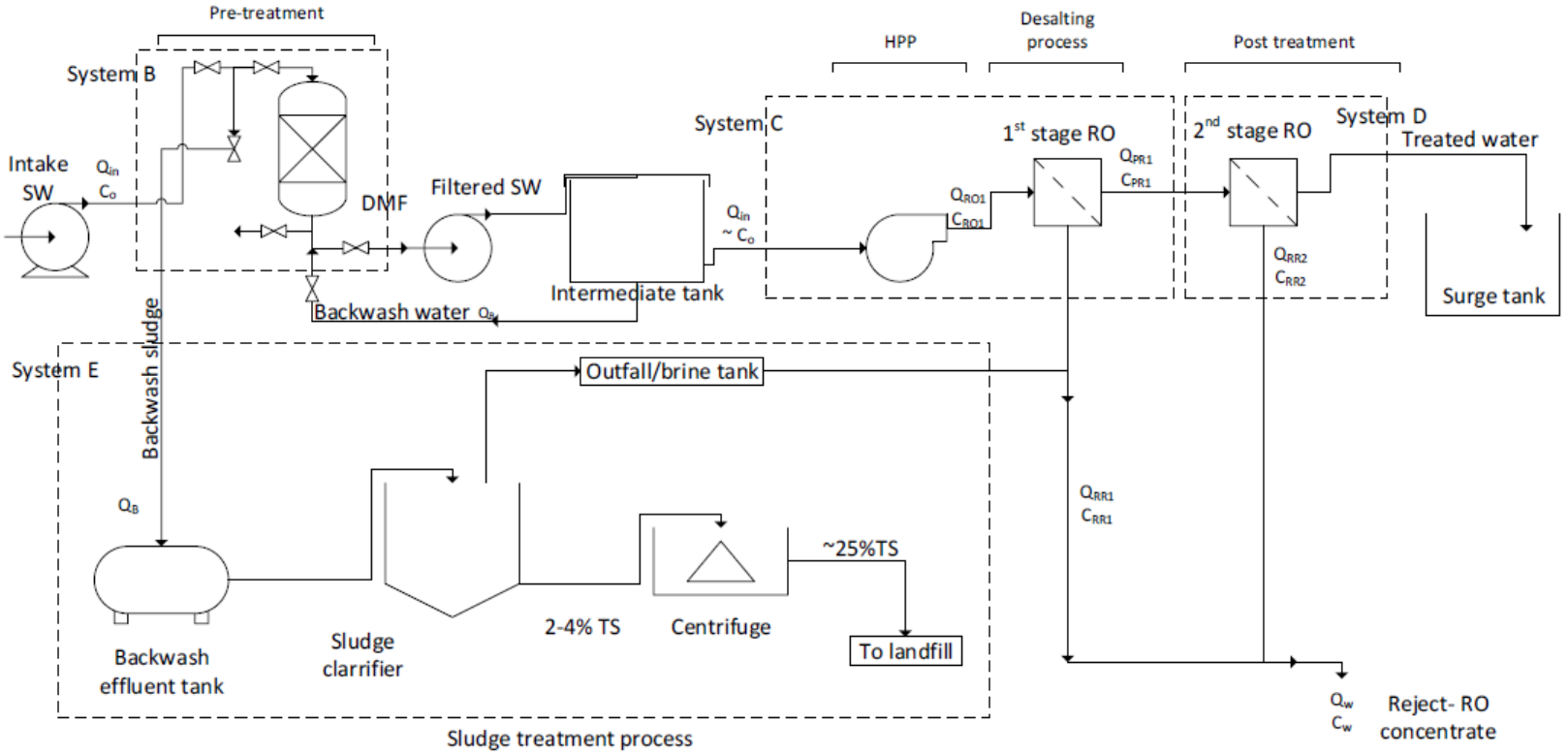

Figure 47: Typical sludge treatment process in a seawater desalination plant

The following three options of RO/FO hybrid system were considered, and mass balance calculations were applied in order to evaluate the feasibility of those systems:

Option 1:

In addition to an existing 2 stage RO desalination process, a FO system is proposed to reduce the volume of pre-treatment sludge. This Option is suggested for the RO processes, where 2nd pass RO concentrate (significantly low salt concentration since 2nd pass RO treats the permeate from 1st pass) is used to backwash media filter. Figure 48 shows the process flow diagram. An optimised proportion of 1stpass RO concentrate is used to draw water through FO as it has high concentration (hence high conductivity and osmotic pressure). Diluted 1st pass RO concentrate, which gets blended with pre-treated seawater, recirculates to the 1stpass RO for desalting in order to increase overall water recovery.

Option 2:

This Option is suggested for existing desalination processes, where filtered/polished seawater is used to backwash media filters. The additional proposed FO system uses 1st pass RO concentrate to draw water through FO as it has high concentration (hence high conductivity and osmotic pressure) as shown in Figure 49. Diluted 1st pass RO concentrate gets blended with pre-treated seawater sent back to the 1stpass RO for further desalting in order to increase the overall water recovery.

Option 3:

Figure 50 shows the process flow diagram of option 3. This Option is applicable for desalination processes where dilution of RO concentrate is important, especially before discharging to a water body. Dilution will significantly increase the discharge rate; hence higher production rate could be obtained. Either filtered/polished water after pre-treatment or concentrate from 2nd pass RO is used to backwash media filter, as suggested in option 1 and 2. 1st pass RO concentrate is used to draw water through FO as it has high TDS (hence high conductivity and osmotic pressure). Diluted brine gets blended with the 1st and 2nd pass concentrate before discharging back to a water body.

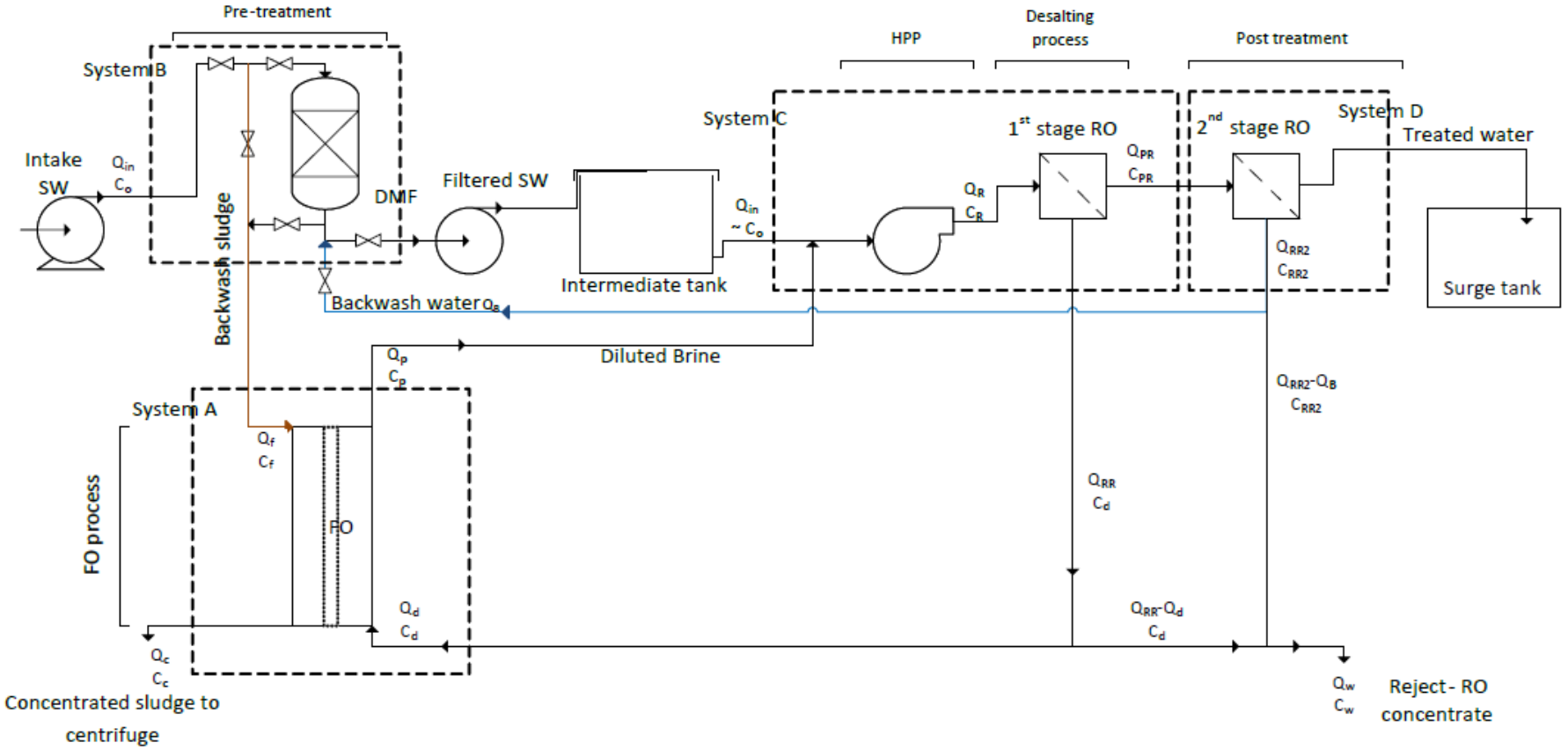

Figure 48: Option 1 - Backwashing of sand filter (used for pre-treatment) by the concentrate from 2nd pass RO, where diluted 1st pass RO concentrate (as draw solution for FO) is recycled in the RO process

Note: HPP-high pressure pumping; MF- media filter; SW-seawater

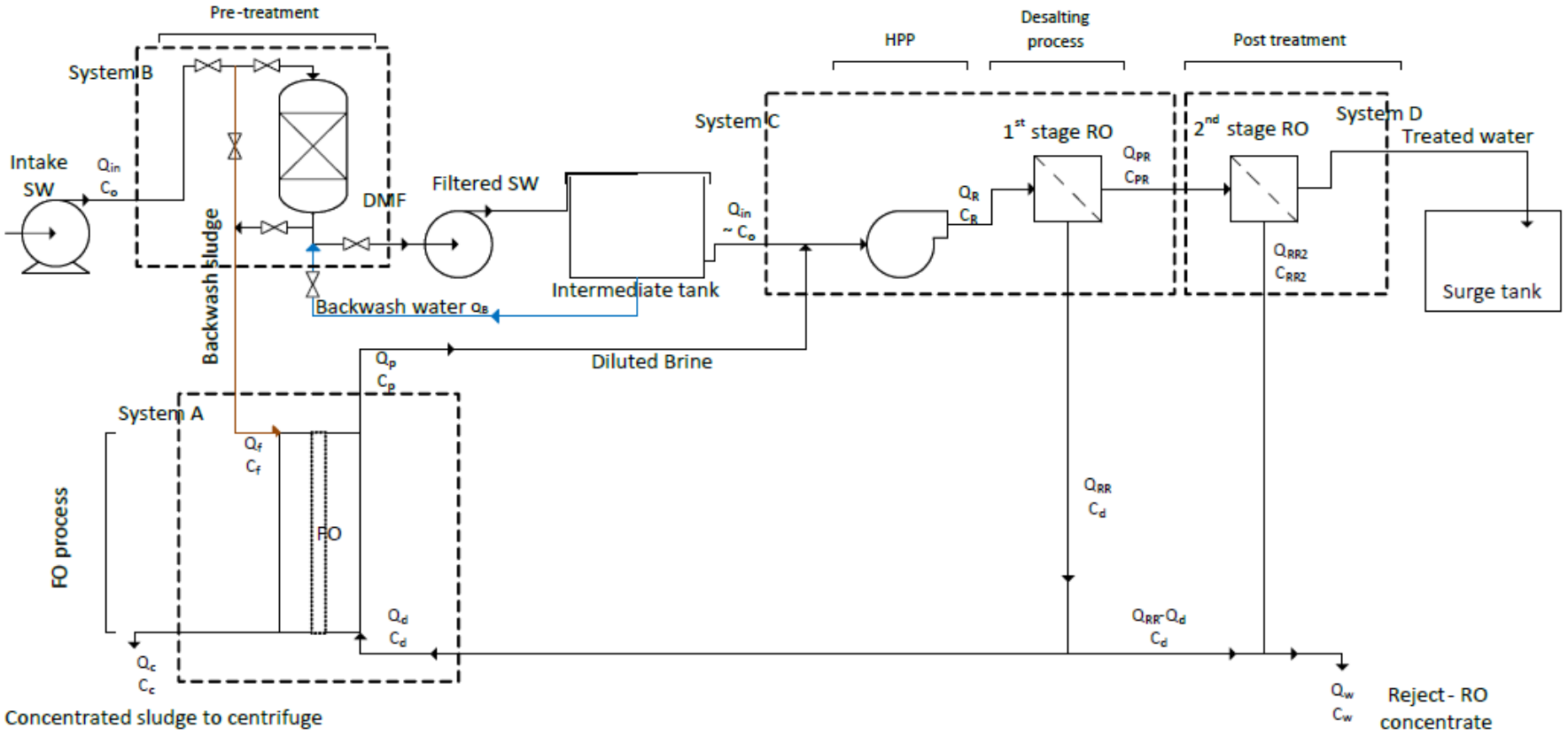

Figure 49: Option 2 - Backwashing of sand filter (used for pre-treatment) by filtered sea water, where diluted 1st pass RO concentrate (as draw solution for FO) is recycled in the RO process

Note: HPP-high pressure pumping; MF- media filter; SW-seawater

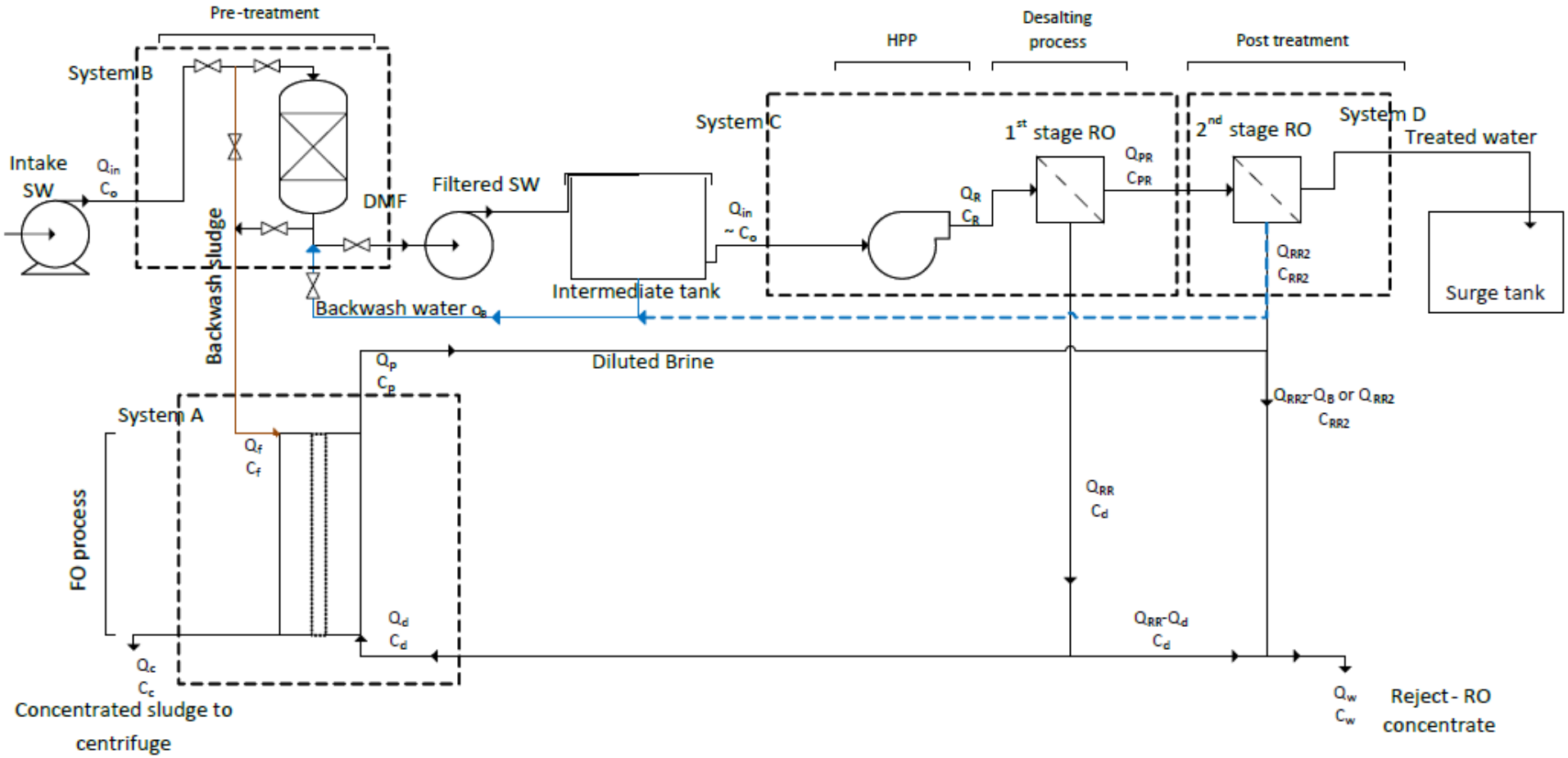

Figure 50: Option 3 – Backwashing of sand filter (used for pre-treatment) either by filtered sea water or by the concentrate from 2nd pass RO, where diluted 1st pass RO concentrate (as draw solution for FO) is not recycled in the RO process

Note: HPP-high pressure pumping; MF- media filter; SW-seawater

8.2 Mass Balance

Several factors need to be considered while conducting the mass balance for a hybrid RO/FO system. It is essential to establish the water recovery of RO at various osmotic pressures of the feed, as the feed will be a mixture of pre-treated sea water and the draw solution from the FO. Information on the amount of backwash water required for the pre-treatment process (generally sand filters) will help to decide how much of this volume could be reduced through the FO process. The above information, along with the performance of FO in terms of water flux, allows estimation of the flow rate of draw solution (RO concentrate) entering to the FO as well as the area of FO membrane.

Mass balance calculations are based on both large scale and a small scale desalination plant conditions. Table 22 shows the initial assumed parameters for the subsequent mass balance calculations.

Table 22: Assumed parameters of RO/FO hybrid system for mass balance calculations

	Large scale plant	Small scale plant	Units
Intake flow rate, Q_{in}	340,000[1]	15,000	m^3/day
RO rejection	100	100	%
Total amount of pre-treatment sludge per day, Q_B	275[1]	100[2]	m^3/day
RO 1 recovery, R1	50	50	%
RO 2 recovery, R2	90	90	%
Overall recovery (Without FO)[3]	45	45	%
Nominal FO membrane surface area of 8-inch spiral wound modules	18.13	18.13	m^2
Initial Solids content of Pre-treatment sludge	4[1]	3	%

[1]-actual figures; [2] 0.7% of intake; [3]- R1*R2

8.2.1 Mass balance for Option 1

FO system uses 1st pass RO brine as the draw solution. Applying mass balance and salt balance to the FO system (System A in Figure 48):

$$Q_c = Q_f - 0.024\, J_w A \qquad (1)$$

and

$$C_p = 2\left[\frac{Q_d}{Q_d + 0.024\,J_w A}\right] C_0 \qquad (2)$$

$$where;\ Q_f \leq\ Q_d \leq\ (Q_{in} + Q_{p)}(1 - R1\%)$$

Q_c= concentrate flow rate (m^3/day), Q_f = Feed flow rate to the FO system (m^3/day), J_w = water flux through FO unit (LMH), A = FO membrane area (m^2), C_p= salt concentration of diluted brine (mg/L), Q_d= draw flow rate to the FO unit (m^3/day), C_o= salt concentration of intake seawater (mg/L), Q_{in}= intake flow rate (m^3/day), Q_p= diluted brine flow rate (m^3/day), $R1$= recovery of the 1st pass RO unit (%).

Lower Q_d (less than Q_f) may reduce the water flux through FO, due to dilution of draw solution during filtration. Therefore, the minimum Q_d value was set to be equal to the volume of Q_f. Further concentration of draw solution is assumed as twice seawater concentration to simplify the equations (Sim et al., 2013). According to equations 1 and 2, higher water flux will lower not only the concentration of diluted brine but also the concentrated sludge volume. However, J_w significantly depends on the performance of the FO membrane and properties of draw and feed solutions, hence they need to be obtained experimentally (refer Section 8.3).

Diluted brine gets blended with pre-treated seawater before entering the 1st pass RO system. Hence, it is required to check the concentration of the inlet to 1st pass RO, C_R, as higher concentration would decrease the recovery of RO if the operating pressure remains same. Applying mass balance and salt balance to the System C in Figure 48, concentration of the inlet water to the RO is given by following equation:

$$C_R = \frac{\left[Q_{in} + {C_p}/{C_0}\, Q_P\right]}{Q_{in} + Q_P} C_o \qquad (3)$$

Where ${C_p}/{C_0}$ can be obtained through equation (2) and C_R= salt concentration of RO 1st pass inlet (mg/L).

Increased overall recovery of the system is given by:

$$R = R1 \times R2 \times (Q_{in} + Q_P) \qquad (4)$$

Where, R= overall recovery of the RO/FO hybrid system (%), R2 = recovery of the 2nd pass RO unit (%).

Furthermore, to check the dilution of the concentrated brine waste before discharging, it is important to check the concentration of concentrated brine waste. Assuming concentration of reject from 2nd pass RO, C_{RR2} is negligible (Personnel communication with Wonthaggi seawater desalination plant, 2014), $C_w$can be obtained using following relationship:

$$C_w = \frac{(Q_{RR} - Q_d)}{(Q_{RR} - Q_d) + (Q_{RR2} - Q_B)} C_d \quad (5)$$

Where C_w= salt concentration of the blended RO concentrate (reject) (mg/L), C_d= salt concentration of draw solution/ brine from 1st pass unit (mg/L), Q_{RR} = brine flow rate of 1st pass RO unit (m^3/day), Q_{RR2} = reject flow rate of 2nd pass RO unit (m^3/day), Q_B = backwash sludge flow rate (m^3/day).

This relationship can be simplified as:

$$C_w = 2\left[\frac{1}{1 + \frac{R1(1-R2)(Q_{in} + Q_p) - Q_B}{(1-R1)(Q_{in} + Q_p) - Q_d}}\right] C_o \quad (6)$$

Where C_w= salt concentration of the blended RO concentrate (reject) (mg/L),R1= recovery of the 1st pass RO unit (%), R2 = recovery of the 2nd pass RO unit (%), Q_{in}= intake flow rate (m^3/day), Q_p= diluted brine flow rate (m^3/day), Q_B = backwash sludge flow rate (m^3/day), Q_d = draw flow rate to the FO unit (m^3/day), C_o= salt concentration of intake seawater (mg/L).

8.2.2 Mass balance for Option 2

Similar equations obtained in Section 8.2.1 can be applied for the FO system in Option 2 (Figure 49) i.e. equation (1) and (2). However, conditions of feed solution vary as follow:

$$(C_f)_{Option\ 1} < (C_f)_{Option\ 2}$$

Where C_f= salt concentration of backwash sludge (mg/L). Also, the range of Q_d is given by:

$$Q_f \leq Q_d \leq (Q_{in} - Q_B + Q_P)\ (1 - R1\%)$$

Where Q_f = Feed flow rate to the FO system (m^3/day), Q_d= draw flow rate to the FO unit (m^3/day), Q_{in}= intake flow rate (m^3/day),Q_B = backwash sludge flow rate (m^3/day), Q_p= diluted brine flow rate (m^3/day), $R1$= recovery of the 1st pass RO unit (%).

Part of the filtered seawater is used to backwash the pre-treatment system, generally media filter. Therefore, the amount of water enters the 1st pass RO system, Q_R is given by:

$$Q_R = Q_{in} - Q_B + Q_P \quad (7)$$

Thus, the concentration of the fluid stream entering the 1st pass RO system,C_R is given by:

$$C_R = \frac{\left[(Q_{in} - Q_B) + {C_p}/{C_0}\, Q_P\right]}{(Q_{in} - Q_B) + Q_P} C_o \quad (8)$$

Where ${C_p}/{C_0}$ is given by Equation (2).

Due to the increased volume to the desalting process, increased overall water recovery is given by:

$$R\% = R1 \times R2 \times (Q_{in} - Q_B + Q_P) \quad (9)$$

Concentration of the concentrated brine waste is given by:

$$C_w = 2\left[\frac{1}{1 + \frac{R1(1-R2)(Q_{in} - Q_B + Q_p)}{(1-R1)(Q_{in} - Q_B + Q_p) - Q_d}}\right] C_o \quad (10)$$

Where C_w= salt concentration of the blended RO concentrate (reject) (mg/L),R1= recovery of the 1st pass RO unit, R2 = recovery of the 2nd pass RO unit (%),Q_{in}= intake flow rate (m^3/day), Q_B = backwash sludge flow rate (m^3/day), Q_p= diluted brine flow rate (m^3/day), Q_d = draw flow rate to the FO unit (m^3/day), C_o= salt concentration of intake seawater (mg/L).

8.2.3 Mass balance for Option 3

The difference in this Option is, without increasing the overall recovery, diluted brine is used to dilute the blended reject from 1st and 2nd pass RO units. Therefore, the important parameter that is needed to be checked is C_w. However, C_w depends on the backwash method. C_w at each backwash can be obtained using following mass balance relationships;

If 2nd pass RO reject is used as backwash water:

$$C_w = \left[\frac{Q_p \, {C_p}/{C_0} + 2[Q_{in}(1-R1) - Q_d]}{[Q_{in}(1-R1) - Q_d] + [Q_{in}R1(1-R2) - Q_B + Q_p}\right] C_0 \quad (11)$$

If filtered seawater is used as backwash water:

$$C_w = \left[\frac{Q_p \, {C_p}/{C_0} + 2[(Q_{in} - Q_B)(1-R1) - Q_d]}{[(Q_{in} - Q_B)(1-R1) - Q_d] + [(Q_{in} - Q_B)R1(1-R2) + Q_p]}\right] C_0 \quad (12)$$

Where, C_w= salt concentration of the blended RO concentrate (reject) (mg/L),Q_p= diluted brine flow rate (m^3/day), C_p= salt concentration of diluted brine (mg/L),C_o= salt concentration of intake seawater (mg/L), Q_{in}= intake flow rate (m^3/day), R1= recovery of the 1st pass RO unit (%),Q_d = draw flow rate to the FO unit (m^3/day), R2 = recovery of the 2nd pass RO unit (%),Q_B = backwash sludge flow rate (m^3/day).

Water flux through FO would be significantly higher in first option than the second as the salt concentration of backwash sludge is lower in the former.

8.3 Materials and Method for FO Experiments

Flat sheet CTA membranes were purchased from HTI, USA and $Fe(OH)_3$ sludge (feed solution) was obtained from the Perth Seawater Desalination Plant (PSDP), Australia. Draw solution (RO reject) was prepared at laboratory scale following the SWRO process explained in Section 3.2.2. Sludge solids content was varied to four different values while the properties of the draw solution remained constant. Pre-treatment sludge was diluted using de-ionised water (up to 1:4 volume proportion) in order to change the solids content, however, the salt concentration of the feed also changed (hence the EC). EC measurements were used as the

basis to define the salt concentration. To check the effect of salt concentration of feed solution (as the proposed systems' feed solutions have different salt concentrations), experiments were conducted at constant EC value as well.

When the feed solution EC was lowered after dilution, EC was adjusted to its original value using 40% NaCl. These solutions are denoted as EC adjusted samples. Feed and draw solutions were passed through the membrane at 0.5 m/s cross flow velocities in counter current flow configuration. All the experiments were conducted in AL-FS mode as the previous studies showed that AL-FS mode performs better than AL-DS mode (Chapter 5- (Liyanaarachchi et al., 2014a)).Change in the weight of the draw solution was programmed to be stored in a data logger at one minute time intervals to calculate the experimental water flux (J_w).

8.4 Results and Discussion

8.4.1 FO Experiments

Pre-treatment sludge solids content was 3.4% TS, as received. When diluted by 1:4, the solids content reduced to 0.6% TS. Figure 51 shows the effect of solids content on the water flux, along with the solids content values. Significantly higher water flux was observed when EC of the feed solution was not adjusted, compared to constant EC feeds. Water flux of EC adjusted, and constant EC samples were 6.1 and 8.0 LMH, respectively, at 1:4 dilution. Added EC controller increases the salt concentration of the feed solution and this would have led to lower water flux as higher feed concentrations reduce the effective osmotic pressure difference across the membrane. This was further confirmed at lower dilution factors. When sludge was diluted 1:1 with water, the amount of salt added by the EC controller was significantly lower compared to former sample, hence the difference in water flux of EC controlled and un-controlled samples was marginal.

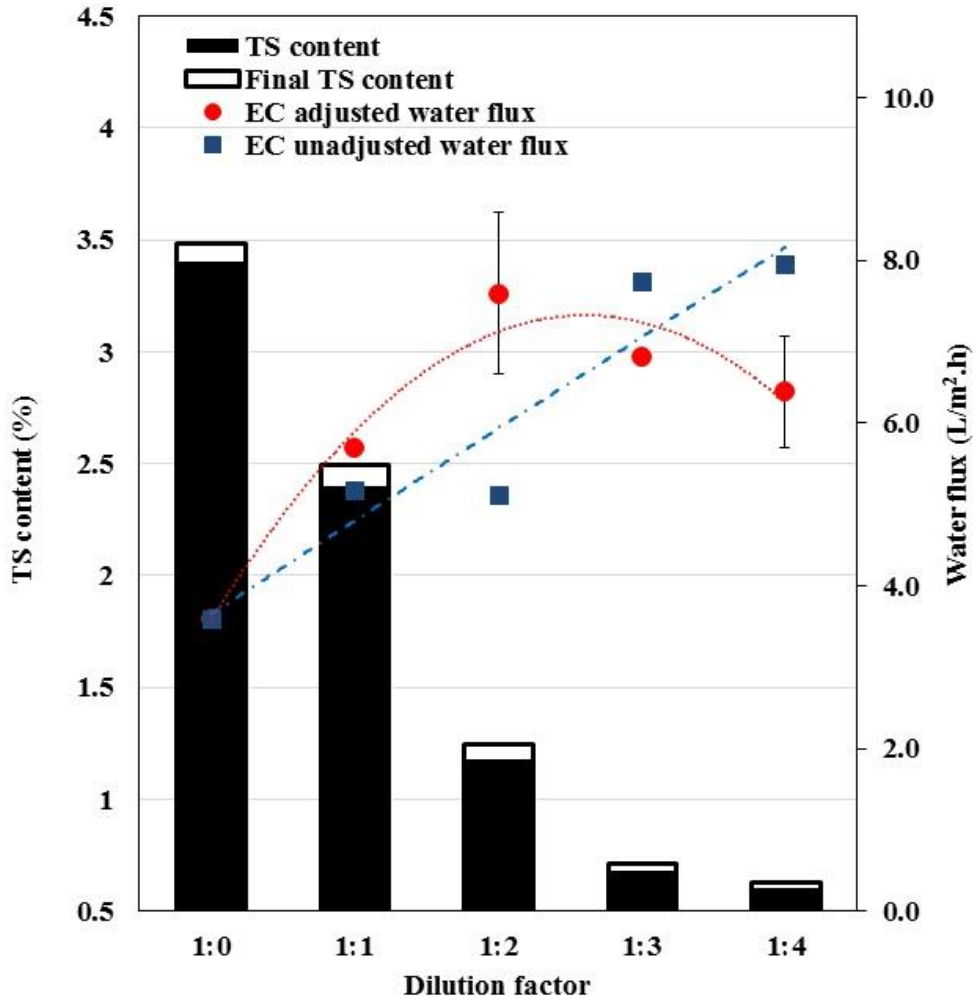

Figure 51: Effect of solids content on water flux. Note: During the experiments feed solution was facing active side of the membrane. Industrial pre-treatment sludge was received with 3.4% TS content; therefore, dilution is 1:0. Water flux obtained at each dilution is presented on secondary Y axis.

Hence, significantly higher flux could be expected in proposed Option 1 than in Option 2. This is due to lower EC value of feed solution in Option 1 than in Option 2. As Figure 51 depicts, water flux at 1:0 dilution was around 3 LMH and when dilution was 1:4 water flux was 6 to 8 LMH depending on the EC of the solution. Therefore, for the mass balance calculations, it was assumed that the water flux in Option 1 is twice that in Option 2.

8.4.2 Option 1

Change in concentration of diluted brine, C_p, was studied when Q_d/Q_f was changed within the given range. Figure 52 shows the change in C_p when FO membrane area increased in large and

small scale desalination plants. When membrane area was 500m^2 and Q_d/Q_f was lowest,C_p was 1.35 and 1.16 times of the concentration of seawater for large scale and small scale processes, respectively. However, when the membrane area was lower, C_p increased significantly as J_w was lower (according to equation (2)), at both scales. However, in both the processes, when Q_d/Q_f increased, $C_p$converged to C_d/C_0 which is nearly equal to the concentration of 1st pass RO reject. Higher concentration of diluted brine would have an effect on the performance of 1st pass RO unit as it would reduce its recovery if it operates under the same operating conditions. However, before entering the RO unit, diluted brine is blended with pre-treated seawater and salt concentrations change to C_R. Consequently, C_R has an effect on the performance of the RO unit. Therefore, change in C_R with $Q_d/Q_f$was studied and given in Figure 52 (c) and (d). As Figure 52 (c) and (d) depict, after blended with filtered seawater, the change in concentration is negligible at each condition for large scale processes. Unfortunately, for small scale processes, the increase in concentration is significantly higher. However, for small scale plants lower $Q_d/Q_f$is suggested, as for lower flow rates C_R/C_o ratio is less than 1.02 (Figure 52).

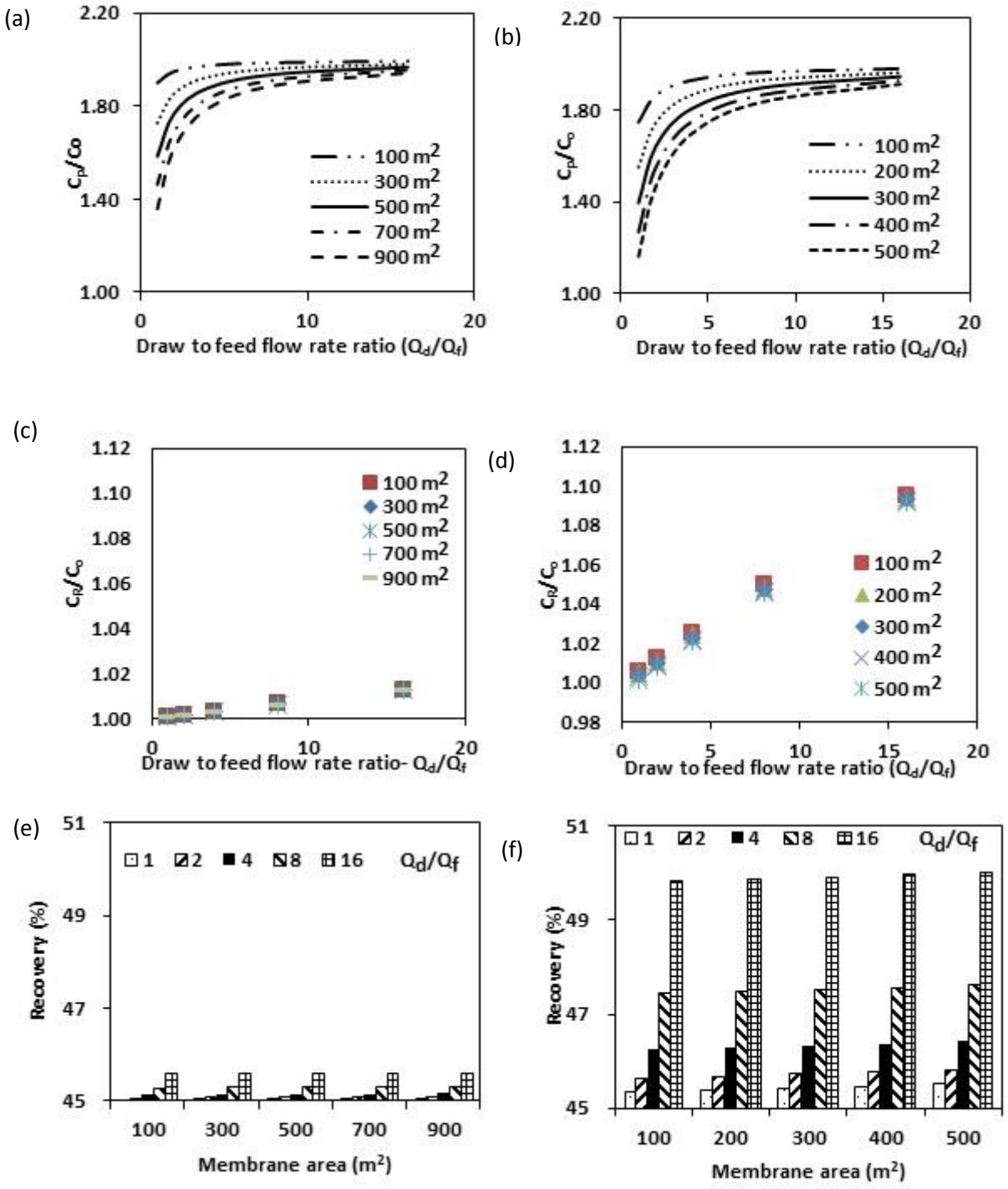

Figure 52: Variation of C_p, C_R and recovery with Q_d at selected FO membrane area for Option 1. (a), (c) and (e) Large scale desalination plant (b), (d) and (f) small scale desalination plant

Overall recovery of a seawater desalination system is assumed to be 45%. Overall recovery after System A is installed was plotted against membrane area at each Q_d and given in Figure 52 (e) and (f). Q_d for large scale and small scale plants was varied up to 16 times. Increase in recovery for the small scale process is higher than that of large scale process, at smaller draw flow rates.

Final solids content after passing through the FO system was calculated and is shown in Figure 53. When the membrane area is 100 m^2 (minimum area considered) it reduces sludge volume by 5.24%, but the final solids content has increased only up to 4.22%. When membrane area increases, both solids content and sludge volume reduction increase in large and small scale plants. When membrane area of a large scale plant is increased to 900 m^2, sludge volume has reduced by 50% with a final solids content of 7.57%.

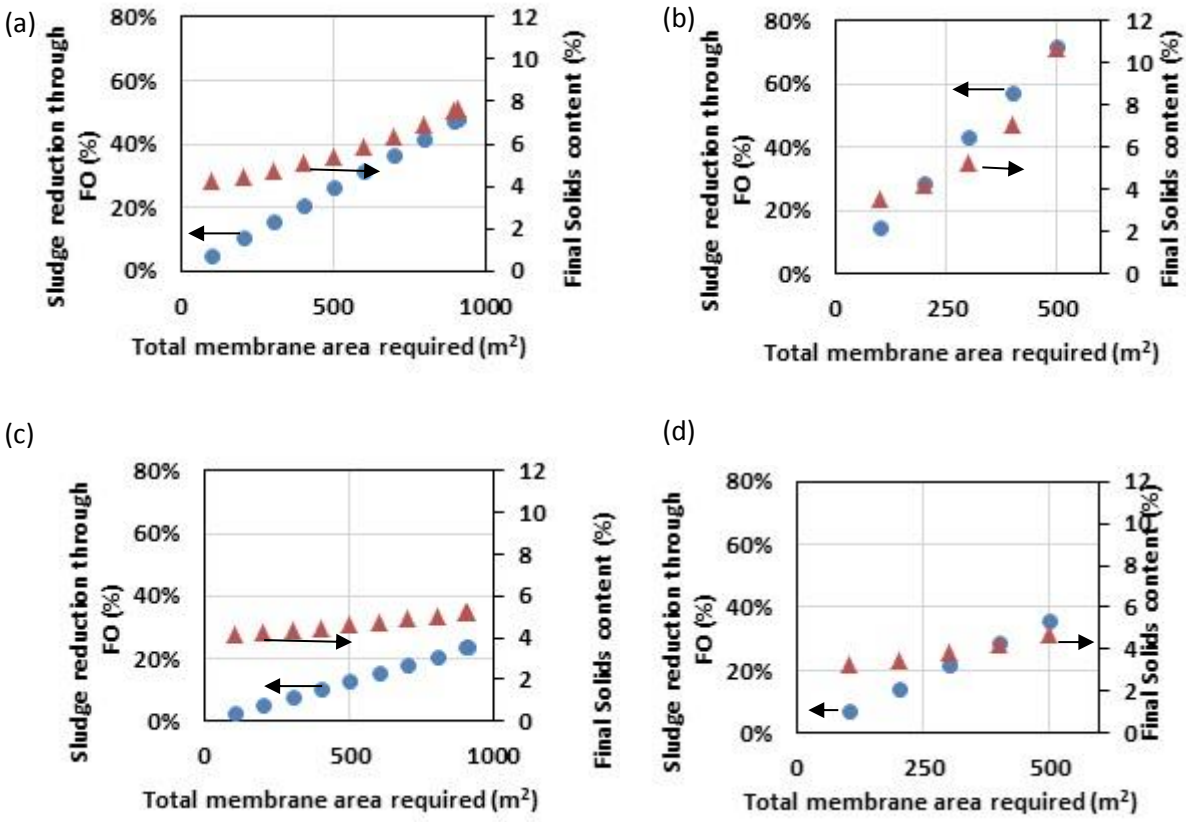

Figure 53: Final solids content of the sludge with different FO membrane area (a) Large scale plant with Option 1 (b) small scale plant with Option 1 (c) Large scale plant with Option 2 (d) small scale plant with Option 2.

Note: circles denote sludge volume reduction through FO and triangles denote final solids content.

8.4.3 Option 2

Figure 54 shows the variation of C_p at selected draw flow rates with different membrane area. In the case of large scale desalination plants, when membrane area increases from 100 to 500 m^2, increase in concentration of diluted brine is marginal at the lowest Q_d/Q_f. However, there is a significant increase in small scale plants in the lowest Q_d/Q_f. As mentioned in Option 1, it is important to check C_R in order to understand the dilution factor to the 1st pass RO. Variation of C_R with Q_d/Q_f is also given in Figure 54. Similar to Option 1, in large scale plants dilution is lower (maximum ratio is 1.013) compared to small scale plants. However, for small scale plants lower membrane area can be suggested since the C_R/C_o ratio is less than 1.01. As far as increase in overall recovery concerned, small scale plants show better performance. Calculated overall recovery values were plotted and are shown in Figure 54 (e) and (f). Maximum change in recovery is by 0.5% in the case of large scale desalination plants. Interestingly, small scale plants show overall recoveries up to ~50 %.

Final solids content after passing through the FO system was calculated and is shown in Figure 53 (c) and (d). When the membrane area is 100 m^2 (minimum area considered) it reduces sludge volume by 7%, but the final solids content has increased only up to 3.2% in small scale plants. When membrane area increases, both solids content and sludge volume reduction increase at both scales. When membrane area of a small scale plant is increased to 500 m^2, sludge volume has reduced by 36% with a final solids content of 4.7%.

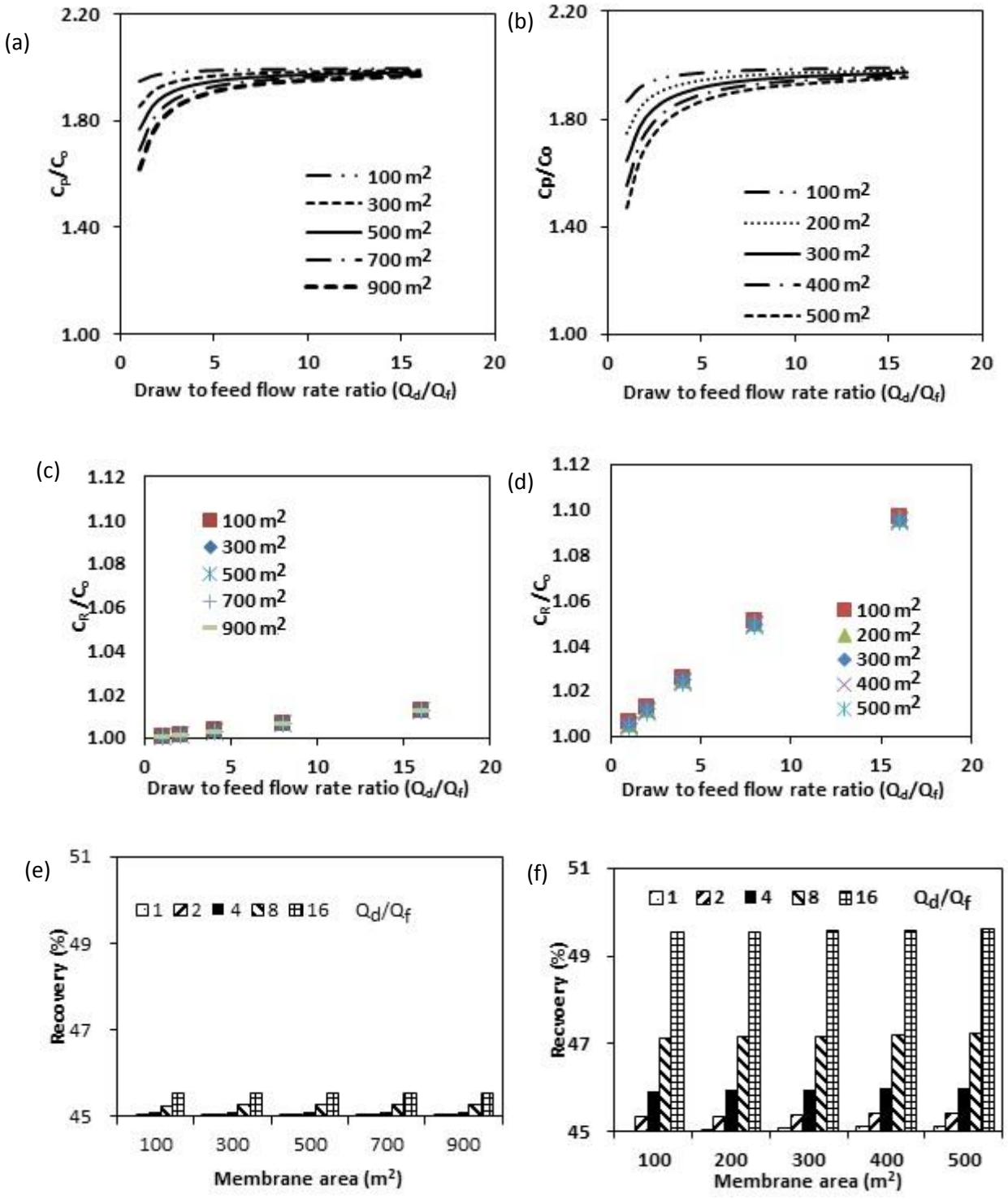

Figure 54: Variation of C_p, C_R and recovery with Q_d at selected FO membrane area for Option 2. (a), (c) and (e) Large scale desalination plant (b), (d) and (f) small scale desalination plant.

8.4.4 Option 3

An important factor to be considered in Option 3 is the dilution factor of brine before discharge. Therefore, ratio of C_w and C_o was calculated and plotted against membrane area as shown in Figure 55. Higher dilution occurs when filtered seawater is used as backwash water in small scale desalination plants. When 100 m^2 of membrane is used, dilution factor is as high as 1.84.

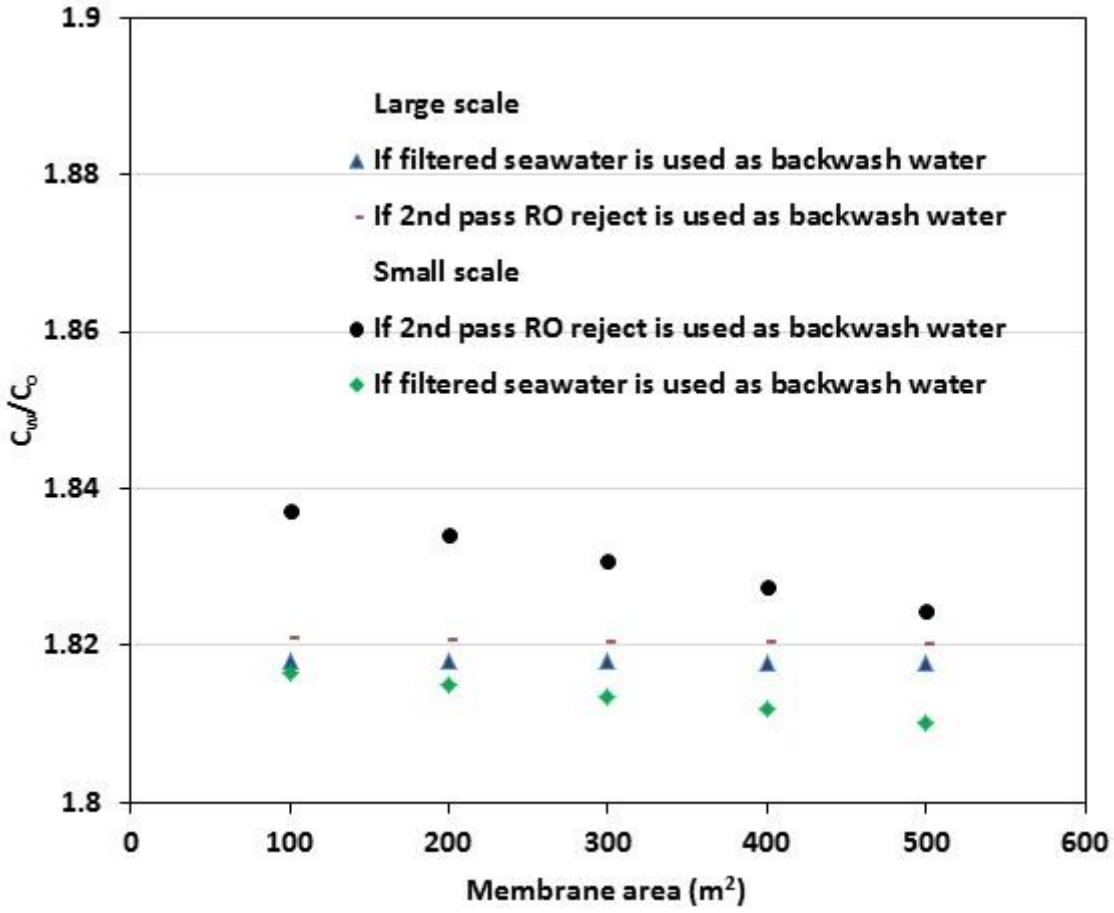

Figure 55: Variation of C_w/C_o with membrane area for large and small scale desalination plants in Option 3.

Note: At both scales, water flux through FO was assumed to be 3 LMH if filtered sea water was used as backwash water and 6 LMH if 2nd pass RO reject was used as backwash water

In summary, the novel proposed FO/RO hybrid system's sludge treatment process shows significant reduction in sludge solids content and a marginal increase in overall water recovery at the selected draw to feed ratio range. An optimum draw to feed ratio should achieve

lower C_P and C_R values and higher recovery values. Therefore, a draw to feed flow ratio of < 4 for both scales would be recommended, with a membrane area of 900 m^2 and 500 m^2 for large and small scale plants, respectively. Table 23 shows the comparison between before and after installing an FO system. After installing an FO system prior to centrifuge of a small scale treatment plant, number of centrifuges in operation can be reduced from 3 to 2, which leads to lower power requirement. Hence, lower capital cost and operational energy costs. As reported in Table 23, annual energy costs of a small scale treatment plant can be reduced to one third. However, number of centrifuges in operation in a large scale treatment plant remains same even after installing the FO unit. But, the annual power requirement reduces nearly to half and the energy cost can be minimised to AUD 8000/annum. The volume of centrate generated through centrifuges can be minimised with the proposed system at both scales. This reduces cleaning in place (CIP) costs of the plants, hence lower operational costs. In addition, existing sludge clarifiers are not necessary for both the systems as sludge flow pass through FO process before entering the mechanical dewatering system, therefore reduction in capital cost can be achieved.

Using the costing data provided in a recent work, (Valladares Linares et al., 2016) the following could be considered as the CAPEX and OPEX of existing RO system and the hybrid FO/RO system proposed in this study: The Engineering, Procurement and Construction (EPC) costs of SWRO and stand-alone FO unit were considered to be USD 1207 and USD 787 per cubic metre of water produced per day. Thus, the CAPEX of 340,000 m^3/d and 15,000 m^3/d RO systems at 45% recovery would be USD 83,102,000 and USD 3,667,000, respectively. If the same RO system is used in the FO/RO hybrid system the EPC will be reduced to USD 1191 in the large scale plant (at 45.6% water recovery) and USD 1095 (at 49.6% water recovery) in the small scale plant per cubic metre of water produced per day. The CAPEX of FO system in the large and small scale FO/RO plants seems to be marginal compared to the CAPEX of RO at USD 115,000 and USD 24,000, respectively. Similarly, the OPEX of SWRO can be computed using the following percentages (Valladares Linares et al., 2016): 3% labour, 3% membrane replacement, 5% chemicals, 12% maintenance and others, 38% energy and 39% amortisation for CAPEX. Introduction of FO as discussed earlier helps to reduce the annual energy cost slightly.

Table 23: Comparison of existing and proposed sludge treatment processes (VOLLPRECHT, 2013, (EPA), (EPA)). (LSP- large scale plants; SSP-small scale plants)

	Existing sludge treatment process	Proposed RO/FO hybrid system
SFR: **SSC:**	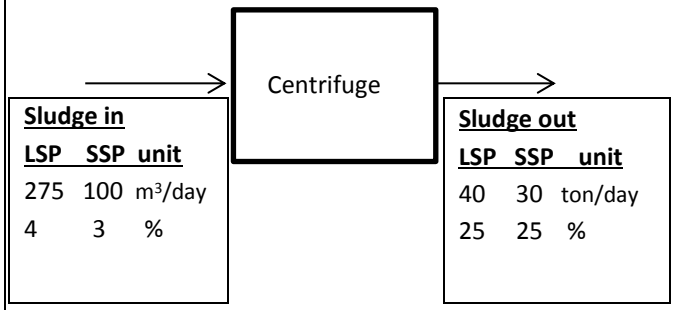	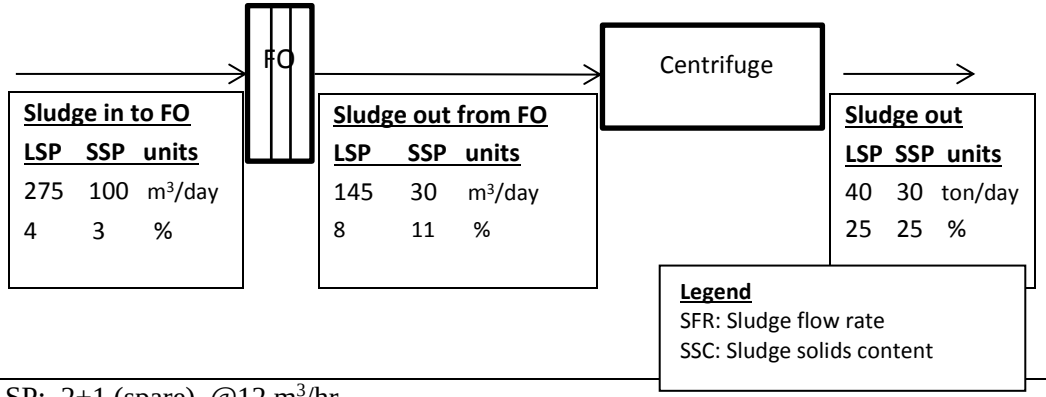
No. of centrifuges	LSP: 2+1 (spare) @12 m^3/hr SSP: 2+1 (spare) @12 m^3/hr	LSP: 2+1 (spare) @12 m^3/hr SSP: 1+1 (spare) @6 m^3/hr
Power requirement	LSP: 415 kW h/day SSP: 150 kW h/day	LSP: 150 kW h/day SSP: 45 kW h/day
Total annual cost	LSP: AUD 15,000 per annum SSP: AUD 5,500 per annum	LSP: AUD 9,000 per annum SSP: AUD 2,600 per annum
Comments	• Centrate needs further treatment. Cannot reuse as solids capturing of centrifuges lie between 85-96	• Reduced number of centrifuges will reduce the capital cost as well as O&M costs for dewatering. • Less centrate to treat in place and could pass through a FO set up if necessary. Centrate from FO (draw solution) can reuse to increase water recovery and/or to dilute RO concentrate • Sludge clarifier (as in Figure 47) is not necessary.

8.5 Conclusions

Experiments and mathematical modelling proved that proposed novel FO/RO hybrid systems are capable of reducing the volume of pre-treatment sludge. Table 24 shows the final volume reduction, increase in water recovery and final solids content of both large and small desalination plants considered.

Table 24: Design outcomes of the RO/FO hybrid system

	Large scale plant (340 ML/day)		**Small scale plant (15 ML/day)**		**Units**
	Option 1	Option 2	Option 1	Option 2	
FO membrane area required	100 - 900	100 - 900	100 - 500	100 - 500	m^2
Volume reduction	5.2 - 47.1	2.6 - 23.6	14.4 - 72.0	7.2 - 36.0	%
Final solids content	4.2 -7.6	4.1 - 5.2	3.5 - 10.7	3.2 - 4.7	%
Water recovery	45.0 - 45.6	45.0 - 45.6	45.3 - 50.0	45.0 - 49.6	%
Number of 8 inch spiral wound modules required	6 - 50	6 - 50	6 - 28	6 - 28	-

By increasing FO membrane area up to 900m^2 (which requires fifty 8" spiral wound membrane modules), pre-treatment sludge volume can be reduced up to 47% in large scale desalination plants. Further final solids content and overall water recovery of RO system can be increase up to 7.6% and 45.6%, respectively. Interestingly in small scale plants, having membrane area up to 500 m^2, the volume of sludge can be reduced by 72%. During dewatering, the final solids content and overall water recovery increased to 10.7% and ~ 50%, respectively. Twenty-eight 8" spiral wound membrane modules are estimated to be required to operate in this mode. Therefore, small scale desalination plants tend to show better performance than large scale plants with the Hybrid system.

Chapter 9: Conclusions and Recommendations

9.1 Conclusions

This study focused on volume reduction of pre-treatment sludge while diluting reverse osmosis (RO) concentrate through emerging forward osmosis (FO) technology where RO concentrate draws water from the pre-treatment sludge in order to reduce volume of pre-treatment sludge and increase the RO water recovery.

Experiments were carried out using two different types of sludge i.e. (1) synthetic pre-treatment sludge (Lab sludge) which has lower salinity and (2) actual sludge from Perth Seawater Desalination Plant, Australia (PSDP sludge) which has higher salinity. These sludge were dewatered using flat sheet as well as hollow fibre FO membranes to find the better type of membrane for this application. Effect of membrane orientation, temperature, cross flow velocity and pH of pre-treatment sludge on water flux was investigated. In addition, fouling tendency of FO membrane during long term filtration was investigated. More over a novel FO/RO hybrid system was proposed for this application in desalination industry.

Experiments and mathematical modelling proved that proposed FO/RO hybrid systems are capable of reducing the volume of pre-treatment sludge. Flat sheet membranes showed a higher water flux compared to hollow fibre membranes. At as is sludge pH (8), and ambient temperature (~20 ^{o}C) the maximum water flux obtained through the flat sheet membranes was around 3 LMH. The long-term filtration showed that membrane needs weekly backwashing to enhance the water flux and the inorganic fouling is reversible as a thin loose layer of metal deposits observed on the filtered membrane surface. With this application, sludge volume can be reduced up to 72% using a FO membrane area of 500 m^2. This reduces the solids content of sludge from 3% to 10.7% and increases the overall RO recovery from 45% to 50%.

9.2 Recommended future work

Feed sludge can be combined with secondary wastewater (WW) effluent. If feed sludge to the FO is combined with a secondary WW effluent, that could increase the water flux through the FO system. This would increase brine dilution as well as the recovery through RO.

In this study fouling of FO was investigated in terms of reduction in water flux. However, the major fouling elements (such as Ca^{2+}, Fe^{3+}, etc) in RO brine and pre-treatment sludge can be identified and then run the FO system, would give a very clear picture of the fouling on FO

during sludge dewatering. This would be one of the recommended future work related to this study.

This research used commercially available CTA flat sheet and PA hollow fibre membranes to check the pre-treatment sludge dewatering capacity. However, both membranes gave a significantly low water flux, as low as 3 LMH. Therefore, surface modifications of the FO membrane to increase the water flux further could be another recommendation. For example, for FO flat sheet CTA membranes are manufactured with dense and a support layer. Therefore, ways of removing the porous support layer (which will then avoid the ICP effect hence lead to significantly higher water flux) could be investigated.

Developing a menu driven program for the proposed FO/RO hybrid system is another future work. This is currently being conducted using Mat Lab, Excel and Visual basic software by other members of the research group that I worked with during my PhD study.

References

Gold Coast Desalination Plant web site [Online]. [Accessed].

http://www.degremont.com.au/media/general/Perth_Seawater_Desalination_Plant.pdf [Online]. [Accessed 10/04/2015].

(EPA), E. Biosolids Technology Fact Sheet-Centrifuge Thickening and Dewatering E.P. agency (Ed.)Office of water, Washington D.C. (2000), pp. 1-8. https://www3.epa.gov/

(EPA), E. Design manual-dewatering municipal wastewater sludges, E.P. agency (Ed.)20460, Office of Research and Development, Washington DC (1987), pp. 1–212. https://www3.epa.gov/.

ABOU RAYAN, M. & KHALED, I. 2003. Seawater desalination by reverse osmosis (case study). *Desalination,* 153**,** 245-251.

ACHILLI, A., CATH, T. Y. & CHILDRESS, A. E. 2010. Selection of inorganic-based draw solutions for forward osmosis applications. *Journal of Membrane Science,* 364**,** 233-241.

ACHILLI, A., CATH, T. Y., MARCHAND, E. A. & CHILDRESS, A. E. 2009. The forward osmosis membrane bioreactor: A low fouling alternative to MBR processes. *Desalination,* 239**,** 10–21.

AGUS, E., VOUTCHKOV, N. & SEDLAK, D. L. 2009. Disinfection by-products and their potential impact on the quality of water produced by desalination systems: A literature review. *Desalination,* 237**,** 214-237.

AHMED, M., SHAYYA, W. H., HOEY, D. & AL-HANDALY, J. 2001. Brine disposal from reverse osmosis desalination plants in Oman and the United Arab Emirates. *Desalination,* 133**,** 135-147.

AL-SARKAL, T. & ARAFAT, H. A. 2013. Ultrafiltration versus sedimentation-based pretreatment in Fujairah-1 RO plant: Environmental impact study. *Desalination,* 317**,** 55-66.

ALEJO, T., ARRUEBO, M., CARCELEN, V., MONSALVO, V. M. & SEBASTIAN, V. 2017. Advances in draw solutes for forward osmosis: Hybrid organic-inorganic nanoparticles and conventional solutes. *Chemical Engineering Journal,* 309**,** 738-752.

ALNAIZY, R., AIDAN, A. & QASIM, M. 2013a. Copper sulfate as draw solute in forward osmosis desalination. *Journal of Environmental Chemical Engineering,* 1**,** 424-430.

ALNAIZY, R., AIDAN, A. & QASIM, M. 2013b. Draw solute recovery by metathesis precipitation in forward osmosis desalination. *Desalination and Water Treatment,* 51**,** 5516-5525.

ARKHANGELSKY, E., WICAKSANA, F., CHOU, S., AL-RABIAH, A. A., AL-ZAHRANI, S. M. & WANG, R. 2012. Effects of scaling and cleaning on the performance of forward osmosis hollow fiber membranes. *Journal of Membrane Science,* 415–416**,** 101-108.

BAOXIA, M. I. & ELIMELECH, M. 2010. Gypsum scaling and cleaning in forward osmosis: Measurements and mechanisms. *Environmental Science and Technology,* 44**,** 2022-2028.

BLANK, J. E., TUSEL, G. F. & NISAN, S. 2007a. The real cost of desalted water and how to reduce it further. *Desalination,* 205**,** 298-311.

BLANK, J. E., TUSEL, G. F. & NISANC, S. 2007b. The real cost of desalted water and how to reduce it further. *Desalination,* 205**,** 298-311.

BOWDEN, K. S., ACHILLI, A. & CHILDRESS, A. E. 2012. Organic ionic salt draw solutions for osmotic membrane bioreactors. *Bioresource Technology,* 122**,** 207-216.

BREHANT, A., BONNELYE, V. & PEREZ, M. 2002. Comparison of MF/UF pretreatment with conventional filtration prior to RO membranes for surface seawater desalination. *Desalination,* 144**,** 353-360.

CATH, T. Y., CHILDRESS, A. E. & ELIMELECH, M. 2006. Forward osmosis: Principles, applications, and recent developments. *Journal of Membrane Science,* 281**,** 70-87.

CATH, T. Y., ELIMELECH, M., MCCUTCHEON, J. R., MCGINNIS, R. L., ACHILLI, A., ANASTASIO, D., BRADY, A. R., CHILDRESS, A. E., FARR, I. V., HANCOCK, N. T., LAMPI, J., NGHIEM, L. D., XIE, M. & YIP, N. Y. 2013a. Standard Methodology for Evaluating Membrane Performance in Osmotically Driven Membrane Processes. *Desalination,* 312**,** 31-38.

CATH, T. Y., ELIMELECH, M., MCCUTCHEON, J. R., MCGINNIS, R. L., ACHILLI, A., ANASTASIO, D., BRADY, A. R., CHILDRESS, A. E., FARR, I. V., HANCOCK, N. T., LAMPI, J., NGHIEM, L. D., XIE, M. & YIP, N. Y. 2013b. Standard Methodology for Evaluating Membrane Performance in Osmotically Driven Membrane Processes. *Desalination,* 312**,** 31-38.

CATH, T. Y., HANCOCK, N. T., LUNDIN, C. D., HOPPE-JONES, C. & DREWES, J. E. 2010. A multi-barrier osmotic dilution process for simultaneous desalination and purification of impaired water. *Journal of Membrane Science,* 362**,** 417-426.

CHARCOSSET, C. 2009. A review of membrane processes and renewable energies for desalination. *Desalination,* 245**,** 214-231.

CHEKLI, L., PHUNTSHO, S., KIM, J. E., KIM, J., CHOI, J. Y., CHOI, J.-S., KIM, S., KIM, J. H., HONG, S., SOHN, J. & SHON, H. K. 2016. A comprehensive review of hybrid forward osmosis systems: Performance, applications and future prospects. *Journal of Membrane Science,* 497**,** 430-449.

CHU, C. P., LEE, D. J. & CHANG, C. Y. 2005. Energy demand in sludge dewatering. *Water Research,* 39**,** 1858-1868.

CHUN, Y., ZAVISKA, F., CORNELISSEN, E. & ZOU, L. 2015. A case study of fouling development and flux reversibility of treating actual lake water by forward osmosis process. *Desalination,* 357**,** 55-64.

CORNELISSEN, E. R., HARMSEN, D., DE KORTE, K. F., RUIKEN, C. J., QIN, J.-J., OO, H. & WESSELS, L. P. 2008. Membrane fouling and process performance of forward osmosis membranes on activated sludge. *Journal of Membrane Science,* 319**,** 158-168.

DREIZIN, Y. 2006. Ashkelon seawater desalination project — off-taker's self costs, supplied water costs, total costs and benefits. *Desalination,* 190**,** 104-116.

DUAN, J., LITWILLER, E., CHOI, S. H. & PINNAU, I. 2014. Evaluation of sodium lignin sulfonate as draw solute in forward osmosis for desert restoration. *Journal of Membrane Science,* 453**,** 463-470.

EBRAHIM, S. & ABDEL-JAWAD, M. 1994. Economics of seawater desalination by reverse osmosis. *Desalination,* 99**,** 39-55.

EL-SADEK, A. 2010. Water desalination: An imperative measure for water security in Egypt. *Desalination,* 250**,** 876-884.

ELIMELECH, M. 2007. Yale constructs forward osmosis desalination pilot plant. *Membrane Technology,* 2007**,** 7-8.

ELIMELECH, M. & PHILLIP, W. A. 2011. The Future of Seawater Desalination: Energy, Technology, and the Environment. *Science,* 333**,** 712-717.

FRITZMANN, C., LÖWENBERG, J., WINTGENS, T. & MELIN, T. 2007. State-of-the-art of reverse osmosis desalination. *Desalination,* 216**,** 1-76.

GAO, Y., W. LI, W.C.L. LAY, H.G.L. COSTER, A.G. FANE, C.Y. TANG, 2013. Characterization of forward osmosis membranes by electrochemical impedance spectroscopy. *Desalination,* 312**,** 45-51.

GE, Q. & CHUNG, T. S. 2013. Hydroacid complexes: A new class of draw solutes to promote forward osmosis (FO) processes. *Chemical Communications,* 49**,** 8471-8473.

GE, Q., LING, M. & CHUNG, T.-S. 2013. Draw solutions for forward osmosis processes: Developments, challenges, and prospects for the future. *Journal of Membrane Science,* 442**,** 225-237.

GE, Q., SU, J., AMY, G. L. & CHUNG, T. S. 2012a. Exploration of polyelectrolytes as draw solutes in forward osmosis processes. *Water Research,* 46**,** 1318-1326.

GE, Q., SU, J., CHUNG, T.-S. & AMY, G. 2011. Hydrophilic Superparamagnetic Nanoparticles: Synthesis, Characterization, and Performance in Forward Osmosis Processes. *Industrial & Engineering Chemistry Research,* 50**,** 382-388.

GE, Q., WANG, P., WAN, C. & CHUNG, T. S. 2012b. Polyelectrolyte-promoted Forward Osmosis-Membrane Distillation (FO-MD) hybrid process for dye wastewater treatment. *Environmental Science and Technology,* 46**,** 6236-6243.

GOH, K., SETIAWAN, L., WEI, L., JIANG, W., WANG, R. & CHEN, Y. 2013. Fabrication of novel functionalized multi-walled carbon nanotube immobilized hollow fiber membranes for

enhanced performance in forward osmosis process. *Journal of Membrane Science,* 446**,** 244-254.
GRAY, G. T., MCCUTCHEON, J. R. & ELIMELECH, M. 2006. Internal concentration polarization in forward osmosis: role of membrane orientation. *Desalination,* 197**,** 1-8.
GREENLEE, L. F., LAWLER, D. F., FREEMAN, B. D., MARROT, B. & MOULIN, P. 2009. Reverse osmosis desalination: Water sources, technology, and today's challenges. *Water Research,* 43**,** 2317-2348.
GUO, C. X., ZHAO, D., ZHAO, Q., WANG, P. & LU, X. 2014. Na+-functionalized carbon quantum dots: A new draw solute in forward osmosis for seawater desalination. *Chemical Communications,* 50**,** 7318-7321.
HANCOCK, N. T. & CATH, T. Y. 2009. Solute Coupled Diffusion in Osmotically Driven Membrane Processes. *Environmental Science & Technology,* 43**,** 6769-6775
HAU, N. T., CHEN, S. S., NGUYEN, N. C., HUANG, K. Z., NGO, H. H. & GUO, W. 2014. Exploration of EDTA sodium salt as novel draw solution in forward osmosis process for dewatering of high nutrient sludge. *Journal of Membrane Science,* 455**,** 305-311.
HAWARI, A. H., KAMAL, N. & ALTAEE, A. 2016. Combined influence of temperature and flow rate of feeds on the performance of forward osmosis. *Desalination,* 398**,** 98-105.
HOANG, M., BOLTO, B., HASKARD, C., BARRON, O., GRAY, S. & LESLIE, G. 2009. Desalination in Australia. *CSIRO: Water for a Healthy Country National Research Flagship*.
HOLLOWAY, R. W., MALTOS, R., VANNESTE, J. & CATH, T. Y. 2015. Mixed draw solutions for improved forward osmosis performance. *Journal of Membrane Science,* 491**,** 121-131.
HTTPS://WWW.LENNTECH.COM/COMPOSITION-SEAWATER.HTM, R.-.-., 2018. [Accessed].
J.E.MILLER Review of water resources and desalination technologies, Sandia National Laboratories Report, SAND-2003-08002003.
JACOB, C. 2007. Seawater desalination: Boron removal by ion exchange technology. *Desalination,* 205**,** 47-52.
JAMALY, S., DARWISH, N. N., AHMED, I. & HASAN, S. W. 2014. A short review on reverse osmosis pretreatment technologies. *Desalination,* 354**,** 30-38.
JEONG, S., KIM, S.-J., HEE KIM, L., SEOP SHIN, M., VIGNESWARAN, S., VINH NGUYEN, T. & KIM, I. S. 2013. Foulant analysis of a reverse osmosis membrane used pretreated seawater. *Journal of Membrane Science,* 428**,** 434-444.
JEPPESEN, T., SHU, L., KEIR, G. & JEGATHEESAN, V. 2009. Metal recovery from reverse osmosis concentrate. *Journal of Cleaner Production,* 17**,** 703-707.
JI, X., CURCIO, E., AL OBAIDANI, S., DI PROFIO, G., FONTANANOVA, E. & DRIOLI, E. 2010. Membrane distillation-crystallization of seawater reverse osmosis brines. *Separation and Purification Technology,* 71**,** 76-82.
K.L, L., R.W., B. & H.K., L. 1981. Membrane for power generation by pressure-retarded osmosis. *Journal of Membrane Science,* 8**,** 141-171.
KARAGIANNIS, I. C. & SOLDATOS, P. G. 2008. Water desalination cost literature: review and assessment. *Desalination,* 223**,** 448-456.
KATZIR, L., VOLKMANN, Y., DALTROPHE, N., KORNGOLD, E., MESALEM, R., OREN, Y. & GILRON, J. 2010. WAIV - Wind aided intensified evaporation for brine volume reduction and generating mineral byproducts. *Desalination and Water Treatment,* 13**,** 63-73.
KIM, J., BLANDIN, G., PHUNTSHO, S., VERLIEFDE, A., LE-CLECH, P. & SHON, H. 2017. Practical considerations for operability of an 8" spiral wound forward osmosis module: Hydrodynamics, fouling behaviour and cleaning strategy. *Desalination,* 404**,** 249-258.
KIM, Y., ELIMELECH, M., SHON, H. K. & HONG, S. 2014. Combined organic and colloidal fouling in forward osmosis: Fouling reversibility and the role of applied pressure. *Journal of Membrane Science,* 460**,** 206-212.

KIM, Y., LEE, S., SHON, H. K. & HONG, S. 2015. Organic fouling mechanisms in forward osmosis membrane process under elevated feed and draw solution temperatures. *Desalination,* 355**,** 169-177.

KIM, Y. M., KIM, S. J., KIM, Y. S., LEE, S., KIM, I. S. & KIM, J. H. 2009. Overview of systems engineering approaches for a large-scale seawater desalination plant with a reverse osmosis network. *Desalination,* 238**,** 312-332.

KRAVATH, R. E. & DAVIS, J. A. 1975. Desalination of sea water by direct osmosis. *Desalination,* 16**,** 151-155.

KREMEN, S. S. & TANNER, M. 1998. Silt density indices (SDI), percent plugging factor (%PF): their relation to actual foulant deposition. *Desalination,* 119**,** 259-262.

LATORRE, M. 2005. Environmental impact of brine disposal on Posidonia seagrasses. *Desalination,* 182**,** 517-524.

LEE, K. L., BAKER, R. W. & LONSDALE, H. K. 1981. Membranes for power generation by pressure-retarded osmosis. *Journal of Membrane Science,* 8**,** 141-171.

LEE, S., BOO, C., ELIMELECH, M. & HONG, S. 2010a. Comparison of fouling behavior in forward osmosis (FO) and reverse osmosis (RO). *Journal of Membrane Science,* 365**,** 34-39.

LEE, S., BOO, C., ELIMELECH, M. & HONG, S. 2010b. Comparison of fouling behavior in forward osmosis (FO) and reverse osmosis (RO). *Journal of Membrane Science,* 365**,** 34-39.

LI, D., ZHANG, X., YAO, J., SIMON, G. P. & WANG, H. 2011a. Stimuli-responsive polymer hydrogels as a new class of draw agent for forward osmosis desalination. *Chemical Communications,* 47**,** 1710-1712.

LI, D., ZHANG, X., YAO, J., ZENG, Y., SIMON, G. P. & WANG, H. 2011b. Composite polymer hydrogels as draw agents in forward osmosis and solar dewatering. *Soft Matter,* 7**,** 10048-10056.

LI, Z.-Y., YANGALI-QUINTANILLA, V., VALLADARES-LINARES, R., LI, Q., ZHAN, T. & AMY, G. 2012a. Flux patterns and membrane fouling propensity during desalination of seawater by forward osmosis. *Water Research,* 46**,** 195-204.

LI, Z. Y., YANGALI-QUINTANILLA, V., VALLADARES-LINARES, R., LI, Q., ZHAN, T. & AMY, G. 2012b. Flux patterns and membrane fouling propensity during desalination of seawater by forward osmosis. *Water Research,* 46**,** 195-204.

LING, M. M. & CHUNG, T. S. 2011. Desalination process using super hydrophilic nanoparticles via forward osmosis integrated with ultrafiltration regeneration. *Desalination,* 278**,** 194-202.

LING, M. M. & CHUNG, T. S. 2012. Surface-dissociated nanoparticle draw solutions in forward osmosis and the regeneration in an integrated electric field and nanofiltration System. *Industrial and Engineering Chemistry Research,* 51**,** 15463-15471.

LING, M. M., WANG, K. Y. & CHUNG, T.-S. 2010a. Highly Water-Soluble Magnetic Nanoparticles as Novel Draw Solutes in Forward Osmosis for Water Reuse. *Industrial & Engineering Chemistry Research,* 49**,** 5869-5876.

LING, M. M., WANG, K. Y. & CHUNG, T. S. 2010b. Highly water-soluble magnetic nanoparticles as novel draw solutes in forward osmosis for water reuse. *Industrial and Engineering Chemistry Research,* 49**,** 5869-5876.

LIU, Y. & MI, B. 2012. Combined fouling of forward osmosis membranes: Synergistic foulant interaction and direct observation of fouling layer formation. *Journal of Membrane Science,* 407–408**,** 136-144.

LIU, Z., BAI, H., LEE, J. & SUN, D. D. 2011. A low-energy forward osmosis process to produce drinking water. *Energy and Environmental Science,* 4**,** 2582-2585.

LIYANAARACHCHI, S., JEGATHEESAN, V., MUTHUKUMARAN, S., GRAY, S. & SHU, L. 2016. Mass balance for a novel RO/FO hybrid system in seawater desalination. *Journal of Membrane Science,* 501**,** 199-208.

LIYANAARACHCHI, S., JEGATHEESAN, V., OBAGBEMI, I., MUTHUKUMARAN, S. & SHU, L. 2014a. Effect of feed temperature and membrane orientation on pre-treatment sludge volume reduction through forward osmosis. *Desalination and Water Treatment,* 54**,** 1-7.

LIYANAARACHCHI, S., JEGATHEESAN, V., OBAGBEMI, I., MUTHUKUMARAN, S. & SHU, L. 2015. Effect of feed temperature and membrane orientation on pre-treatment sludge volume reduction through forward osmosis. *Desalination and Water Treatment,* 54**,** 838-844.

LIYANAARACHCHI, S., JEGATHEESAN, V., SHU, L., MUTHUKUMARAN, S. & BASKARAN, K. 2014b. A preliminary study on the volume reduction of pre-treatment sludge in seawater desalination by forward osmosis. *Desalination and Water Treatment,* 52**,** 556-563.

LIYANAARACHCHI, S., SHU, L., MUTHUKUMARAN, S., JEGATHEESAN, V. & BASKARAN, K. 2013. Problems in seawater industrial desalination processes and potential sustainable solutions: a review. *Reviews in Environmental Science and Bio/Technology***,** 1-12.

LOEB, S., TITELMAN, L., KORNGOLD, E. & FREIMAN, J. 1997. Effect of porous support fabric on osmosis through a Loeb-Sourirajan type asymmetric membrane. *Journal of Membrane Science,* 129**,** 243-249.

LOTFI, F., PHUNTSHO, S., MAJEED, T., KIM, K., HAN, D. S., ABDEL-WAHAB, A. & SHON, H. K. 2015. Thin film composite hollow fibre forward osmosis membrane module for the desalination of brackish groundwater for fertigation. *Desalination,* 364**,** 108-118.

LUO, M. & WANG, Z. 2001. Complex fouling and cleaning-in-place of a reverse osmosis desalination system. *Desalination,* 141**,** 15-22.

MAJEED, T. 2014. *Fertilizer drawn hollow fiber forward osmosis for desalination.* PhD, University of Technology, Sydney.

MARTINETTI, C. R., CHILDRESS, A. E. & CATH, T. Y. 2009. High recovery of concentrated RO brines using forward osmosis and membrane distillation. *Journal of Membrane Science,* 331**,** 31-39.

MATHEW, R., PADUANO, L., ALBRIGHT, J. G., MILLER, D. G. & RARD, J. A. 1989. Isothermal Diffusion Coefficients for NaCl-MgCl,-H2O at 25 oC. 3. Low MgCl2 Concentrations with a Wide Range of NaCl Concentrations

J . Phys. Chem., 93**,** 4370-4374.

MATIN, A., KHAN, Z., ZAIDI, S. M. J. & BOYCE, M. C. 2011. Biofouling in reverse osmosis membranes for seawater desalination: Phenomena and prevention. *Desalination,* 281**,** 1-16.

MCCORMICK, P., PELLEGRINO, J., MANTOVANI, F. & SARTI, G. 2008. Water, salt, and ethanol diffusion through membranes for water recovery by forward (direct) osmosis processes. *Journal of Membrane Science,* 325**,** 467-478.

MCCUTCHEON, J. R. & ELIMELECH, M. 2006. Influence of concentrative and dilutive internal concentration polarization on flux behavior in forward osmosis. *Journal of Membrane Science,* 284**,** 237-247.

MCCUTCHEON, J. R., MCGINNIS, R. L. & ELIMELECH, M. 2005. A novel ammonia—carbon dioxide forward (direct) osmosis desalination process. *Desalination,* 174**,** 1-11.

MCCUTCHEON, J. R., MCGINNIS, R. L. & ELIMELECH, M. 2006a. Desalination by ammonia-carbon dioxide forward osmosis: Influence of draw and feed solution concentrations on process performance. *Journal of Membrane Science,* 278**,** 114-123.

MCCUTCHEON, J. R., MCGINNIS, R. L. & ELIMELECH, M. 2006b. Desalination by ammonia–carbon dioxide forward osmosis: Influence of draw and feed solution concentrations on process performance. *Journal of Membrane Science,* 278**,** 114-123.

MCGINNIS, R. L. & ELIMELECH, M. 2007. Energy requirements of ammonia–carbon dioxide forward osmosis desalination. *Desalination,* 207**,** 370-382.

MI, B. & ELIMELECH, M. 2008. Chemical and physical aspects of organic fouling of forward osmosis membranes. *Journal of Membrane Science,* 320**,** 292-302.

MILLER, D. G., LEE, C. M. & RARD, J. A. 2007. Ternary Isothermal Diffusion Coefficients of NaCl-MgCl2-H2O at 25 °C. 7. Seawater Composition. *Journal of Solution Chemistry,* 36**,** 1559-1567.

MISDAN, N., LAU, W. J. & ISMAIL, A. F. 2012. Seawater Reverse Osmosis (SWRO) desalination by thin-film composite membrane—Current development, challenges and future prospects. *Desalination,* 287**,** 228-237.

MOHAMED, A. M. O., MARAQA, M. & AL HANDHALY, J. 2005. Impact of land disposal of reject brine from desalination plants on soil and groundwater. *Desalination,* 182**,** 411-433.

MORTON, A. J., CALLISTER, I. K. & WADE, N. M. 1997. Environmental impacts of seawater distillation and reverse osmosis processes. *Desalination,* 108**,** 1-10.

NA, Y., YANG, S. & LEE, S. 2014. Evaluation of citrate-coated magnetic nanoparticles as draw solute for forward osmosis. *Desalination,* 347**,** 34-42.

NCED 2010. Australian desalination research road map, National Centre of Excellence in Desalination.

NGUYEN, T., RODDICK, F. & FAN, L. 2012. Biofouling of Water Treatment Membranes: A Review of the Underlying Causes, Monitoring Techniques and Control Measures. *Membranes,* 2**,** 804-840.

NICOLL, P. Forward Osmosis and Some Applications. Membranes & Desalination Specialist Network Update, Australian Water Association Technical Director, Modern Water plc.

NOOIJEN, W. F. J. M. & WOUTERS, J. W. 1992. Optimizing and planning of seawater desalination. *Desalination,* 89**,** 1-19.

OU, R., WANG, Y., WANG, H. & XU, T. 2013. Thermo-sensitive polyelectrolytes as draw solutions in forward osmosis process. *Desalination,* 318**,** 48-55.

PALMER, N. 2012. Changing perception of the value of urban water in Australia following investment in seawater desalination. *Desalination and Water Treatment,* 43**,** 298-307.

PERSONNEL COMMUNICATION WITH WONTHAGGI SEAWATER DESALINATION PLANT, A. 2014.

PETROTOS, K. B., QUANTICK, P. C. & PETROPAKIS, H. 1999. Direct osmotic concentration of tomato juice in tubular membrane – module configuration. II. The effect of using clarified tomato juice on the process performance. *Journal of Membrane Science,* 160**,** 171-177.

PHUNTSHO, S., SHON, H., HONG, S., LEE, S., VIGNESWARAN, S. & KANDASAMY, J. 2012. Fertiliser drawn forward osmosis desalination: the concept, performance and limitations for fertigation. *Reviews in Environmental Science and Bio/Technology,* 11**,** 147-168.

PHUNTSHO, S., SHON, H. K., HONG, S., LEE, S. & VIGNESWARAN, S. 2011. A novel low energy fertilizer driven forward osmosis desalination for direct fertigation: Evaluating the performance of fertilizer draw solutions. *Journal of Membrane Science,* 375**,** 172-181.

PUGUAN, J. M. C., KIM, H. S., LEE, K. J. & KIM, H. 2014. Low internal concentration polarization in forward osmosis membranes with hydrophilic crosslinked PVA nanofibers as porous support layer. *Desalination,* 336**,** 24-31.

QASIM, M., DARWISH, N. A., SARP, S. & HILAL, N. 2015. Water desalination by forward (direct) osmosis phenomenon: A comprehensive review. *Desalination,* 374**,** 47-69.

QIU, C., SETIAWAN, L., WANG, R., TANG, C. Y. & FANE, A. G. 2012. High performance flat sheet forward osmosis membrane with an NF-like selective layer on a woven fabric embedded substrate. *Desalination,* 287**,** 266-270.

RAZMJOU, A., BARATI, M. R., SIMON, G. P., SUZUKI, K. & WANG, H. 2013a. Fast deswelling of nanocomposite polymer hydrogels via magnetic field-induced heating for emerging FO desalination. *Environmental Science and Technology,* 47**,** 6297-6305.

RAZMJOU, A., SIMON, G. P. & WANG, H. 2013b. Effect of particle size on the performance of forward osmosis desalination by stimuli-responsive polymer hydrogels as a draw agent. *Chemical Engineering Journal,* 215-216**,** 913-920.

SADHWANI, J. J., VEZA, J. M. & SANTANA, C. 2005. Case studies on environmental impact of seawater desalination. *Desalination,* 185**,** 1-8.

SARP, S., LEE, S., REN, X., LEE, E., CHON, K., CHOI, S. H., KIM, S., KIM, I. S. & CHO, J. 2008. Boron removal from seawater using NF and RO membranes, and effects of boron on HEK 293 human embryonic kidney cell with respect to toxicities. *Desalination,* 223**,** 23-30.

SEMIAT, R. 2008. Energy Issues in Desalination Processes. *Environmental Science & Technology,* 42**,** 8193-8201.

SETHI, S., WALKER, S., DREWES, J., & XU, P. 2006. Existing & emerging concentrate minimization & disposal practices for membrane systems. *Florida Water Resources Journal***,** 38-48.

SETIAWAN, L., WANG, R., LI, K. & FANE, A. G. 2011. Fabrication of novel poly(amide-imide) forward osmosis hollow fiber membranes with a positively charged nanofiltration-like selective layer. *Journal of Membrane Science,* 369**,** 196-205.

SETIAWAN, L., WANG, R., LI, K. & FANE, A. G. 2012. Fabrication and characterization of forward osmosis hollow fiber membranes with antifouling NF-like selective layer. *Journal of Membrane Science,* 394-395**,** 80-88.

SHIBUYA, M., YASUKAWA, M., MISHIMA, S., TANAKA, Y., TAKAHASHI, T. & MATSUYAMA, H. 2017. A thin-film composite-hollow fiber forward osmosis membrane with a polyketone hollow fiber membrane as a support. *Desalination,* 402**,** 33-41.

SIM, V., SHE, Q., CHONG, T., TANG, C., FANE, A. & KRANTZ, W. 2013. Strategic Co-Location in a Hybrid Process Involving Desalination and Pressure Retarded Osmosis (PRO). *Membranes,* 3**,** 98.

SIVERTSEN, E., HOLT, T., THELIN, W. & BREKKE, G. 2012. Modelling mass transport in hollow fibre membranes used for pressure retarded osmosis. *Journal of Membrane Science,* 417**–**418**,** 69-79.

STONE, M. L., RAE, C., STEWART, F. F. & WILSON, A. D. 2013. Switchable polarity solvents as draw solutes for forward osmosis. *Desalination,* 312**,** 124-129.

SU, J., CHUNG, T.-S., HELMER, B. J. & DE WIT, J. S. 2012. Enhanced double-skinned FO membranes with inner dense layer for wastewater treatment and macromolecule recycle using Sucrose as draw solute. *Journal of Membrane Science,* 396**,** 92-100.

SU, J., YANG, Q., TEO, J. F. & CHUNG, T.-S. 2010. Cellulose acetate nanofiltration hollow fiber membranes for forward osmosis processes. *Journal of Membrane Science,* 355**,** 36-44.

TAN, C. H. & NG, H. Y. 2008. Modified models to predict flux behavior in forward osmosis in consideration of external and internal concentration polarizations. *Journal of Membrane Science,* 324**,** 209-219.

TAN, C. H. & NG, H. Y. 2010. A novel hybrid forward osmosis - nanofiltration (FO-NF) process for seawater desalination: Draw solution selection and system configuration. *Desalination and Water Treatment,* 13**,** 356-361.

TANG, C. Y., SHE, Q., LAY, W. C. L., WANG, R. & FANE, A. G. 2010. Coupled effects of internal concentration polarization and fouling on flux behavior of forward osmosis membranes during humic acid filtration. *Journal of Membrane Science,* 354**,** 123-133.

TOUATI, K. & TADEO, F. 2016. Study of the Reverse Salt Diffusion in pressure retarded osmosis: Influence on concentration polarization and effect of the operating conditions. *Desalination,* 389**,** 171-186.

TULARAM, G. A. & ILAHEE, M. 2007. Environmental concerns of desalinating seawater using reverse osmosis. *Journal of Environmental Monitoring,* 9**,** 805-813.

VALLADARES LINARES, R., LI, Z., YANGALI-QUINTANILLA, V., GHAFFOUR, N., AMY, G., LEIKNES, T. & VROUWENVELDER, J. S. 2016. Life cycle cost of a hybrid forward osmosis – low pressure reverse osmosis system for seawater desalination and wastewater recovery. *Water Research,* 88**,** 225-234.

VEDAVYASAN, C. V. 2007. Pretreatment trends — an overview. *Desalination,* 203**,** 296-299.

VOLLPRECHT, R. 2013. Personnel communication with DEGREMONT PTY LTD,Perth Seawater Desalination Plant, Lot 3003 Barter Road, 6165 NAVAL BASE - WA - AUSTRALIA

WANG, K. Y., TEOH, M. M., NUGROHO, A. & CHUNG, T. S. 2011. Integrated forward osmosis-membrane distillation (FO-MD) hybrid system for the concentration of protein solutions. *Chemical Engineering Science,* 66**,** 2421-2430.

WANG, R., SHI, L., TANG, C. Y., CHOU, S., QIU, C. & FANE, A. G. 2010. Characterization of novel forward osmosis hollow fiber membranes. *Journal of Membrane Science,* 355**,** 158-167.

WATER-TECHNOLOGY.NET. 2013. *Perth Seawater Desalination Plant, Australia* [Online]. Available: http://www.water-technology.net/projects/perth/ [Accessed 31-10-2013 2013].

WATERREUSEASSOCIATION 2011. Seawater Desalination Power Consumption, White paper November 2011.

WILF, M. & KLINKO, K. 1998. Effective new pretreatment for seawater reverse osmosis systems. *Desalination,* 117**,** 323-331.

WITTHOLZ, M. K., O'NEILL, B. K., COLBY, C. B. & LEWIS, D. 2008. Estimating the cost of desalination plants using a cost database. *Desalination,* 229**,** 10-20.

XIE, M., NGHIEM, L. D., PRICE, W. E. & ELIMELECH, M. 2012. Comparison of the removal of hydrophobic trace organic contaminants by forward osmosis and reverse osmosis. *Water Research,* 46**,** 2683-2692.

XIE, M., NGHIEM, L. D., PRICE, W. E. & ELIMELECH, M. 2013. A forward osmosis-membrane distillation hybrid process for direct sewer mining: System performance and limitations. *Environmental Science and Technology,* 47**,** 13486-13493.

XIONG, S., ZUO, J., MA, Y. G., LIU, L., WU, H. & WANG, Y. 2016. Novel thin film composite forward osmosis membrane of enhanced water flux and anti-fouling property with N-[3-(trimethoxysilyl) propyl] ethylenediamine incorporated. *Journal of Membrane Science,* 520**,** 400-414.

YANGALI-QUINTANILLA, V., LI, Z., VALLADARES, R., LI, Q. & AMY, G. 2011. Indirect desalination of Red Sea water with forward osmosis and low pressure reverse osmosis for water reuse. *Desalination,* 280**,** 160-166.

YEN, S. K., MEHNAS HAJA N, F., SU, M., WANG, K. Y. & CHUNG, T.-S. 2010a. Study of draw solutes using 2-methylimidazole-based compounds in forward osmosis. *Journal of Membrane Science,* 364**,** 242-252.

YEN, S. K., MEHNAS HAJA N, F., SU, M., WANG, K. Y. & CHUNG, T. S. 2010b. Study of draw solutes using 2-methylimidazole-based compounds in forward osmosis. *Journal of Membrane Science,* 364**,** 242-252.

YONG, J. S., PHILLIP, W. A. & ELIMELECH, M. 2012. Coupled reverse draw solute permeation and water flux in forward osmosis with neutral draw solutes. *Journal of Membrane Science,* 392–393**,** 9-17.

YOON, H., BAEK, Y., YU, J. & YOON, J. 2013. Biofouling occurrence process and its control in the forward osmosis. *Desalination,* 325**,** 30-36.

ZHANG, H., MA, Y., JIANG, T., ZHANG, G. & YANG, F. 2012. Influence of activated sludge properties on flux behavior in osmosis membrane bioreactor (OMBR). *Journal of Membrane Science,* 390–391**,** 270-276.

ZHANG, S., WANG, P., FU, X. & CHUNG, T. S. 2014. Sustainable water recovery from oily wastewater via forward osmosis-membrane distillation (FO-MD). *Water Research,* 52**,** 112-121.

ZHANG, Y., PINOY, L., MEESSCHAERT, B. & VAN DER BRUGGEN, B. 2013. A natural driven membrane process for brackish and wastewater treatment: Photovoltaic powered ED and FO hybrid system. *Environmental Science and Technology,* 47**,** 10548-10555.

ZHAO, D., WANG, P., ZHAO, Q., CHEN, N. & LU, X. 2014. Thermoresponsive copolymer-based draw solution for seawater desalination in a combined process of forward osmosis and membrane distillation. *Desalination,* 348**,** 26-32.

ZHAO, P., GAO, B., YUE, Q., LIU, S. & SHON, H. K. 2016. Effect of high salinity on the performance of forward osmosis: Water flux, membrane scaling and removal efficiency. *Desalination,* 378**,** 67-73.

ZHAO, S. & ZOU, L. 2011. Relating solution physicochemical properties to internal concentration polarization in forward osmosis. *Journal of Membrane Science,* 379**,** 459-467.

ZHAO, S., ZOU, L. & MULCAHY, D. 2011. Effects of membrane orientation on process performance in forward osmosis applications. *Journal of Membrane Science,* 382**,** 308-315.

ZHAO, S., ZOU, L. & MULCAHY, D. 2012. Brackish water desalination by a hybrid forward osmosis-nanofiltration system using divalent draw solute. *Desalination,* 284**,** 175-181.

Appendices

Chapter 3 related appendices

Table A1: Jar test conducted to find the optimum coagulant dose.

Dosage (mg/L)	Volume of $FeCl_3$ added/ mL	Coagulant added pH	Settled water turbidity (NTU)			Settled water pH	EC (mS/cm)	TDS (ppm)
			sample 1 (after 30 min)	sample 2 (after 1 hr)	sample 3 (after 1.5 hr)			
5	1	7.85	1.07	0.40	0.42	7.91	50.6	33902
10	2	7.97	0.76	0.55	0.54	8.00	50.9	34103
15	3	7.73	1.12	0.67	0.45	7.78	51	34170
20	4	7.55	1.00	0.44	0.41	7.61	50.9	34103
25	5	7.33	2.54	0.53	0.32	7.43	50.9	34103
30	6	7.25	1.72	0.38	0.43	7.33	50.9	34103

DMF filtration test

minimum container volume=	100	L			
Q=	250	mL/min			
total run time=	400	min			

Back wash rate was adjusted manually so that sand will not pass through the outlet.

after test, washed container and pump with tap water to prevent from corrosion.

DMF data		mm			
depth of sand bed	300				
size of sand grains	1				
porosity of sand bed	0.4				
depth of anthracite bed	400				
size of anthraciste particles	2				
porosity of anthracite bed	0.45				
influent turbidity	29.1	NTU	35.2	30.2	21.9
flow rate	250	mL/min			

Filtrate properties

Collected time (hours)		Turbidity (NTU)	pH	T (oC)	Conductivity (mS/cm)
0	(before coagulant addition)	0	7.28	19.6	38.2
0	(after coagulant additon)	1.53	7.44	20.2	40.9
1		0.31	7.72	19.9	44.1
1.5		0.32			
2		0.45	7.77	20.1	44.3
2.5		0.49			
3		0.34	7.79	20.1	43.8
3.5		0.69			
Average values					
Intake seawater		29.1	8.42	20.0	44.5
Filtrate		0.45	7.68	21.2	44.7
Sludge			7.51	21.1	13.8
				20.2	

After DMF treatment;

Total collected filtrate volume~	30	L
Total collected Sludge volume~	7	L

Chapter 4 related appendices

Effective diffusion coefficient calculations

NOTE: For the specimen calculation, the pure $K_2 SO_4$ 30mg/L data from Table 14;

Water flux, J_w, can be calculated using equation (1) (theoretical) or can be obtained experimentally.

In this study J_w was obtained experimentally ($J_{w,e}$) and reported in Table 1, in Section 3.1.

Therefore J_w = 2.08 LMH (ALFS mode)

And, J_w = 3.15 LMH (ALDS mode)

$$J_w = A\sigma[\pi_{D,b}\exp(-J_w K_D) - \pi_{F,b}\exp(-\frac{J_w}{k_f})] \quad (4)$$

Since the feed solution used in this study is distilled water, above equation can be rearranged as;

$$K_D = \frac{\ln(\frac{J_w}{A\pi_{D,b}})}{-J_w} \quad (10)$$

Substituting known values from Table 14;

$$K_D = \frac{\ln(\frac{2.08}{0.36*8.52709})*3600*10^3}{-2.08}$$

$$\underline{K_D = 1.87 * 10^6\ (s/m)}$$

Similarly, equation (5) can be rearranged as;

$$k_d = \frac{-J_w}{\ln(\frac{J_w}{A\pi_{D,b}})} \quad (11)$$

Therefore, substituting known values,

$$k_d = \frac{-3.15*}{\ln(\frac{3.15}{0.36*8.52709})} * 10^{-3}/3600$$

$$\underline{k_d = 1.31 * 10^{-6}\ (m/s)}$$

Once k_d and K_D calculated,

$$D_{eff} = \frac{k_d\, t\tau}{\varepsilon} \qquad (8)$$

Also, $D_{eff} = \frac{k_d\, d_h}{sh}$, substituting at equation 8;

$$D_{eff} = \frac{k_d\, d_h}{1.85\ (Re*Sc*\frac{dh}{L})^{0.33}}$$

$$\underline{\therefore D_{eff} = 4.30 * 10^{-7}}$$

Similarly, effective diffusion coefficient for each salt was calculated and given in the chapter.

Chapter 5 related appendices

The results in Table 16 and Table 17 are obtained using the step by step calculations shown in Figure A1. These calculations will be included in the appendix section. Yellow highlighted cells are the inputs to this excel sheet.

Further A value was obtained experimentally and given below in Figure A2. To obtain A, water flux at different pressure values were obtained through a RO type experiment. Water flux vs pressure difference was plotted, and the gradient of the curve gives the value of A.

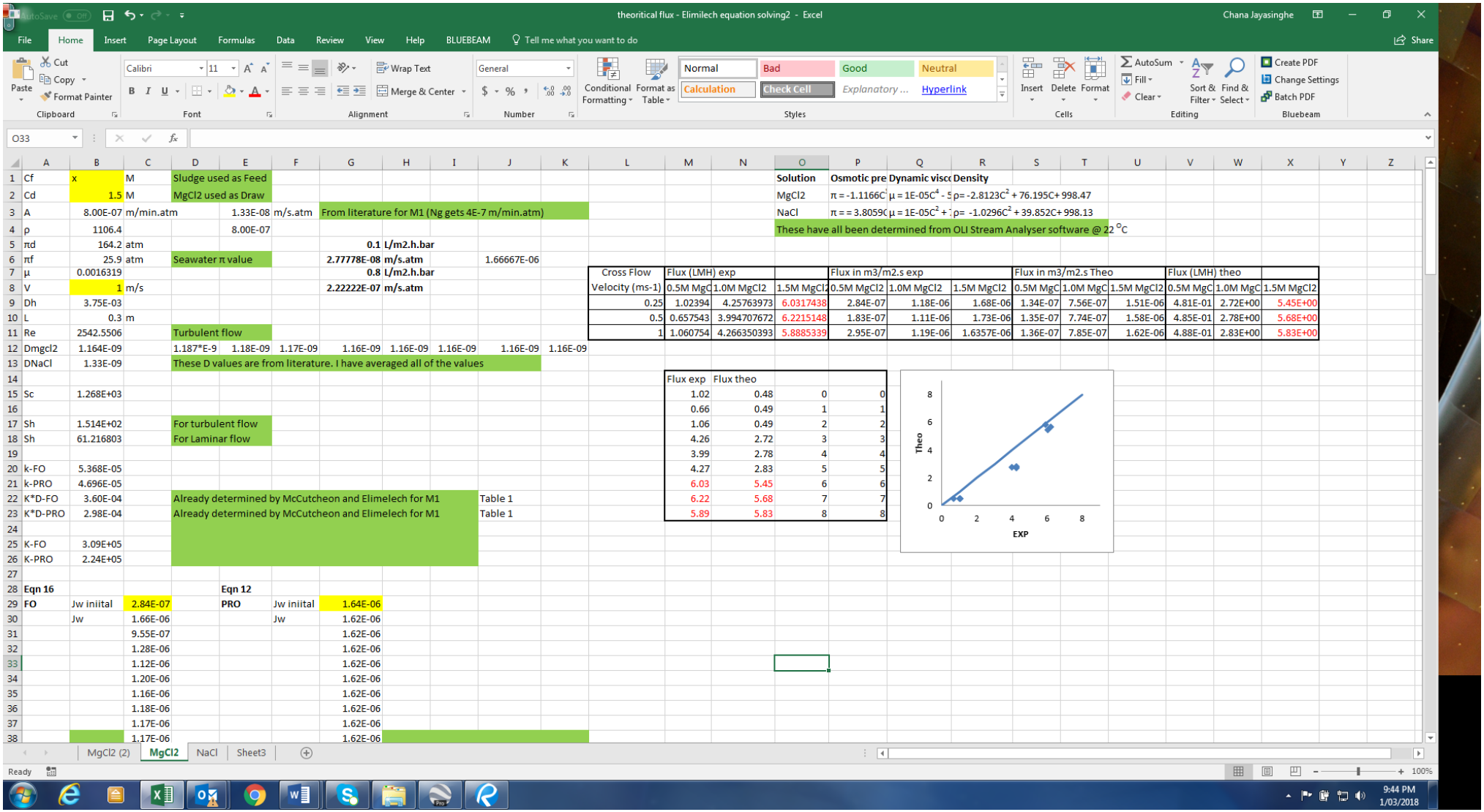

Figure A1: Calculations of theoretical water flux

water fulx (g/min)					Flux					Area of the membrane		
5oo kPa	600 kPa	700 kPa	800 kPa	Pressure (kPa)	500	600	700	800		0.00229022		
				Pressure (bar)	5	6	7	8				
0.13000	0.21000	0.18000	0.23000	Flux	3.40578479	5.501652	4.715702	6.025619		From graph; y=2*10-7x		
0.17000	0.18000	0.23000	0.32000		4.453718572	4.715702	6.025619	8.38347		therefore,		
0.15000	0.20000	0.18000	0.25000		3.929751681	5.239669	4.715702	6.549586		**A**	**2.00E-07**	m/s. Bar
0.19000	0.18000	0.25000	0.29000		4.977685463	4.715702	6.549586	7.59752			**1.20E-05**	m/min.bar
0.15000	0.19000	0.21000	0.29000		3.929751681	4.977685	5.501652	7.59752				
0.16000	0.21000	0.22000	0.24000		4.191735127	5.501652	5.763636	6.287603				
0.17000	0.21000	0.25000	0.24000		4.453718572	5.501652	6.549586	6.287603				
0.15000		0.23000	0.19000		3.929751681		6.025619	4.977685		McCutcheor	5.06E-12	m /Pa s
0.19000		0.23000	0.28000		4.977685463		6.025619	7.335536			5.06E-07	m/s. Bar
0.15000		0.22000	0.20000		3.929751681		5.763636	5.239669			3.04E-05	m/min.bar
				Average flux (LMH)	**4.217933471**	**5.164816**	**5.763636**	**6.628181**				
				Average flux (m3/m2.s)	**1.17165E-06**	**1.43E-06**	**1.6E-06**	**1.84E-06**				
										Wollongong		
									pouch	A1	0.745	L/m2.h/bar
									catridge	A2	1.13	L/m2.h/bar
											2.06944E-07	m/s. Bar
											3.13889E-07	m/s. Bar

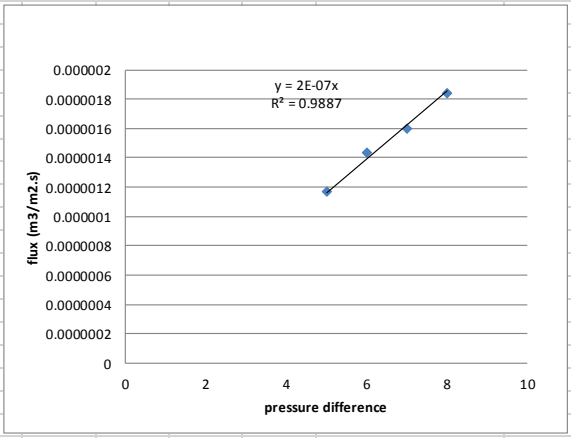

Figure A2: Calculations of permeability coefficient, A.

Chapter 6 related appendices

$$Re = \frac{\rho v d}{\mu}$$

$$v = \frac{Re \times \mu}{\rho d} = \frac{Q}{A}$$

At 1000 and 2000 Re values, the required flowrate was calculated using the μ and ρ values given in Table 18. For example, for Na_2SO_4 solution;

$$\frac{1000 \times 0.00112}{1557 \times 0.0009} = \frac{Q}{\pi \times 0.45^2 \times 10^{-6}}$$

Where, Radius of the hollow fiber membrane is 0.45 mm. therefore, the required flow rate of Na_2SO_4 solution to obtain a 1000Re is,

$$\underline{Q = 0.3\ l/min}$$

Chapter 7 related appendices

EDX images of the 8-weeks trail.

Major 12 elements found on the membrane feed side surface is given below.

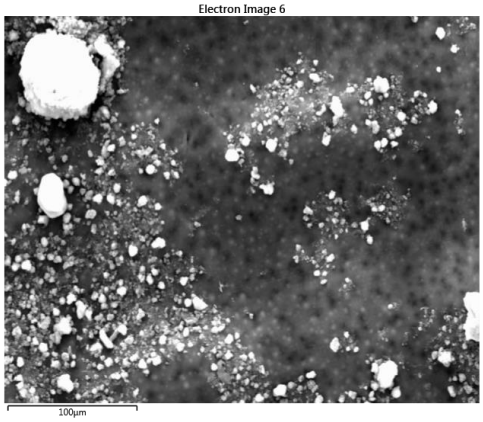

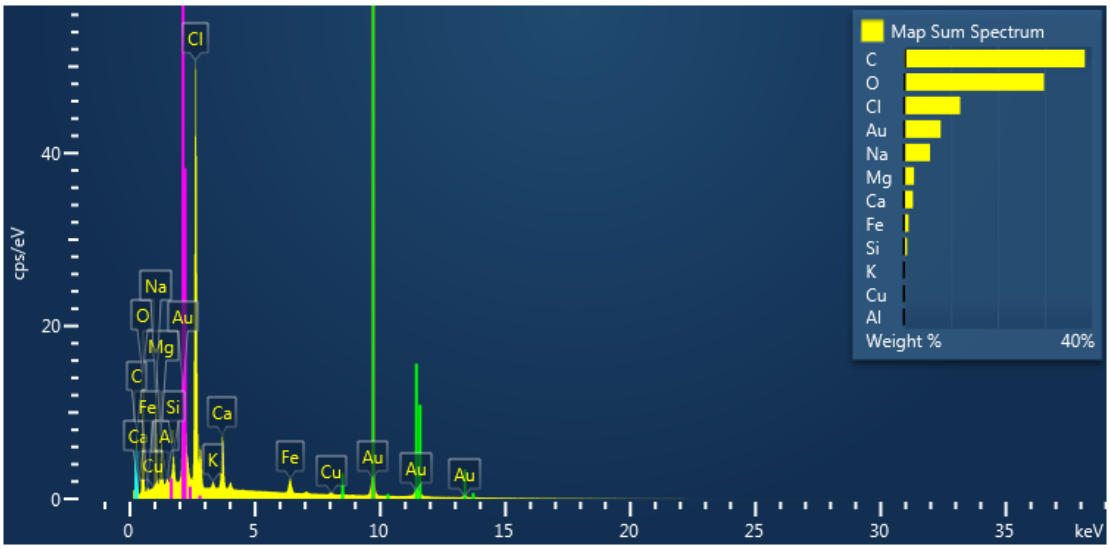

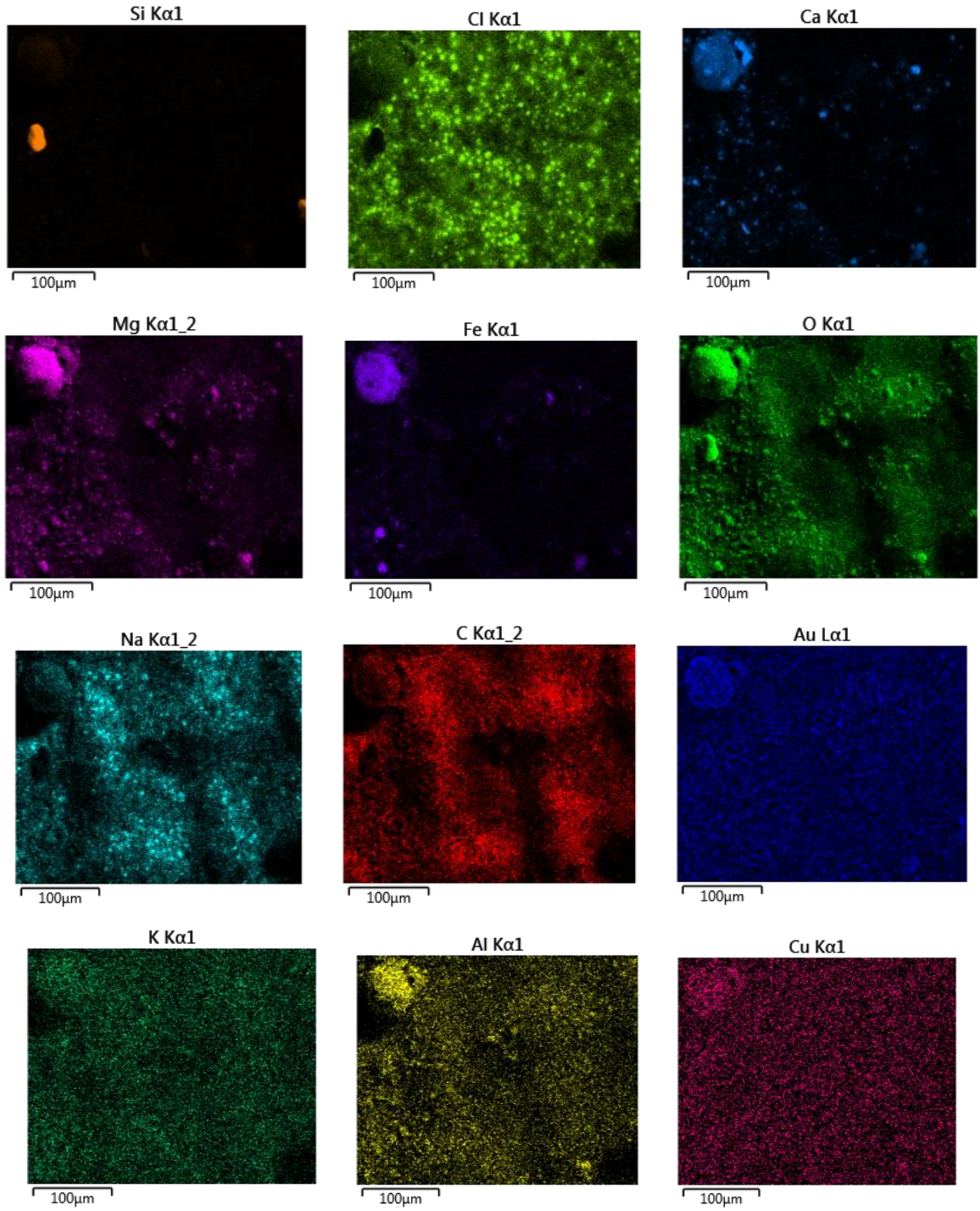

Figure: (a) SEM image (b) EDX spectrum of feed side membrane (c) to (n) main 12 elements found on the membrane surface through EDX analysis.

Draw side membrane surface image and the elements found on it are given below.

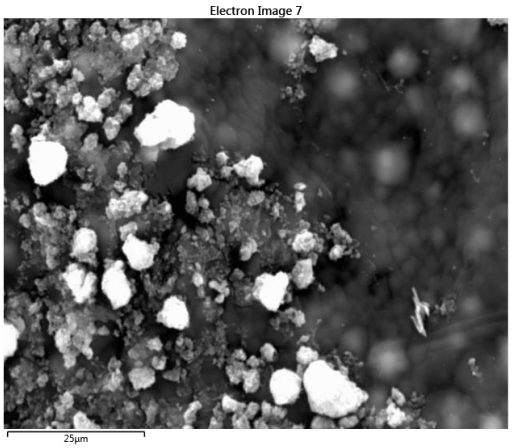

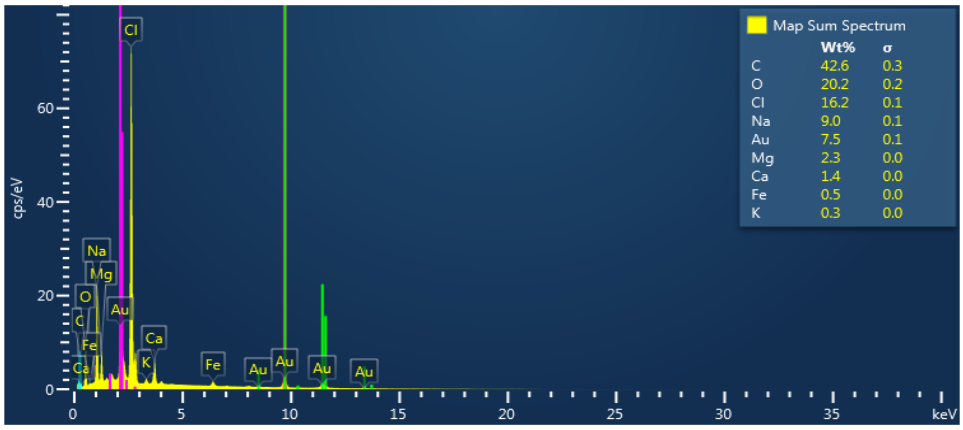

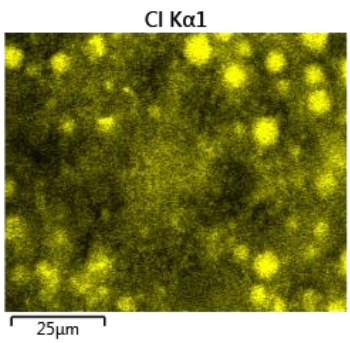

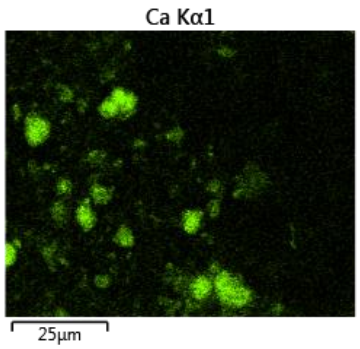

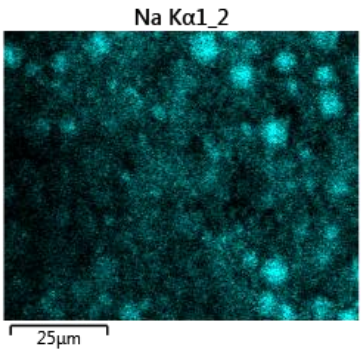

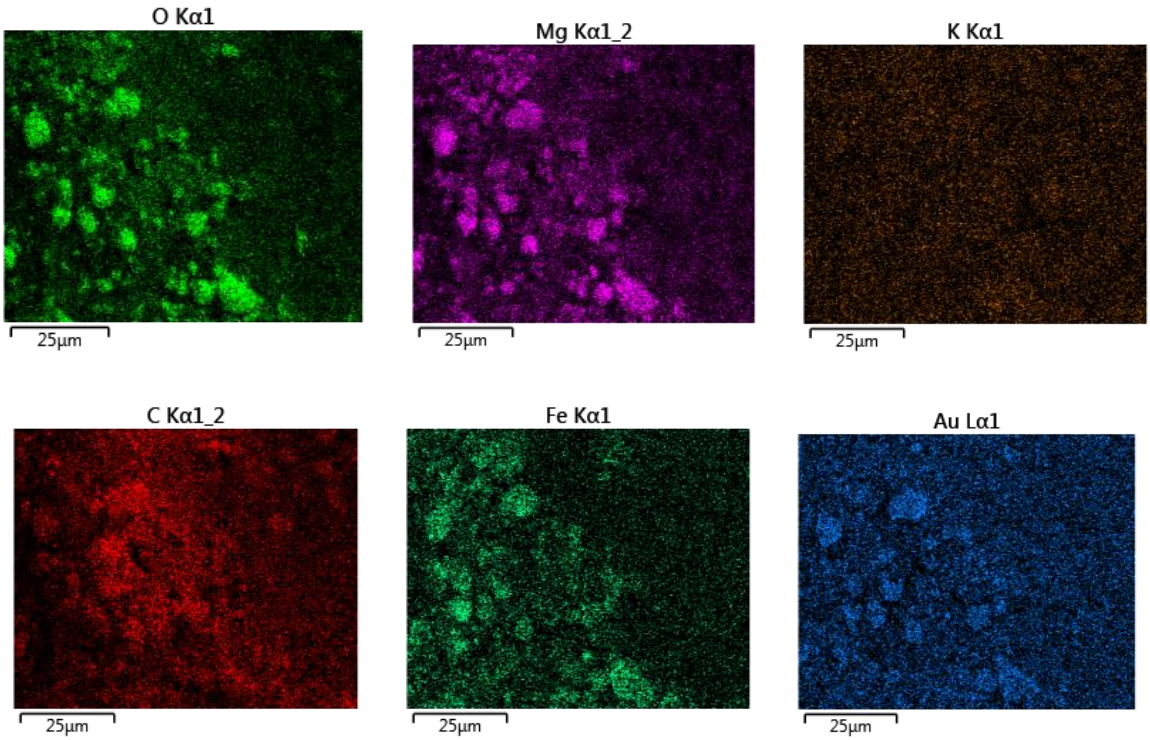

Figure: (a) SEM image (b) EDX spectrum of draw side membrane (c) to (k) main 12 elements found on the membrane surface through EDX analysis.

TOC results of the 5-weeks trial

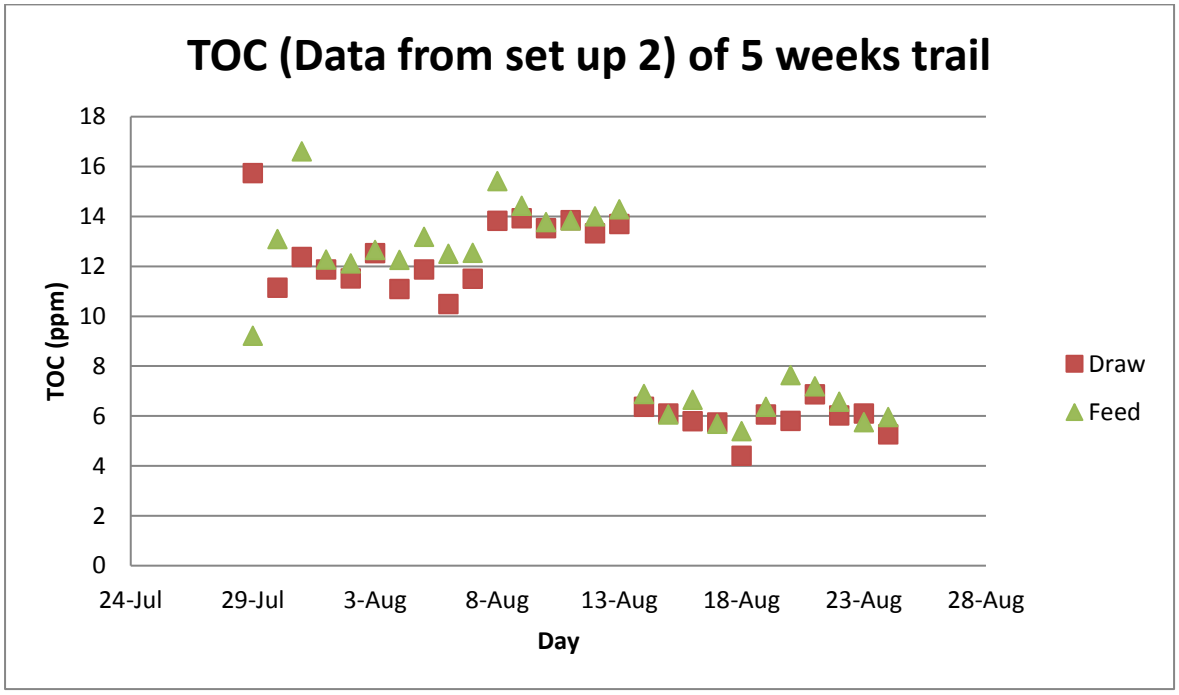

Figure: TOC of feed and draw solutions after filtration during 5 weeks filtration.

Table: TOC of feed and draw solutions after filtration during 5 weeks filtration in ppm.

Daily TOC results		Feed			Draw		
Sample date		Set up 1	Set up 2	Set up 3	Set up 1	Set up 2	Set up 3
	29-Jul	10.3	9.23	8.96	16.9	15.7	7.5
	30-Jul	13.5	13.1	13.3	12.3	11.2	11.6
	31-Jul	14.1	16.6	12.9	12.2	12.4	11.5
	1-Aug	12.8	12.3	12.6	12.4	11.9	13
	2-Aug	13.5	12.1	12.7	12.3	11.5	11.8
	3-Aug	12.8	12.7	12.1	13.2	12.5	11.1
	4-Aug	14.2	12.3	12.7	11.7	11.1	11.3
	5-Aug	13.5	13.2	12.6	12.4	11.9	11.7
	6-Aug	13.4	12.5	12.5	11.1	10.5	10.8
	7-Aug	13.5	12.5	12.5	12.1	11.5	11.3
	8-Aug	17.9	15.4	15.3	14.4	13.8	13.9
	9-Aug	16.1	14.4	15	14.5	13.9	14.6
	10-Aug	15.5	13.8	14.1	14.2	13.5	14
	11-Aug	15.5	13.8	13.6	13.9	13.9	13.7
	12-Aug	15.7	14	14.1	13.8	13.3	13.5
	13-Aug	16.1	14.3	14.4	14.1	13.7	13.9
	14-Aug	7.32	6.89	6.98	5.39	6.38	6.78
	15-Aug	7.01	6.07	6	5.44	6.1	5.79
	16-Aug	7.18	6.65	6.75	5.8	5.79	6.17
	17-Aug	7.37	5.69	6.23	5.08	5.75	5.48
	18-Aug	6.37	5.4	5.39	4.96	4.41	5.13
	19-Aug	6.79	6.38	6.77	5.69	6.07	5.96
	20-Aug	8.53	7.64	7.49	6.27	5.81	6.64
	21-Aug	7.04	7.19	7.36	6.26	6.88	6.94

22-Aug	6.68	6.58	6.72	5.57	6.03	6.43
23-Aug	7.27	5.76	6.74	5.35	6.1	5.2
24-Aug	6.16	5.97	6.26	5.58	5.27	5.25

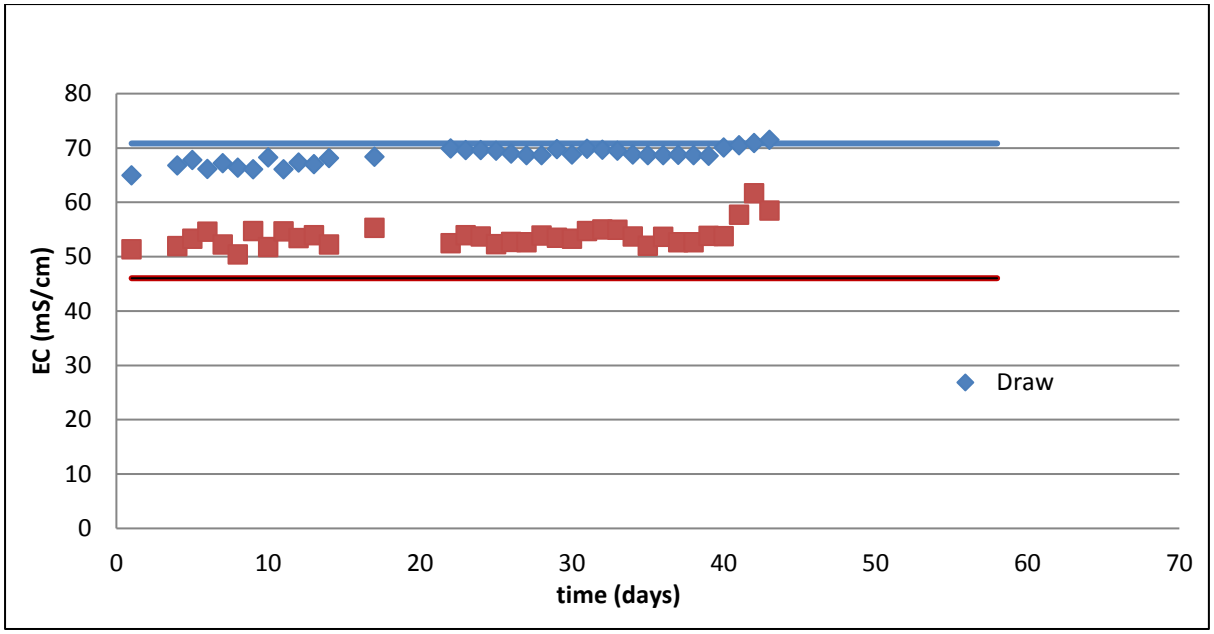

Table: EC of feed and draw solutions after filtration during 8 weeks filtration.

Chapter 8 related appendices

EPC cost calculations

Engineering , Procurement and construction cost (EPC) cost								
	Approach 1 (water reseach ref)				texas reference		Approach 2 (texas reference)	
	SWRO		RO/FO hybrid system		FO stand alone system		SWRO	
	LSP	SSP	LSP	SSP	LSP	SSP	LSP	SSP
Total cost								
Procduction capacity of the plant (m3/day)	153,000	6,750	155,040	7,440	130	72	153,000	6,750
Equipment and materials	46,167,750	2,036,813	46,783,320	2,245,020				
membranes	10,156,905	448,099	10,292,330	493,904				
pressure vessels	2,770,065	122,209	2,806,999	134,701				
pumps	13,480,983	594,749	13,660,729	655,546				
energy recovery	3,693,420	162,945	3,742,666	179,602				
piping and high grade alloy materials	23,083,875	1,018,406	23,391,660	1,122,510				
others	85,318,002	3,764,030	86,455,575	4,148,797				
Equipment and materials + memrbanes	30.5%	30.5%	30.5%	30.5%	2,136,566	1,837,523		4,845,192
Construction	69.5%	69.5%	69.5%	69.5%	3,839,133	3,466,185		18,275,724
Process Eqiupment cost					1,436,566	1,242,523		
Mechanical (piping)					300,000	200,000		
Instrumentation and control					300,000	300,000		
Electrical csosts					100,000	95,000		
Total cost (USD) to produce water	184,671,000	8,147,250	187,133,280	8,980,080	5,975,699	5,303,708		23,120,916
Total O&M cost					220,251	174,284		3,131,967
Total	**0.739**	0.739	**0.739**		**0.024**	**0.481**		**2.098**
CAPEX amortization	**0.288**	0.288	**0.288**		**0.009**	**0.188**		**0.818**
OPEX	**0.451**	0.451	0.451		**0.01**	**0.29**		**1.28**
Energy	0.281	0.281	0.281					
maintannce	0.089	0.089	0.089					
chemicals	0.037	0.037	0.037					
labour	0.022	0.022	0.022					
membrane replacement	0.022	0.022	0.022					

Mass balance calculations

Specimen calculations for a LSP

Assumptions;		
100% RO rejection		
Intake flow rate	340,000	m^3/day
Backwash water flow rate	275.000	m^3/day
RO 1 recovery	50	%
RO 2 recovery	90	%
Overall recovery (Without FO)	45	%
Flux through FO	6	LMH
Nominal membrane surface area of 8 inch spiral wound modules	18.13	m^2
Initial Solids content of sludge	4	%

salt transport through FO is negligible.

Calculations

For FO system

Total amount of sludge per day	275	m3/day
Assume backwash frequency is 4 times a day		
backwash cycles per day	4	cycles/day
Therefore every 6 hours the amount of sludge received	68.75	m3/cycle
Therefore, we can recirculate 6 hours through FO system to get the maximum flux		
Flux through FO	6	LMH
Recirculation time	6	h
Therefore, flux through FO in one circle	36	L/m2

Total membrane area required (m2)	Total permeate through FO (m3/cycle)	Total permeate per day (m3)	Sludge volume reduction through FO (%)	# of modules needed	Final Solids content (%)
100	3.6	14.4	5.2%	6	4.2
200	7.2	28.8	10.5%	11	4.5
300	10.8	43.2	15.7%	17	4.7
400	14.4	57.6	20.9%	22	5.1
500	18	72	26.2%	28	5.4
600	21.6	86.4	31.4%	33	5.8
700	25.2	100.8	36.7%	39	6.3
800	28.8	115.2	41.9%	44	6.9
900	32.4	129.6	47.1%	50	7.6
910	32.76	131.04	47.7%	50	8

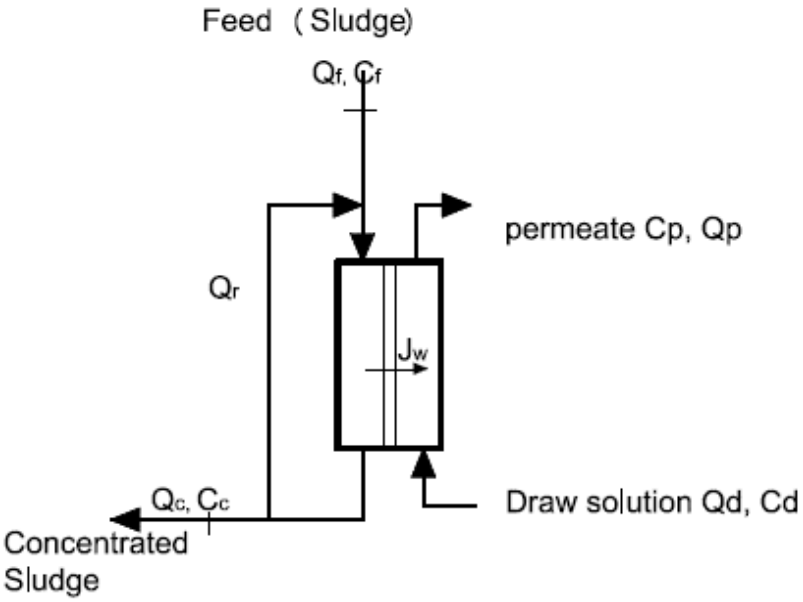

Salt balance for FO system;

Qd*Cd+Qf*Cf= Qc*Cc+Qp*Cp

For System 1 where filtered seawater used to backwash the pre-treatment system;

Qd*Cd=Cp*Qp

Cp= Qd*Cd/Qp

Cp= Qd*Cd/(Qd+Jw)

Assume Cd~2 Co (if recovery is 50 %)

Cp=Qd*2*Co/(Qd+Jw)

If Qd is equal to Qf; Qd=2Qf: Qd=4Qf: Qd=8Qf Qd=16 Qf …….

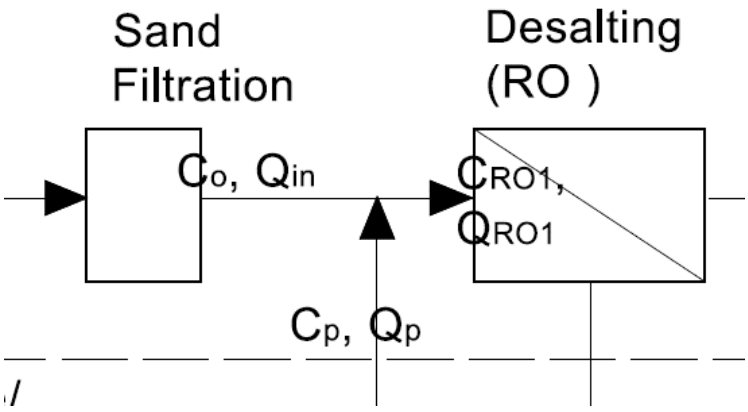

CRO1= (CoQin+Cp*Qp)/(QRO1)

If Qd is equal to Qf : Qd=2Qf: Qd=4Qf: Qd=8Qf Qd=16 Qf …….

Never doubt that a small group of thoughtful, committed citizens can change the world; indeed, it's the only thing that ever has.
-Margaret Mead